The Function and Regulation of Macrophage Matrix Metalloproteinase 10 (MMP-10) in Lung Injury and Fibrosis

Tyler C. Vandivort

A dissertation
submitted in partial fulfillment of the
requirements for the degree of

Doctor of Philosophy

University of Washington
2015

Reading Committee
William C. Parks, Chair
David L. Eaton, Chair
Terrance J. Kavanagh

Program Authorized to Offer Degree:

Environmental and Occupational Health Sciences

University of Washington

Abstract

The Function and Regulation of Macrophage Matrix Metalloproteinase 10 (MMP-10) in Lung Injury and Fibrosis

Tyler C. Vandivort

Chairs of the Supervisory Committee:
William C. Parks, PhD
Dept. of Medicine
David L. Eaton, PhD
Dept. of Environmental and Occupational Health Sciences

Matrix metalloproteinases (MMPs) are a family of zinc-dependent endopeptidases long assumed to primarily function in the breakdown of extracellular matrix (ECM). However, a growing body of work indicates that distinct MMPs are important for the innate response to injury. *Mmp10* (also stromelysin-2) has also been linked with this response in various models (e.g. partial hepatectomy and bile duct ligation, colitis, *P. aeruginosa* infection in the lungs), and its expression is sustained in a number of diseases including atherosclerosis, cystic fibrosis, and idiopathic pulmonary fibrosis. Here I used mice deficient in *Mmp10* to ascertain the role of MMP-10 in two pulmonary models of sterile damage: the pro-fibrotic drug bleomycin, and long multi-walled carbon nanotubes (L-MWCNT), a type of engineered nanomaterial with properties similar to asbestosis. I found that macrophage *Mmp10* was protective in both models through somewhat dissimilar mechanisms. Whereas *Mmp10* ablation resulted in increased inflammation and fibrogenesis with bleomycin, likely resulting from enhanced CCL2-mediated macrophage recruitment, no difference in CCL2 was seen post-L-MWCNT. Instead, *Mmp10* promoted pulmonary clearance of these particles, and protected macrophages from inflammation and death at 24 hours post-exposure. As MMPs are largely regulated transcriptionally, I examined macrophage *Mmp10* signaling *in vitro* with four disparate stimuli: LPS, bronchoalveolar lavage post-bleomycin, PMA, and L-MWCNT. I found these agents differ in their potency, temporal pattern of induction, and utilization of signaling components (i.e. TLR4, protein kinase C, and mitogen activated protein kinases), but that each was ultimately NFκB-dependent. I conclude that *Mmp10* is a well-conserved, protective component of the macrophage response to sterile lung damage.

TABLE OF CONTENTS

Page

List of Figures ..……..……..……i

List of Tables .....……..…….iv

List of Abbreviations ……...……...v

Acknowledgements……...……....vii

Chapter 1: Introduction

1.1. Vertebrate matrix metalloproteinases (MMPs) ……1

1.2. Regulation of MMPs…….……2

1.3. Matrix metalloproteinase 10 (stromelysin-2) ……5

1.4. Generation of *Mmp10* null mice……..5

1.5. *In vitro Mmp10* studies……..6

1.6. Macrophage polarization……..8

1.7. Macrophages and fibrosis……9

1.8. Previous studies: *P.* aeruginosa and MMP-10……10

1.9. Rodent models of lung disease……12

1.10. Acute lung injury and fibrosis in humans……...13

1.11. The bleomycin model……14

1.12. Multi-walled carbon nanotubes……15

1.13. Central Hypothesis……16

1.14. Figures / Tables……17

Chapter 2: Pulmonary Stromelysin-2 (MMP-10) Protects against Acute Lung Injury and Fibrogenesis in Mice

2.1. Introduction……..26

2.2. Results ……..….28

2.3. Discussion ……..….31

2.4. Figures / Tables……..……..35

Chapter 3: Stromelysin-2 (MMP-10) Facilitates Clearance and Moderates Inflammation and Cell Death Following Lung Exposure to Long Multi-walled Carbon Nanotubes (L-MWCNT)

3.1. Introduction ……..…….41

3.2. Results ……..……..…….43

3.3. Discussion ……..…….47

3.4. Figures / Tables……..……..51

Chapter 4: Induction of Stromelysin-2 (MMP-10) in Macrophages Is Mediated via Diverse Signaling Pathways That Converge on NFκB

4.1. Introduction ……..…….60

4.2. Results ……..……..…….62

4.3. Discussion ……..….68

4.4. Figures / Tables……..……..72

Chapter 5: Conclusions

5.1. Summary...……..……..…….81

5.2. Macrophage *Mmp10* is a major *in vivo* mediator

of the response to lung injury……..….82

5.3. Macrophage *Mmp10* orchestrates inflammation via distinct

but conserved mechanisms *in vitro*……...*84*

Chapter 6: Materials and Methods...……....88

References ...……...……95

Curriculum Vitae……...…….106

LIST OF FIGURES

Figure Number Page

Chapter 1:
1.1. Targeting construct for generating *Mmp10* null mice……...17

1.2. Simplified diagram of the major MAPK signaling pathways……19

1.3. Macrophage polarization in response to the pulmonary environment……...20

1.4. *Mmp10* is associated with reduced mortality and weight loss following *Pseudomonas* aeruginosa infection……...……21

1.5. Macrophage *Mmp10* is protective against weight loss post-*P.* aeruginosa infection……..22

1.6. MMP-10 is Expressed by activated macrophages in the lung……...……23

1.7.Stages of the typical murine response to bleomycin. ……...24

1.8. Transmission electron microscopy (TEM) image of multi-walled carbon nanotubes (95wt%, 20-30nm OD)……..…25

Chapter 2:
2.1. *Mmp10* expression in lung is associated with reduced mortality post-exposure to bleomycin……..…35

2.2. Weight loss and inflammation are enhanced in *Mmp10*$^{-/-}$ mice……..…36

2.3. MMP-10 attenuates peak immune cell infiltration post-bleomycin exposure. ……..…37

2.4. *Mmp10*$^{-/-}$ lungs contain increased macrophage and lymphocyte cells at 10 and 14 days post-bleomycin……..……38

2.5. MMP-10 regulates macrophage recruitment into the lung post-bleomycin……...…39

2.6. The fibrogenic response to bleomycin is exacerbated in *Mmp10*$^{-/-}$ lungs……..……40

Chapter 3:
3.1. MMP-10 protects against MWCNT-associated losses of BAL macrophages……..…52

3.2. Macrophage and neutrophil recruitment is MWCNT, but not genotype dependent……..……..…53

3.3. MWCNT induce a robust inflammatory response in lungs treated with MWCNT……..……..…54

3.4. MMP10 attenuates the pro-inflammatory response to MWCNT in BMDMs……55

3.5. *Mmp10* deficient mice exhibit reduced clearance following exposure to MWCNT……56

3.6. MWCNT sensitivity in *Mmp10*$^{-/-}$ animals is mediated by contact, but not enhanced endocytosis……57

3.7. MWCNT are associated with enhanced cell death in *Mmp10*$^{-/-}$ BAL pellets, but not whole lung lysates……..58

3.8. *Mmp10* ablation confers sensitivity to apoptosis in BMDMs without an increase in endocytosis……59

Chapter 4:

4.1. *Mmp10* is induced during *in vitro* derivation of BMDMs from bone marrow……72

4.2. Day 4 post bleomycin (BLM) BAL shows a dose-dependent induction of *Mmp10* that is greater than untreated BAL alone…….……73

4.3. BMDM *Mmp10* is up-regulated by treatment with BAL collected from BLM treated animals. ……74

4.4. *Mmp10* stimuli show distinct temporal induction profiles in treated BMDMs……..75

4.5. PMA, but not LPS, MWCNT, or BLM BAL signaling is protein kinase C dependent……76

4.6. MWCNT and PMA, but not LPS or BLM BAL are modified by *Tlr4* and *Myd88* ablation……77

4.7. *Mmp10* stimuli utilize diverse MAPK signaling cascades that converge on NFκB……...78

4.8. *Mmp10* signaling inhibitors have minimal or no impact on baseline *Mmp10* expression……..79

LIST OF TABLES

Table Number Page

1.1. Summary of existing *in vitro* studies of *Mmp10* regulation……..18

3.1. Physiochemical properties of L-MWCNTs……..……51

4.1. Summary of results for experiments regarding *Mmp10* signaling with various stimuli……80

LIST OF ABBREVIATIONS (alphabetical)

AAV - adenoviral associated vector
ALI culture - air liquid interface culture
ARDS - acute respiratory distress syndrome
αSMA - alpha smooth muscle actin
ASP - aspartic acid
BAL - bronchoalveolar lavage
BIS - bisindolymaleimide
BLM - bleomycin
BM - bone marrow
BMDMs - bone marrow derived macrophage
CBD - chronic beryllium disease-
CF - cystic fibrosis
Cfu - colony forming unit
CNT/CNF - carbon nanotube/carbon nanofiber
CS-BTRC - Cedars-Sinai Biobank and Translational Research Core
CSCs - cancer stem cells
Ct - threshold cycle
DAMP - damage associated molecular pattern
DM - dispersion media
ECM - extracellular matrix
GFP - green fluorescent protein
GM-CSF - granulocyte macrophage colony-stimulating factor
H&E - hematoxylin and eosin
HBE - human bronchial epithelial cells
i.t. - intratracheal intubation
IgM - immunoglobulin M
IHC - immunohistochemistry
IPF - idiopathic pulmonary fibrosis
L-MWCNT - long multi-walled carbon nanotubes
LPS - lipopolysaccharide
M-CSF - macrophage colony stimulating factor
M-CSFR- M-CSF receptor
MAPK - mitogen activated protein kinases
MMP-10 - *matrix metalloproteinase 10*
$Mmp10^{-/-}$ - Mmp10 null mouse
MNs – mononuclear cells
MPO - myeloperoxidase
MWCNT - multi-walled carbon nanotubes
MyD88 - myeloid differentiation primary response gene 88
NCI - National Cancer Institute
NCL - Nanotechnology Characterization Laboratory.

NCNHIR - Nanotechnology Health Implications Research Consortia
NIEHS - National Institute of Environmental Health Sciences
OD - outside diameter
OPA - oropharyngeal aspiration
OSHA - Occupational Safety and Health Administration
PAK - pseudomonas aeruginosa strain K
PEL - permissible exposure limit
PKC - protein kinase C
PMA - phorbol 12-myristate 13-acetate
PmB - polymyxin B
PMN - polymorphonuclear leukocytes (neutrophils)
qPCR - quantitative polymerase chain reaction
RSV - respiratory syncytial virus
RTK - receptor tyrosine kinase
SWCNT - single-walled carbon nanotube
TEM - transmission electron microscopy
TIMP - tissue inhibitors of MMPs
TLR4 - Toll-like receptor 4
WT - wild type

ACKNOWLEDGMENTS

This work would not be possible without the tremendous support I received from both my department (Environmental and Occupational Health Sciences) at the University of Washington, and my committee. In particular, I would like to recognize my Graduate Program Manager, Rory Murphy, Professor Terrance Kavanagh, and Professor David Eaton for their wisdom and direction over the last 5 years.

I would also like to acknowledge the contributions of my mentor and principal investigator, William Parks, for his continued financial and moral support, as well as all members of the Parks' laboratory, both past and present.

Finally, I would like to thank my wife, Nikki, who will never know the full measure of her contribution to this and all things that I do.

CHAPTER 1

Introduction

1.1 Vertebrate matrix metalloproteinases (MMPs)

First identified in 1962 by Gross and Lapiere, matrix metalloproteinases (MMPs) were a result of the pair's search for a vertebrate collagenase capable of collagen degradation at neutral pH and physiological temperature. This distinction was important as several bacterial collagenases had been identified previously, as well as a class of lysosomal proteins known as cysteine cathepsins, which are largely unstable at neutral pH [1]. However, Gross and Lapiere reasoned that certain rapid, large-scale, post-natal remodeling events, such as the involution of the post-partum uterus, [2] would require the presence of a ubiquitous extracellular collagenase, and they proceeded to describe the first MMP in the regressing frog tadpole tail during metamorphosis [3].

Since that time, vertebrate MMPs have grown to comprise a family of 24 extracellular peptidases, and as their name implies, their primary function has long been assumed to be turnover of extracellular matrix (ECM) that surrounds and supports most cells in the body. In addition, the high sequence homology and low substrate specificity seen *in vitro* led many to assume that individual MMPs are largely redundant [4,5].

Several pieces of evidence have uprooted these conclusions. In particular, of the more than 18 MMP-specific knockout mice that have been produced, most (with the exception of *Mmp14*$^{-/-}$ mice, which show severe skeletal deformations and impaired angiogenesis [6]) show only minimal or transient phenotypes – a far

cry from what would be expected in the absence of normal ECM turnover. While MMP redundancy is a possible explanation for the lack of a developmental/adult phenotype, many of these same knockout mice have shown profoundly distinct phenotypes following injury. For example, Li et al. described a mechanism by which MMP-7 selectively sheds syndecan-1 from the surface of the pulmonary epithelium following bleomycin exposure, resulting in enhanced neutrophil infiltration and fibrosis. In contrast, several other MMPs, including MMP-1, 2, and 8, have been shown to be protective following bleomycin exposure [7].

Finally, while *in vitro* activity assays have demonstrated that MMPs show considerable, but somewhat non-specific activity against many ECM components [8] much of these data have failed to be reproduced *in vivo*, likely due to the absence of various physiologically relevant factors known to regulate their activity (e.g. substrate and/or MMP concentration, presence of tissue inhibitors, compartmentalization, etc. [9,10]). This is not to say that MMPs do not degrade ECM products (for example, MMP-13 functions as a collagenase in mice), but that MMPs are also capable of cleaving an assortment of extracellular proteins, including latent cytokines, chemokines, receptors, and antimicrobial agents in the pericellular space [11]. These findings, together with many others, have led to an emerging view of MMPs as regulators of innate immunity [12, 13, 14].

1.2. Regulation of MMPs

Given the destructive potential of MMPs, it is not surprising that their function is tightly controlled at both the transcriptional and post-transcriptional levels.

Transcriptional Control

Transcriptional control is considered the primary regulatory point for MMPs, which largely show low, baseline expression in most tissues. However, many MMPs are induced following injury, with transcriptional levels often strongly correlating with outcomes. Analysis of human MMP promoters has shown that MMPs contain a rich diversity of transcription factor responsive *cis*-elements that make this possible (e.g. AP-1, PEA3, Sp-1, NF-kB, etc.) [15] [16].

Post-transcriptional control

Post-transcriptionally, MMPs are controlled in four different ways: inactivation (zymogen), tissue inhibitors of matrix metalloproteinases (TIMPs), compartmentalization, and substrate availability [16].

Zymogen. MMPs are broadly classified based on the high degree of homology seen in their pro and catalytic regions, which is necessary to preserve the translated protein in an inactive, zymogen state. Known as the cysteine-switch mechanism, this state is maintained via ligation of the thiol group of a cysteine residue in the pro-domain to a Zn^{2+} ion held by

three conserved histidine residues in the catalytic domain. Disruption of this mechanism is necessary for MMP activity [17].

Tissue inhibitors of MMPs (TIMPs). Having first been identified and sequenced in 1985, tissue inhibitors of matrix metalloproteinase have long been understood to be integral to MMP regulation [18,19]. Four tissue inhibitors (TIMP-1, 2, 3, 4) have been described with the collective ability to inhibit all MMPs. Composed of two different domains (amino and carboxy-terminal), these proteins inhibit MMPs through an interaction between the folded N-terminal end and the active site of the MMP [20,21].

Compartmentalization. By establishing areas of high enzyme concentration (e.g. near a particular membrane receptor), cells are able to tightly control the amount of cleaved product being produced, and thus conserve resources and minimize off-target effects [16].

Substrate availability and affinity. Though the apparent affinity of MMPs for various substrates has been somewhat misleading *in vitro*, studies show that MMPs do show specificity, even in culture. Likewise, the absence of a substrate can also modify the contribution of MMPs to a phenotype [16]. For example, in the previously described mechanism by Li et al. where MMP7 recruits neutrophils through shedding of syndecan-1 from lung epithelium, both *Mmp7*$^{-/-}$ and *Syn1*$^{-/-}$ deficient mice

demonstrated reduced neutrophil numbers in the lung post-bleomycin, highlighting the importance of substrate availability in mediating neutrophil recruitment in this model [11].

1.3. Matrix metalloproteinase 10 (stromelysin-2)

Despite having been cloned almost 20 years ago, MMP-10 (stromelysin-2) has received substantially less attention than other MMPs, especially MMP-2, and 9 [22]. But while the majority of the MMP-10 research that has been conducted has focused on the role it plays in either cardiovascular disease [23, 24], or the maintenance and tumorigenic potential of cancer stem cells (CSCs) [25,26], *Mmp10* has also been shown to be up-regulated in the serum and lungs of patients with idiopathic pulmonary fibrosis [27,28].

Like the majority of MMPs, MMP-10 is not expressed in most developing or adult tissues, including lung [22,29-32]. However, in response to injury or infection, MMP10 is induced by macrophages and to a lesser extent epithelial cells in many tissues [30,32-46,47]. This widespread expression suggests that MMP-10 serves key roles in the host response to environmental insults.

1.4. Generation of *Mmp10* null mice

Mmp10 null mice were generated through the use of a neomycin-containing construct targeted to exons 3 to 5 of the *Mmp10* gene (also see Figure 1.1), which includes the catalytic domain [48]. These mice have since been

crossbred for more than 11 generations with C57BL/6 mice. *Mmp10* null mice are viable and show no discernable defects.

Studies conducted with these animals have revealed that *Mmp10* deficiency is associated with several consistent murine phenotypes. Chief among these are an exaggerated and sustained inflammatory response [49,50,unpublished data], and inappropriate wound scarring / fibrosis [47], though not necessarily in the same model. Furthermore, although epithelial cells are also a known source, these findings have largely been attributed to macrophage MMP-10.

Based on these data, I hypothesized that macrophage MMP-10 is also a well-conserved component of the macrophage response to sterile lung injury (i.e. injury occurring in the absence of a pathogen). To test this hypothesis, I utilized two models of injury: exposure to the pro-fibrotic drug bleomycin, as well as to a specific type of engineered nanomaterial known as long multi-walled carbon nanotubes (L-MWCNT) (see sections 1.11 and 1.12 for details). Furthermore, to explore the nature of *Mmp10* conservation in lung injury (both sterile and non-sterile), I decided to examine the signaling mechanisms responsible for *Mmp10* induction in macrophages with both of these stimuli, as well as with *Pseudomonas aeruginosa* (see section 1.8).

1.5. *In vitro Mmp10* studies

Although little work has been done on its gene regulation, a number of cell surface receptors, signaling pathways, and transcription factors have been suggested to control of *Mmp10* expression (see Table 1.1). Most notable among

these are the major mitogen activated protein kinases (MAPK) (i.e. ERK, JNK, and P38). MAPKs are rapidly and highly conserved intracellular phosphorylation cascades that control a multitude of cellular events from growth and differentiation to apoptosis and survival [51,52]. As illustrated in Figure 1.2, generic MAPK signaling involves stepwise activation of three classes of kinases (MAPKKK, MAPKK, MAPK), which typically activate various transcription factors (e.g. AP-1 and NFκB) to generate a specific gene program.

In one of the few studies on MMP-10 regulation, Sampieri et al. examined PMA-dependent gene induction in MRC-5 cells, a human fibroblast line. They found that *Mmp10* signaling proceeded through a protein kinase C (PKC) => MEK-1/2 => ERK-1/2 mechanism in these cells [53]. Hirakawa et al. demonstrated a similar, PKC-dependent mechanism for respiratory syncytial virus (RSV) in human nasal epithelial cells (HNECs). Furthermore, they found that this process was NFκB dependent. Orbe et al. were also able to implicate ERK and JNK in thrombin-dependent signaling in a series of human and mouse endothelial cell types (HUVECs, HUVECs, HAECs, BAECs), and they concluded that AP-1, not NFkB was responsible for *Mmp10* transcription [23]. However, a caveat with the Orbe et al. findings is that MMP-10 has not been shown to be expressed by endothelial cells *in vivo* [47]. Finally, Lisboa et al. implicated NFκB in LPS and mechanical force-mediated signaling in human periodontal fibroblasts, but instead found that p38 and JNK, and not ERK were the relevant MAPK members behind this response [54]. While not complete (see table 1.1 for a more in-depth summary of studies examining *Mmp10* expression), the above results illustrate

the highly stimulus-specific and, to a lesser extent, cell-type specific nature of *Mmp10* signaling.

This last point is relevant as very few of these studies have been conducted in macrophages, and *Mmp10* has been shown to yield cell specific phenotypes. For example, Treiber et al. examined the contribution of murine RelA/p65, a component of the NFκB complex, to the pathogenesis of chronic pancreatitis. By selectively ablating this subunit in acinar or myeloid cells they were able to show that whereas the former protects against chronic inflammation, the later promotes a fibrotic response that is attenuated by macrophage MMP-10 [55]. These findings support the idea that macrophage MMP-10 is anti-fibrotic and indicate that macrophage-dependent *Mmp10* signaling warrants further study.

1.6. Macrophages and fibrosis

Macrophage responses are important for a wide range of tissue processes, including clearance of approximately $2x10^{11}$ erythrocytes each day, wound repair, and amplifying and carrying out complex activities that are essential for both host defense and immune suppression [56]. These responses are highly plastic and tissue specific, involving the rapid and precise development of distinct transcriptional responses to stimuli [57 58 59].

The M1/M2 polarization concept has evolved as a way to describe the responses of activated macrophages to their environment. As illustrated in Figure 1.3, M1 polarized, or classically activated macrophages, are induced by infection and pro-inflammatory T_H1 cytokines [60]. They produce high levels of iNOS and

release large quantities of pro-inflammatory cytokines (e.g., IL-1, TNFa, IL-6) to facilitate pathogen clearance. On the other extreme are M2 cells, or alternatively activated macrophages (as well as sub-M2 types)[61-64], which are induced by T_H2 cytokines IL4 and IL13 and other factors [60,64]. These cells produce Arg1 and secrete factors associated with immunosuppression and repair (e.g., IL-10, TGFb1, IL-1ra) [65,66]. As iNOS and Arginase 1 both compete for L-arginine to produce nitric oxide (NO), or L-ornithine (which contribute to inflammation or repair, respectively), the ratio of these two markers is thought to be indicative of the underlying polarization state [67,68].

Although dividing macrophages into M1 vs. M2 classes greatly oversimplifies the complex continuum of functional and reversible states that the cells exist in *in vivo* [69,70], it is helpful for describing the overall macrophage disposition at specific points during acute and chronic illness.

1.7. Macrophages and fibrosis

Considering their tissue distribution and ample capacity for cytokine synthesis, it is not surprising that macrophages directly influence the severity of BLM-induced lung fibrosis.

This effect can be exerted during both the early, predominately M1-biased phase of the model, as well as the later, M2-biased resolution phase [56,71,72]. For example, studies have shown that M2 polarization promotes the fibrotic response to bleomycin [73], possibly through the expression of known pro-fibrotic factors like TGFβ1 and arginase-1, which can stimulate synthesis of proline, a highly

abundant amino acid in collagens [74]. However, other studies have shown that M1 macrophages are capable of promoting fibrogenesis through tissue damage associated with excess inflammation [75].

In addition to polarization, the number of recruited macrophages also seems to be an important determinant for the bleomycin response. For example, whereas ablation of the major monocyte attractant, CCL2, as well as its receptor, CCR2, have been shown to be protective against fibrosis through attenuated macrophage recruitment [76-78], macrophage depletion at both early and late phases results in impaired wound healing. In the short-term this is due to inadequate formation of vascularized granulation tissue (the precursor to scar) [79,80], and in the late phase, to an inability to resolve scars [81,82].

These points stress the importance of macrophage number and polarity in the fibrotic response to bleomycin.

1.8. Previous studies: *Pseudomonas aeruginosa* and MMP-10

Earlier studies in the Parks lab assessed the role of MMP-10 in host response to *Pseudomonas aeruginosa* (note: PAK is a specific strain of *P. aeruginosa*). The conclusions of these studies are important as they corroborate, and indeed helped guide the studies outlined in the remaining chapters. The following is an overview of relevant findings.

Cystic fibrosis (CF) is a life-limiting disorder that impacts approximately 70,000 people worldwide. While CF impacts many organ systems (e.g. pancreas, liver, kidneys, and intestines), lungs are severely affected due to persistent *P.*

aeruginosa colonization leading to excessive viscous mucus secretions that cause obstructions, impaired mucociliary clearance, and inflammation [83]. *P. aeruginosa* is the most common clinical isolate from the lungs of CF patients, and chronic *P. aeruginosa* colonization is associated with reduced survival [84,85]. Interestingly, *Mmp10* was found to be up-regulated in the lungs of CF transplant recipients (n = 5) relative to normal lungs (n=3), suggesting that MMP-10 might be involved in mediating the pulmonary response to infection (unpublished data – not shown).

Given these facts, the impact of *P. aeruginosa* infection on WT and *Mmp10*$^{-/-}$ mice was subsequently investigated. The Parks lab found that infection via oropharyngeal aspiration (OPA) of 10^7 cfu of live PAK resulted in rapid weight loss that peaked at 48 hours (~10%) in the WT animals before steadily improving (Figure 1.4.C). This was accompanied by a robust increase in *Mmp10* mRNA in whole lung (~300 fold) (Figure 1.4.B). However, while no mortality was observed in the WT animal, infection resulted in ~50% mortality in *Mmp10*$^{-/-}$ (Figure 1.4.A) and sustained weight loss in surviving animals (Figure 1.4.C). These data suggest that MMP-10 is protective against infection with *P. aeruginosa*.

Macrophages modulate the pulmonary response to infection through a host of direct (i.e. phagocytosis) and indirect (i.e. antigen presentation, cytokine production, etc.) bactericidal activities. But while these processes are important for clearance, they can also result in residual damage to the tissues themselves [64]. Interestingly, whereas cell counts and myeloperoxidase (MPO) levels indicated that neutrophil recruitment did not differ between the genotypes (data

not shown), macrophages counts were significantly increased in the BAL of *Mmp10*$^{-/-}$ mice at 48 hours post-infection (Figure 1.5.A). To test the impact of macrophage *Mmp10* on the weight loss phenotype, *Mmp10*$^{-/-}$ animals were infected as before, and administered 2x10^{6} of WT or *Mmp10*$^{-/-}$ bone marrow-derived macrophages (BMDMs) via retro-orbital injection 24 hours later. The Parks lab found that the addition of WT, but not *Mmp10*$^{-/-}$ BMDMs significantly reduced the weight loss post-infection (Figure 1.5.B).

To determine the macrophage-specific contribution to whole lung *Mmp10* levels (Figure 1.4.A), the Parks lab conducted *in situ* hybridization for *Mmp10* on WT lung sections collected 48 hours post-infection. As seen in Figure 1.6, whereas no *Mmp10* mRNA was observed in untreated lungs (A), *P.* aeruginosa resulted in a robust increase in expression (B) that appeared to localize to extravasating macrophages (C). Immunostaining with the pan macrophage marker, Mac2, showed co-localization of these signals, suggesting that macrophages were the major source of *Mmp10* in this model.

Together, these experiments, which were conducted before I joined the Parks lab, indicate that macrophage MMP-10 is protective against excess pulmonary inflammation and weight loss following infection.

1.9. Rodent models of lung disease

In spite of some anatomical and physiological differences [86], murine models continue to be invaluable for modeling human biology and disease pathogenesis [87]. From a husbandry standpoint, mice are easy to handle, have a

short breeding time, an accelerated lifespan, and are relatively inexpensive to house. With the development of diverse genetic strains and strategies (conditional knock-outs, reporter mice, lineage-tracing approaches, etc.), as well as the wide range of available reagents (antibodies, recombinant proteins, inhibitors, etc.), mice have become an essential organism to model human homeostasis and disease processes [88].

1.10. Acute lung injury and fibrosis in humans

Mice have been especially valuable for studying lung development and pulmonary disease, including acute lung injury (ALI) and pulmonary fibrosis [89]. ALI in humans can be caused by trauma, injury, or sepsis and is characterized by epithelial and endothelial leak (i.e., edema), inflammation, and nascent fibrosis. In many patients, ALI progresses to its severe form, acute respiratory distress syndrome (ARDS), which often results in fibrosis and death due to respiratory failure [90,91].

Pulmonary fibrosis is a progressive, fatal pathology characterized by the excess deposition of collagen-rich extracellular matrix leading to impaired lung function [92,93]. The most common manifestation of fibrosis is idiopathic pulmonary fibrosis (IPF), which has an exceedingly poor prognosis (approximately 2-3 years) [94]. In addition, fibrosis can result from many known causes, such as a range of occupational exposures including silicosis, asbestosis, and chronic beryllium disease (CBD or berylliosis) [95], and more recently, engineered nanomaterials like carbon nanotubes [96]. While research interest in these

occupational exposures has often taken a backseat to IPF, it's important to note that the WHO estimates that pneumoconiosis were responsible for approximately 260,000 of the estimated 56,000,000 global deaths in 2013 [97].

1.11. The bleomycin model

Administration of bleomycin (BLM) is the most widely used and best characterized model for inducing both ALI and fibrosis in experimental mammals [98]. Although BLM-induced pulmonary fibrosis in rodents does not recapitulate fully the human fibrotic phenotype [99], mouse studies with this model have led to the discovery of many important factors influencing the onset and progression of disease [100]. While the exact mechanism(s) behind BLM-induced fibrogenesis are unknown, the initiating injury is thought to arise from contact-dependent DNA strand breaks in the epithelial cells lining the conducting airways and alveoli, and in particular, type 1 pneumocytes [101].

The stages of the typical mouse response to BLM are presented in Figure 1.7. The first week following exposure is dominated by an epithelial response, with contact-dependent interactions with the pulmonary epithelium resulting in cellular injury, pulmonary edema resulting from barrier dysfunction, recruitment of leukocytes (notably neutrophils and macrophages) into the pulmonary space, weight loss, and mortality. This is followed by a transition period of roughly 4 days, during which time the airways begin to repair the damaged tissues through clearance of dead tissue and deposition of the matrix components necessary to re-establish the epithelial barrier. However, due to a mechanism that is not

entirely understood, these responses fail to abate, instead resulting in excess deposition of fibrous connective tissue (primarily type I and III collagens) by activated fibroblasts (known as myofibroblasts). This occurs over a period of several weeks, culminating in decreased pulmonary compliance [98].

This degree of characterization, along with the establishment of canonical markers associated with each of the stages, makes bleomycin an attractive place to begin to investigate both the innate and fibrotic response to lung damage.

1.12. Multi-walled carbon nanotubes

Engineered nanotubes are a class of synthesized materials whose size, electrical, mechanical, and thermal properties have made exceedingly valuable for a range of biomedical and commercial applications [102]. Multi-walled carbon nanotubes (MWCNTs), concentric tubes comprised of graphene sheets, are one such material (see Figure 1.8 for a TEM image). The growing use of these tubes, together with uncertainly regarding occupational exposure risk, and the lack of an Occupational Safety and Health Administration (OSHA) permissible exposure limit (PEL) for CNT/CNF (NIOSH proposes a recommended exposure limit (REL) of 1 $\mu g/m^3$) [96] have created a real need to understand the factors associated with hazard. Such factors include modifications to the surface, particle rigidity, the diameter of the sheet, and length [102]. The last two factors are particularly important as single-walled carbon nanotubes (SWCNT), and shorter tubes are substantially more expensive to generate. However, longer tubes, and especially those that fit the EPA criteria for fiber classification (5 mm or longer, with a

length-to-diameter ratio of at least 3 to 1) have also been shown to have considerable pro-inflammatory, pro-apoptotic, and pro-fibrotic potential with high dose exposure [103, 104, 105, 106, 107].

While the full mechanism underlying these phenotypes has yet to be described, a mounting body of evidence suggests that the NLRP3 (also known as NALP3) inflammasome is responsible in part for these effects through IL-1β production [105,103,108,109]. In canonical inflammasome activation, this multimeric complex assembles in the cytosol in response to stimuli (in this case, L-MWCNTs), and recruits and activates the pro-caspase-1 zymogen. As part of the NLRP3 complex, caspase-1 cleaves pro-IL-1β at the Asp 116 to convert it into its mature, active state [110,111]. Primarily carried out by monocytes and macrophages, Il-1β produced in this way is released into the surround space where it produces inflammation via binding with the type 1 interleukin-1 receptor (IL1R1) [112].

1.13. Central Hypothesis

Following pulmonary injury, Mmp10 is up-regulated in activated macrophages, and where it functions to modulate both inflammatory and fibrotic pathways.

1.14 Figures / Tables

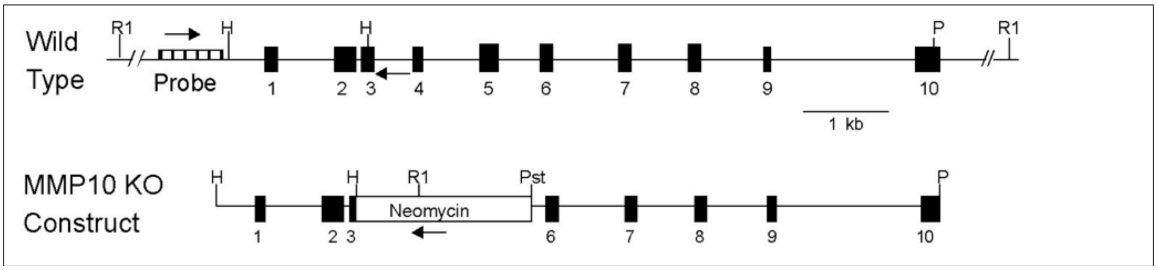

Figure 1.1. Targeting construct for generating *Mmp10* null mice. C57BL/6 mice were previously generated through a functional deletion in the catalytic domain spanning exons 3 to 5 [48]. *Unpublished figure by William C. Parks.*

Table 1.1. Summary of existing *in vitro* studies of *Mmp10* regulation.

Class	Agent	Cell Type	Source
Infection	Lipopolysaccharide (LPS)	Bone marrow derived macrophages (BMDMs), RAW264.7, Kupffer cells- murine Macrophages	113, 49
	P. aeruginosa	Air liquid interface (ALI) cultures - murine epithelial cells	48
	LPS + mechanical stress	Human periodontal fibroblasts	114
	LPS, IL-1, TNF,	Differentiated human macrophages (CD16 +/- monocytes), human keratinocytes	115,116
Virus	Respiratory Syncytial Virus	Human nasal epithelial cells (HNEC)	54
	Influenza A Virus	*N/A*	*Unpublished obs.*
Sterile Injury/Damage	Amphiregulin, Ereg, extra domain A (EDA) of fibronectin, Epidermal growth factor	AML12, Huh7, NMC, Huh28 (mouse hepatocytes, human hepatocellular carcinoma cells, mouse cholangiocytes, human cholangiocarcinoma cells)	49,75
	LPS + mechanical stress	Human periodontal fibroblasts	114
Immune Mediators	C-reactive protein	Ventricular cardiomyocytes	117
	Thrombin	HUVECs, HUVECs, HAECs, BAECs - Human and mouse endothelial cells	23
Mitogens	PMA (TPA)	MRC-5 fibroblasts (Human lung)	53
	TGF-β1, amphiregulin, epiregulin	AML12, Huh7, NMC, Huh28 (above); human keratinocytes	49, 75
	Yin Yang-1	BxPC-3 (human pancreatic epithelial cells)	118

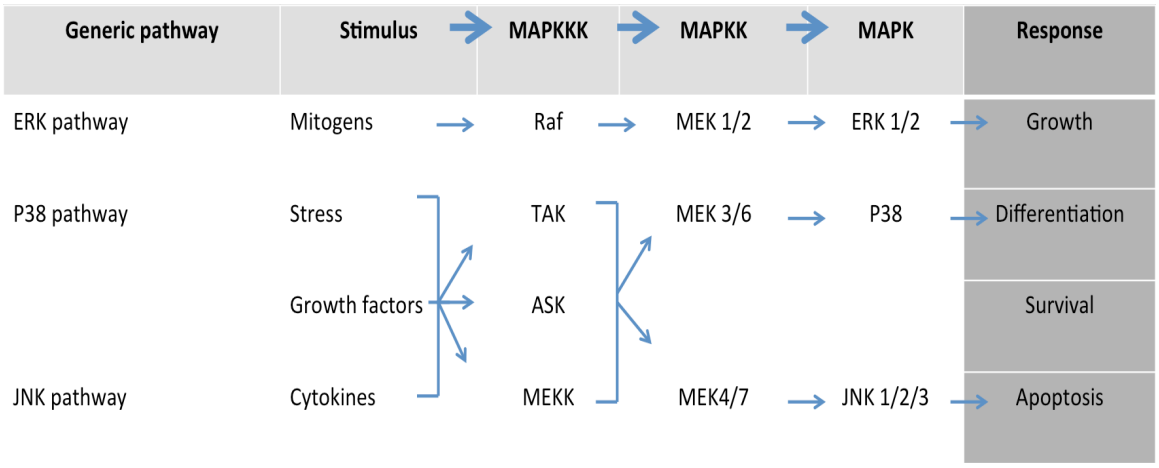

Figure 1.2 Simplified diagram of the major MAPK signaling pathways. The three major MAPK pathways, ERK, p38, and JNK are shown. The generic pathway (top) demonstrates how sequential phosphorylation events lead to a prescribed response from the cell in the form of growth, apoptosis, differentiation, survival, and more. *Modified from Batchelor and Winder, 2006* [119] [51].

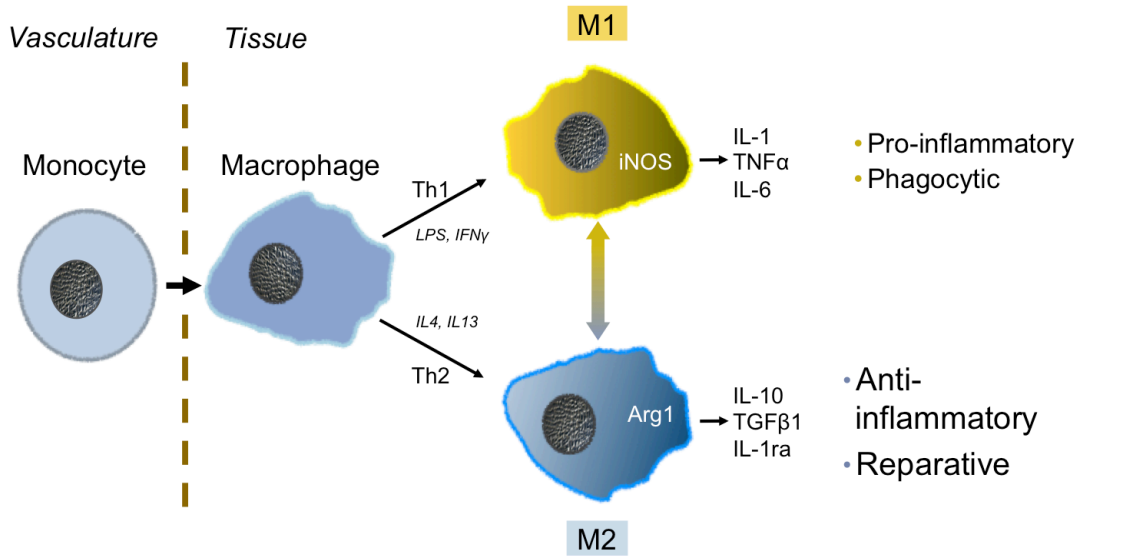

Figure 1.3. Macrophage polarization in response to the pulmonary environment. Upon extravasation, macrophages initiate a spectrum of transcriptional responses based on signals in the pulmonary environment. At one extreme are M1 polarized cells, which release pro-inflammatory cytokines (e.g. IL-1, TNFα, IL-6), and on the other are M2 cells, which produce factors associated with repair (e.g IL-10, TGFβ1, IL-1ra) [65,66]. *Unpublished figure by William C. Parks.*

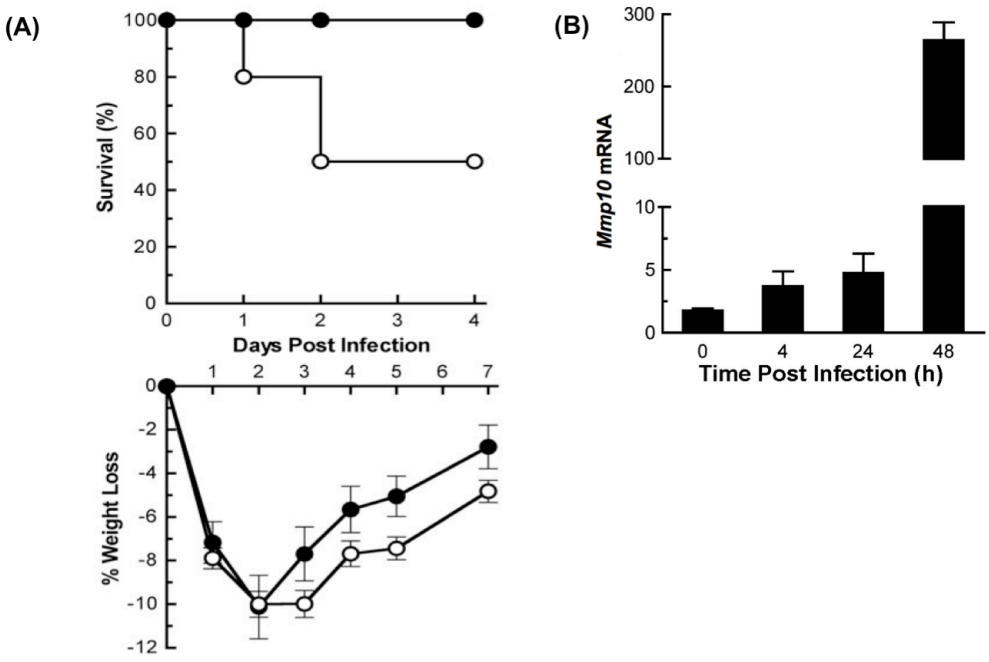

Figure 1.4. *Mmp10* is associated with reduced mortality and weight loss following *Pseudomonas* aeruginosa infection. (A) WT or *Mmp10*$^{-/-}$ mice were infected with 10^7 cfu live PAK and mortality and weight loss were observed (n = 14). **(B)** *Mmp10* mRNA expression was assayed in lungs at various days post-infection (n = 6). *Source: unpublished observations*

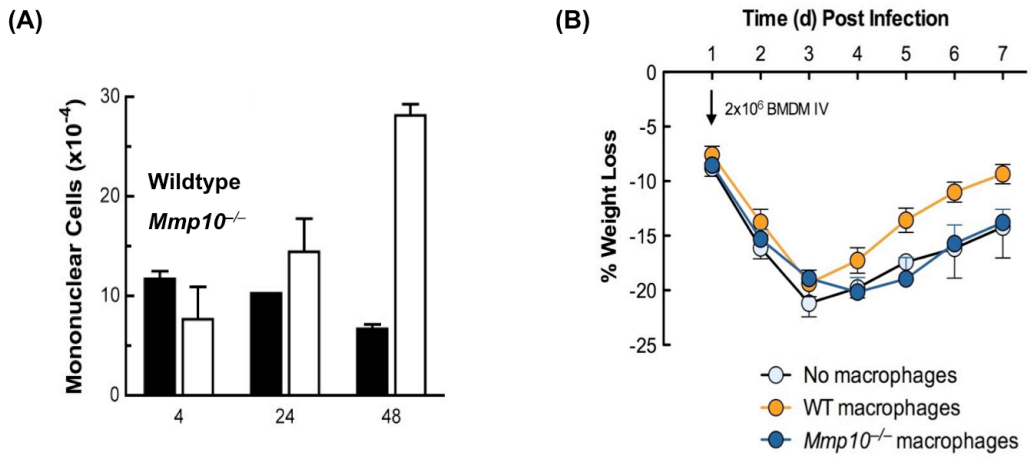

Figure 1.5. Macrophage *Mmp10* is protective against weight loss post-PAK infection. (A) Macrophages in BAL were quantified via differential counts at 4, 24 and 48 hours post-infection with PAK (n = 4). **(B)** *Mmp10*$^{-/-}$ animals were infected with PAK as before, and administered 2x10^6 BMDMs of either genotype via retro-orbital injection at 24 hours post-infection. Weight loss was recorded over the next 7 days. *Source: unpublished observations*

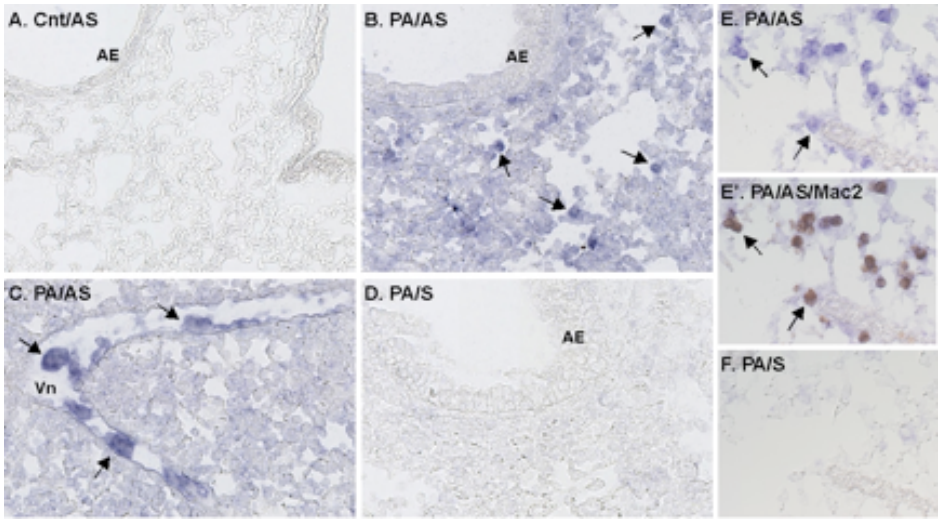

1.6. MMP10 is expressed by activated macrophages in the lung. (A-D) Sections of control **(Cnt)** and infected lungs **(PA)** were hybridized with digoxigenin anti-sense **(AS)** or sense **(S)** RNA probes. Arrows point to positive (blue) macrophages. Vn: venule; AE: airway epithelium. **(E)** After *in situ* images were captured, sections were co-stained with MAC-2 antibody. **(F)** Section serial to that in **(E)** was hybridized with sense RNA*. Source: unpublished observations*

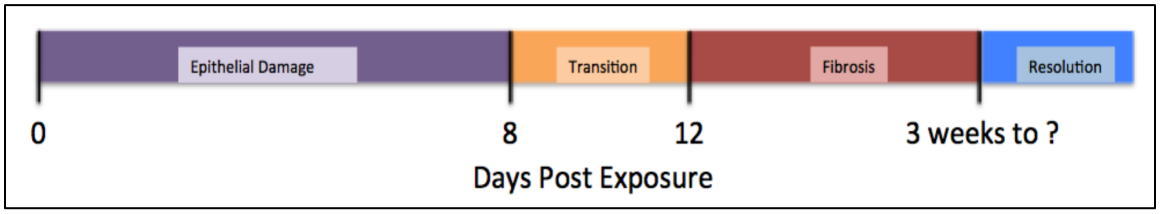

Figure 1.7 Stages of the typical murine response to bleomycin. The typical murine response includes an ALI phase derived from the initial epithelial damage, a transitory period in which markers of damage usually stabilize or attenuate and repair is initiated, and the fibrogenic phase when colllagen production peaks. Resolution generally occurs within 6 months [98, 120].

Figure: 1.8. Transmission electron microscopy (TEM) image of multi-walled carbon nanotubes (95wt%, 20-30nm OD). Provided by Cheap Tubes, Inc. from Cheaptubes.com (http://www.cheaptubes.com/product/multi-walled-carbon-nanotubes-20-30nm/)

CHAPTER 2

Pulmonary Stromelysin-2 (MMP-10) Protects Against Acute Lung Injury and Fibrogenesis in Mice

2.1. Introduction:

Pulmonary fibrosis is a progressive interstitial lung pathology typified by the persistent production of extracellular matrix components, notably type I collagen, leading to restricted lung function [121,92,93]. The most common manifestation of fibrosis is idiopathic pulmonary fibrosis (IPF), which has an exceedingly poor prognosis (approximately 2-3 years) [94], but fibrosis can also result from numerous environmental exposures including silicosis, asbestosis, and chronic beryllium disease (CBD or berylliosis) [95]. While these conditions present with other distinct pathological features (i.e. honeycombing, granulomas, nodules, etc.[122]), inappropriate re-epithelialization is thought to be an important component of the fibrotic response [123].

Administration of bleomycin (BLM) is the best described and most commonly used fibrotic model in experimental animals [98]. A key component of BLM exposure is the development of acute lung injury (ALI) during the first week post-exposure stemming from contact-mediated DNA strand brakes in epithelial cells lining the respiratory track, and in particular, pneumocytes in the distal lung [101]. This is followed by a brief transitory period, (from approximately day 8 to 12) where the airways shift to repairing this damage. However, for reasons that aren't entirely clear, these processes fail to abate, resulting in the excess production of fibrous connective tissue and decreased pulmonary compliance [98]. Importantly,

while BLM doesn't fully recapitulate a particular human phenotype (with the exception of the high dose side effects of BLM treatment), the consistency of this model makes it an attractive place to investigate both the innate response to lung injury and fibrogenesis.

Matrix metalloproteinases are a family of extracellular endopeptidases that mediate a multitude of cellular processes including growth and repair, apoptosis, pathogen clearance, and cellular recruitment. Like most MMPs, MMP-10 (stromelysin-2) is largely unexpressed in adult tissues (with the exception of the small intestine), but is substantially up-regulated in various diseases including, atherosclerosis, lung tumorigenesis and metastasis, and interestingly, in the serum and lungs of patients with IPF [23-28].

Recently, our group found that MMP-10 is protective against weight loss, inflammation, and macrophage recruitment following infection with the gram negative bacteria *Pseudomonas aeruginosa (PAK)*, and that the adoptive transfer of WT bone marrow derived macrophages (BMDMs) into *Mmp10*$^{-/-}$ mice was able to completely rescue the excess weight loss observed in *Mmp10*$^{-/-}$ animals (unpublished data). Given these findings, we hypothesized that MMP-10 might also be involved in mediating the pulmonary response to BLM-induced fibrosis. We found, similar to our observations in PAK, that *Mmp10* is protective against enhanced macrophage recruitment, inflammation, and fibrosis post-BLM.

2.2. Results: *See Chapter 6 for detailed methods.*

MMP-10 Protects Against Mortality, Weight loss, and Inflammation Post-BLM

To investigate the impact of MMP-10 on BLM-induced mortality, 8 WT or *Mmp10*$^{-/-}$ mice, of mixed sex, were treated with a high dose of 0.08U (~3.6U/kg) of BLM by intratracheal intubation (i.t.) and mortality (i.e. premature euthanasia) was observed over the next 16 days (Figure 2.1A). Treatment in this way resulted in a robust mortality response that peaked between days 9 and 11 post-exposure. A lower dose of 1.2 U/kg was subsequently utilized to increase survivorship and minimize bias (though premature euthanasia in *Mmp10*$^{-/-}$ mice would be expected to decrease, not increase the magnitude of the differences between the genotypes in these endpoints), and weight data was collected daily post-exposure. As expected, this dose resulted in substantial weight loss, which reached its nadir at day 9 (consistent with the mortality data), but resulted in 100% survivorship of WT animals (Figure 2.1B). In contrast, we found that *Mmp10*$^{-/-}$ mice showed exacerbated mortality and weight loss in these studies, and that 1.2 U/kg resulted in the premature euthanasia of 2 animals (75% survival) (data not shown). Interestingly, *Mmp10* mRNA levels in left lung homogenates from these animals showed a similar pattern, peaking at more than 170-fold above baseline at day 10 (Figure 2.1C.)

To assess how bleomycin-induced damage varies between the genotypes (i.e.), we analyzed BAL collected from WT or *Mmp10*$^{-/-}$ mice for IgM (Figure 2.2A) and total protein (Figure 2.2B) (n = 4 to 6) as markers of endothelial/epithelial

barrier dysfunction. We found that while both endpoints were significantly elevated with treatment (>60 fold and ~3 fold respectively), that neither differed significantly with genotype. However, we did observe a trend toward elevated protein in the *Mmp10*$^{-/-}$ that was absent from the IgM values, suggesting a possible disparity in cytokine synthesis in these lungs. Given this finding, lung RNAs were then probed for changes in different pro-inflammatory transcripts including *Il6*, *Il1b*, and *Tnfa* (Figure 2.2C). Analysis showed that all three of these transcripts were significantly elevated in *Mmp10*$^{-/-}$ vs. WT lungs at days 4 and 6, which corresponds to the known peak period of epithelial damage in the BLM model [98], with only *Tnfa* remaining elevated relative to WT controls at day 10. These findings were further corroborated by ELISA measurements of each of these cytokines at day 6 (Figure 2.2.D).

Together, these results suggest that MMP-10 is protective against mortality, weight loss, and inflammation post-BLM in a damage-independent manner.

Macrophage Recruitment Is Enhanced in *Mmp10*$^{-/-}$ mice

Having observed a difference in inflammation, we next evaluated whether this difference impacted lung cellularity. To this end, total BAL cell counts were quantified at days 0, 4, 6, 10, 14, 28, and 40 days post-BLM exposure (n = 4 to 6). Consistent with our mortality and weight loss data, we found that cellular recruitment peaked between 6 and 10 days after BLM. This difference was sustained in *Mmp10*$^{-/-}$ lungs, remaining significantly elevated at both the 10 and

14-day time-points (Figure 2.3A), and was easily discernable in H&E sections prepared from day 10 lungs (Figure 2.3B).

Cytospins were generated from these BALs and differential counts of macrophages, neutrophils, and lymphocytes were performed. Figure 2.4 shows the resulting total counts (Figure 2.4A), and percentages (Figure 2.4B), for each cell type during this time, including an initial increase in neutrophils, and a sustained macrophage presence, both of which have been seen in other models [124]. However, while neutrophil numbers did show a mild trend toward an increase in *Mmp10*$^{-/-}$ animals, only macrophages and lymphocytes reached statistical significance. Given that the difference in percentages between macrophages and lymphocytes at day 10 was heavily skewed toward macrophages (~15% vs. 80%) we concluded that the majority of the difference in cellularity observed at day 10 (Figure 2.3B,A) was due to macrophages. This was further confirmed via F4/80 dot blot in BAL from day 10 animals (Figure 2.4C).

Next, we examined whether the observed difference in macrophages could be a result of differential recruitment. Accordingly, we evaluated transcript levels of the major monocyte recruitment factor, *Ccl2*, in whole lung, as well as total CCL2 protein in BAL. In agreement with our differential counts, we found that both *Ccl2* mRNA and protein was significantly up-regulated in *Mmp10*$^{-/-}$ lungs at day 6 post-exposure (Figure 2.5A,B). Furthermore, when WT bone marrow derived macrophages (n = 3) were allowed to migrate in a Boyden chamber plate toward either day 6 WT or *Mmp10*$^{-/-}$ BAL for 3 hours, we saw that *Mmp10*$^{-/-}$ BAL resulted in a 3-fold increase in percent of migrated cells compared to WT BAL

(Figure 2.5C), suggesting that MMP-10 protects against sustained macrophage recruitment following BLM exposure. This is important, as CCL2-induced macrophage recruitment is associated with fibrosis [75,76].

Mmp10$^{-/-}$ Mice Show Enhanced Fibrogenesis Post-BLM

To understand the contribution of MMP-10 to BLM-induced fibrosis, several markers of collagen production were monitored in WT and *Mmp10*$^{-/-}$ mice. At the transcript level, we measured the change in *Col1a1* in lung, which along with *Col1a2* is responsible for producing type I collagen, the most abundantly produced collagen in fibrosis [125]. We found that *Col1a1* mRNA was substantially up-regulated with bleomycin treatment (~6 fold), but that whereas WT levels had begun to attenuate by day 14, *Mmp10*$^{-/-}$ *Col1a1* remained elevated at day post-bleomycin (n was between 8 and 16 animals for each group) (Figure 2.6A). A similar effect was observed in both trichrome stained sections (Figure 2.6B), and hydroxyproline content in left lungs (Figure 2.6C), with both showing a statistically significant increase at day 14 in *Mmp10*$^{-/-}$ mice. Immunohistochemistry was then performed for α–smooth muscle actin (αSMA) a marker of activated fibroblasts (myofibroblasts). In agreement with our other data, we found that αSMA is elevated at day 10, and to a lesser extent at day 14 (Figure 2.6D) in these sections, indicating that MMP-10 is protective against fibroblast activation in this model.

2.3. Discussion:

While MMPs have long been assumed to function primarily in the turnover of ECM, extensive research now indicates that MMPs are a vital component of the innate response to tissue injury. In the present study, we found that *Mmp10* mRNA was rapidly up-regulated in BLM exposure, and that expression was associated with an early attenuation of weight loss and inflammation that culminated in reduced mortality. Notably, while higher doses of BLM did induce an increase in BAL IgM in *Mmp10*$^{-/-}$ animals, we did not observe a difference at 1.2 U/kg, suggesting that the observed weight loss and inflammation disparities are to some extent independent of the degree of tissue damage.

The finding that *Mmp10* is protective against inflammation post-BLM exposure is consistent with findings from other laboratories. For example, Koller et al. demonstrated that lack of MMP-10 exacerbates experimentally induced colitis with *Mmp10* deficient animals expressing significantly more IL1α and TNFα in colonic lavage samples post-dextran sulfate sodium (DSS) injury [50]. Similarly, using partial hepatectomy (PH) and bile duct ligation (BDL) Garcia-Irigoyen et al. found that *Mmp10* ablation was associated with increased liver injury, impaired resolution of necrotic areas, and ultimately, increased fibrogenesis [49]. Importantly, both groups also reported an increase in CCL2 in *Mmp10* deficient mice.

Given that cellular recruitment is well known to result from and even contribute to tissue damage, we measured BAL cellularity in both BAL and tissue sections from these animals. We found that despite the lack of a difference in epithelial barrier damage between the genotypes at any day, *Mmp10*$^{-/-}$ mice had

significantly elevated total BAL cells at days 10 and 14 (~3 and 2 fold, respectively); however, differential counts revealed that while neutrophils and lymphocytes were elevated compared to WT controls (with lymphocytes reaching significance), macrophages made up the majority of the difference. Furthermore, by assaying levels of the major murine chemokine CCL2, as well as the ability of BAL from either genotype to recruit cells, we determined that the observed difference in F4/80 positive macrophages is due to their selective recruitment in the lung.

Our observation that CCL2 is up-regulated in *Mmp10*$^{-/-}$ lungs is interesting as ablation of CCL2, as well as its receptor, CCR2, has been shown to be protective against BLM-induced fibrosis through attenuated macrophage recruitment [76, 77, 78], and BAL samples from IPF patients contain significantly more CCL2 than those of normal volunteers [76]. Pulmonary macrophages play important, diverse roles in the injured lung, including clearance of damaged tissue, pathogen killing, antigen presentation, and the production of secreted factors that support inflammation and wound repair [56]. Somewhat unsurprisingly, studies show that macrophages are capable of influencing fibrogenesis at all phases of development through mechanisms that exaggerate both tissue damage [75] and repair [126,73,127].

In agreement with this idea, we found that the fibrotic response to BLM was significantly greater in the absence of *Mmp10*. Analysis of *Col1a1* mRNA, trichrome staining, and the modified amino acid hydroxyproline in whole lung indicate that collagen synthesis is significantly sustained in *Mmp10*$^{-/-}$ mice. In

addition, αSMA staining via IHC indicated that myofibroblast proliferation was enhanced relative to WT controls at day 10 and to a lesser extent at day 14 post-BLM.

In conclusion, the data presented here indicate that pulmonary MMP-10 is an important mediator of lung injury and fibrosis following BLM exposure. In the short-term, MMP-10 helps to suppress the damage response by limiting the production of various proinflammatory cytokines, as well as the recruitment of macrophages into the lung, contributing to attenuated weight loss and mortality. MMP-10 then goes on to modulate the fibrogenic response in the long-term by restraining fibroblast activation and collagen synthesis. Future studies will focus on the role of CCL2-induced macrophage recruitment in orchestrating these differences.

2.4 Figures/ Tables:

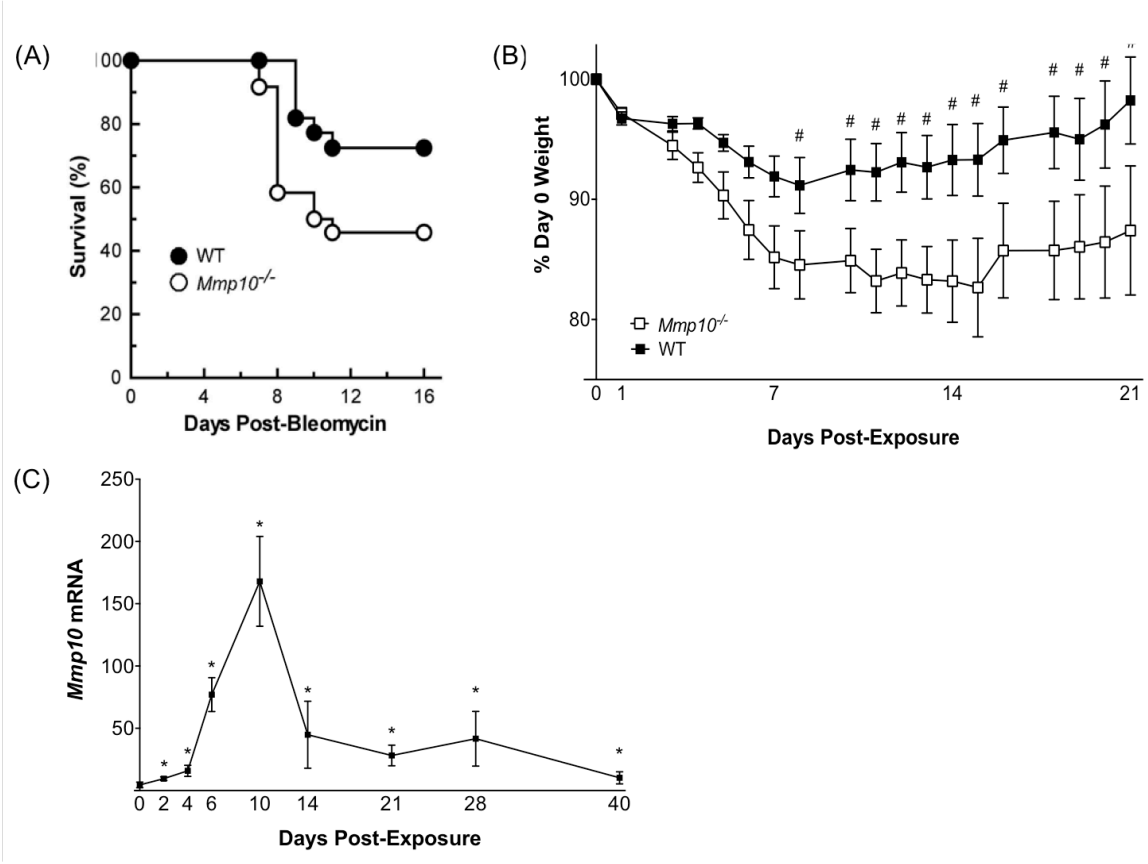

2.1. ***Mmp10 expression in lung is associated with reduced mortality and weight loss post-exposure to BLM. (A)*** *WT or Mmp10$^{-/-}$ animals were administered 0.08 U of bleomycin (~3.6U/kg) by intratracheal intubation and percent survival was recorded.* ***(B)*** *Mice (n=8) were intubated with 1.2U/kg of bleomycin and weight loss was expressed as a percentage of day 0 weight.* ***(C)*** *RNA was collected from homogenized left lungs of WT mice at 0, 4, 10, 14, 21, 28 and 40 days post-intubation of 1.2U/Kg of bleomycin (n = 4 to 6) and assayed for Mmp10 expression. * significant vs. untreated WT control (P<0.05)*

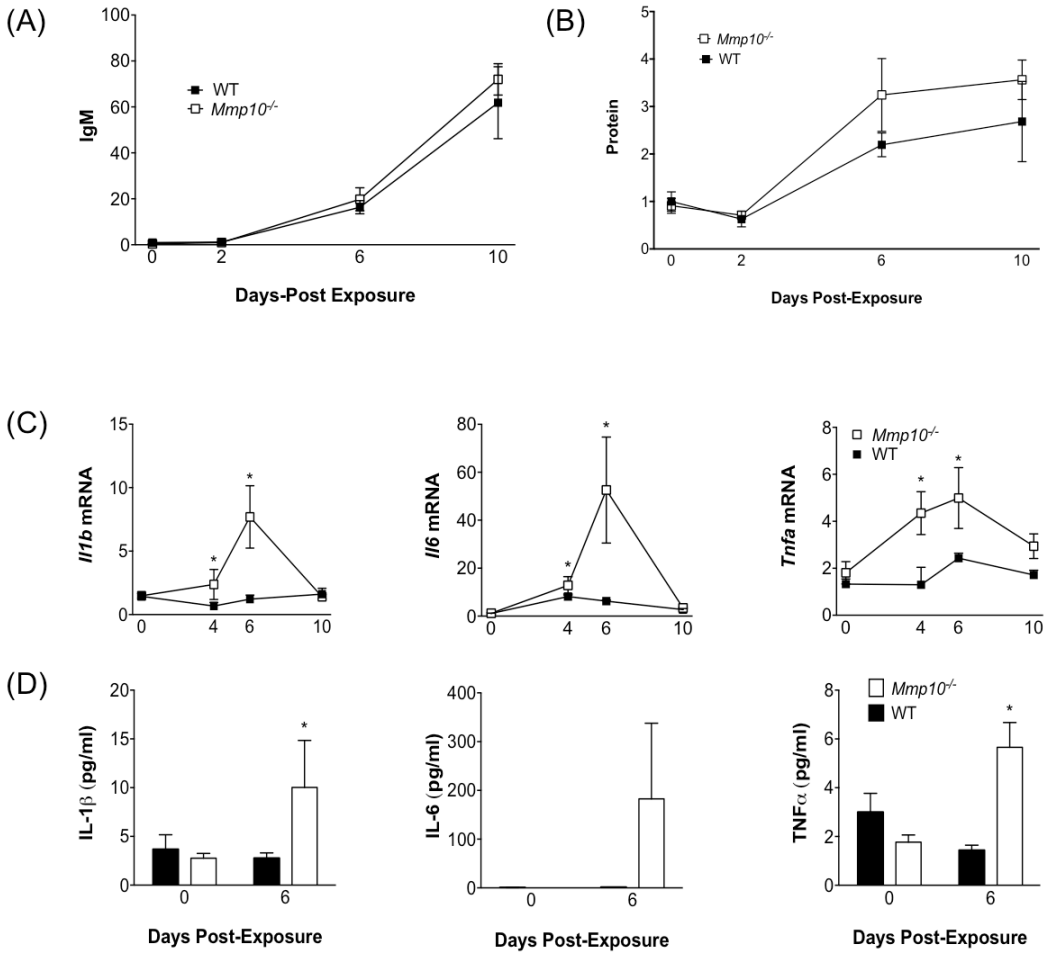

2.2. Inflammation, but not damage is enhanced in *Mmp10*$^{-/-}$ mice. Lungs and BAL (n = 4 to 6) were collected from animals at various days post-exposure. BAL IgM content **(A)** and total protein values **(B)** were determined via ELISA and BCA assay. **(C)** mRNA in whole lung was probed for *Il6*, *Il1b* and *Tnfa* transcripts as markers of inflammation, and **(D)** ELISA for each of these proteins was performed**.** Values shown are expressed relative to untreated WT control. $^{\#}$ significant vs. corresponding WT value. *(P<0.05)*

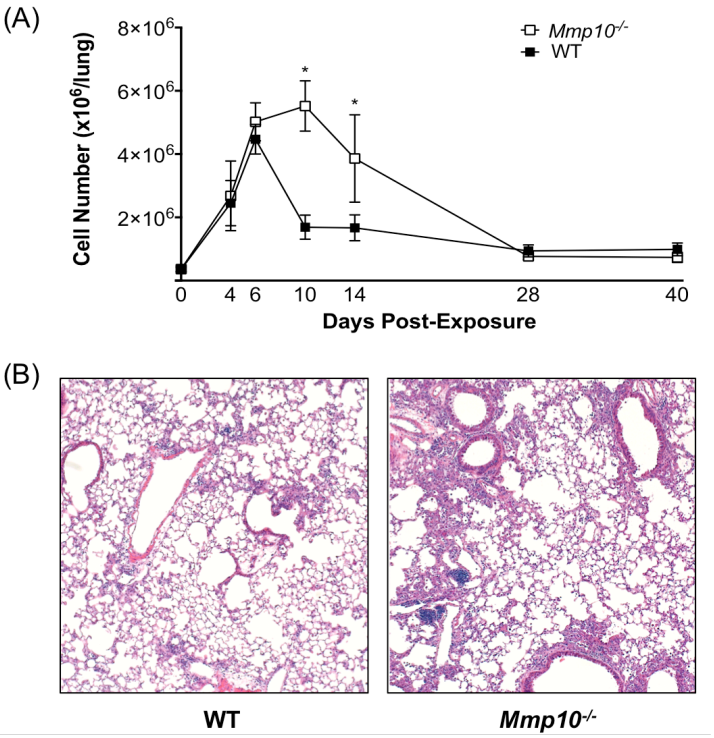

2.3. MMP10 attenuates peak immune cell infiltration post-bleomycin exposure. (A) BAL cellularity was measured via cell counter at various days following 1.2 U/kg BLM exposure (n = 4 to 6) **(B)** Representative H&E sections demonstrating increased cellularity at day 10 post-BLM (5x magnification). Values shown are expressed relative to untreated WT control. # significant vs. corresponding WT value. # significant vs. corresponding WT value. *(P<0.05)*

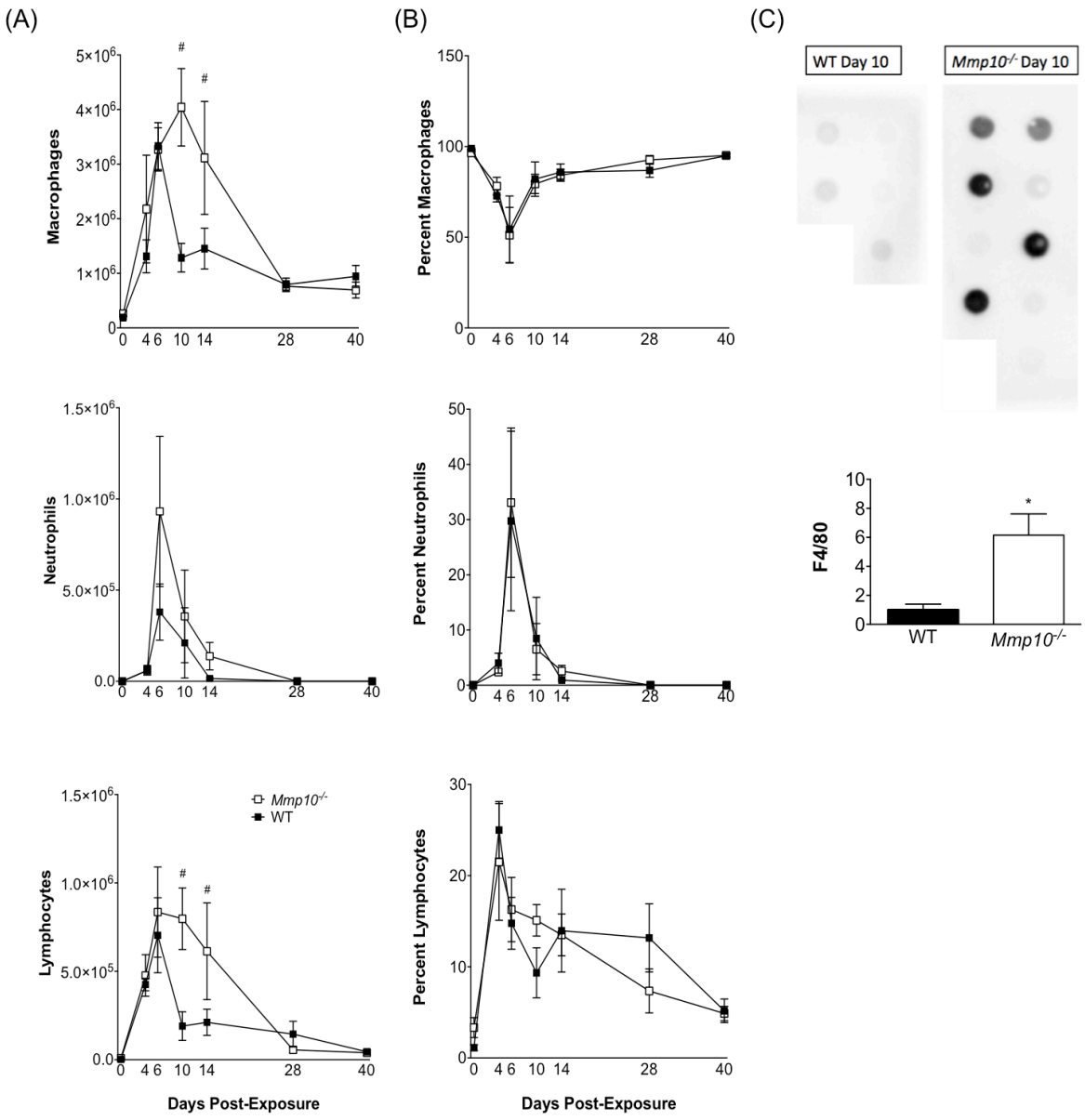

2.4. *Mmp10*$^{-/-}$ lungs contain increased macrophage and lymphocyte cells at 10 and 14 days post-bleomycin. BAL Cytospins were prepared from WT and *Mmp10*$^{-/-}$ animals at various day post-exposure to 1.2 U/kg BLM. Light microscopy was used to determine the number **(A)**, and percentage **(B)** of macrophages, neutrophils, and lymphocytes in each sample (n = 4 to 6). **(C)** An F4/80 dot blot for macrophages was performed on day 10 cellular BAL lysates to confirm the results of the differential counts. # significant vs. corresponding WT value. *(P<0.05)*

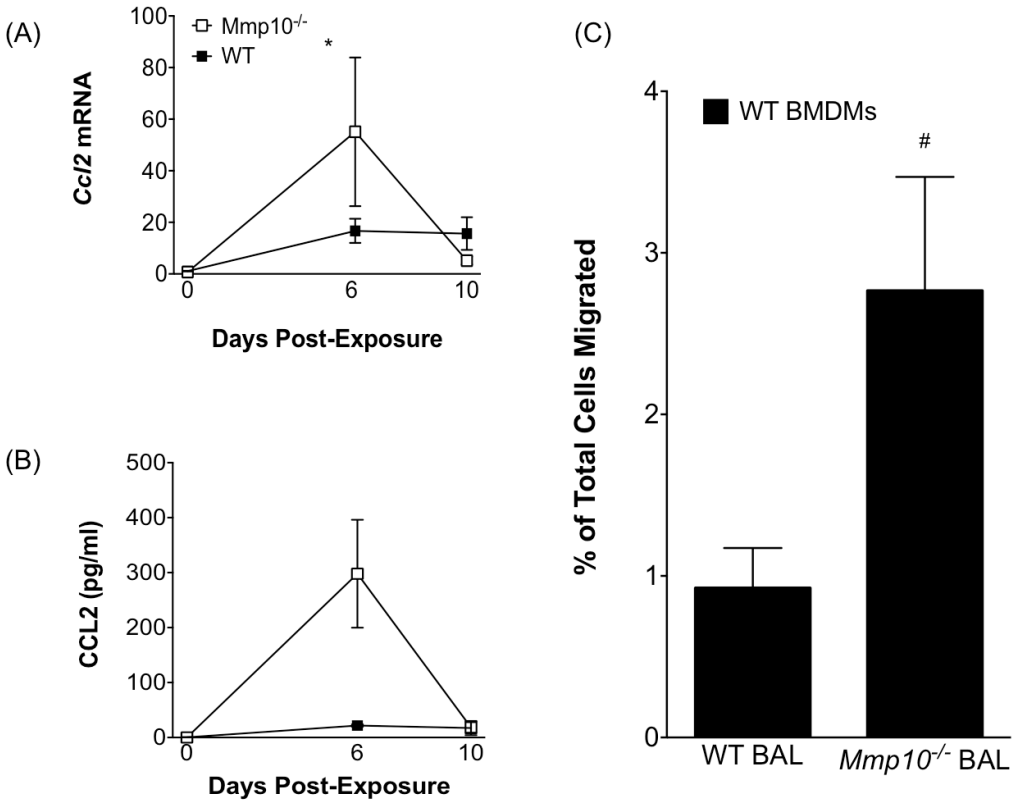

2.5. MMP10 regulates macrophage recruitment into the lung post-bleomycin. (A) RNA was extracted from 1.2 U/kg treated lungs and transcript levels of the major monocyte attractant, *Ccl2*, were quantified at days 4, 6 and 10. **(B**) CCL2 protein was also quantified in lung BAL via ELISA. **(C)** WT BMDMS were allowed to migrate for 3 hours toward day 6 BAL from either WT or *Mmp10*$^{-/-}$ animals and percentage of migrating cells was plotted. N = 3 to 6 for all groups. Values shown are expressed relative to untreated WT control. $^{\#}$ significant vs. corresponding WT value. *(P<0.05)*

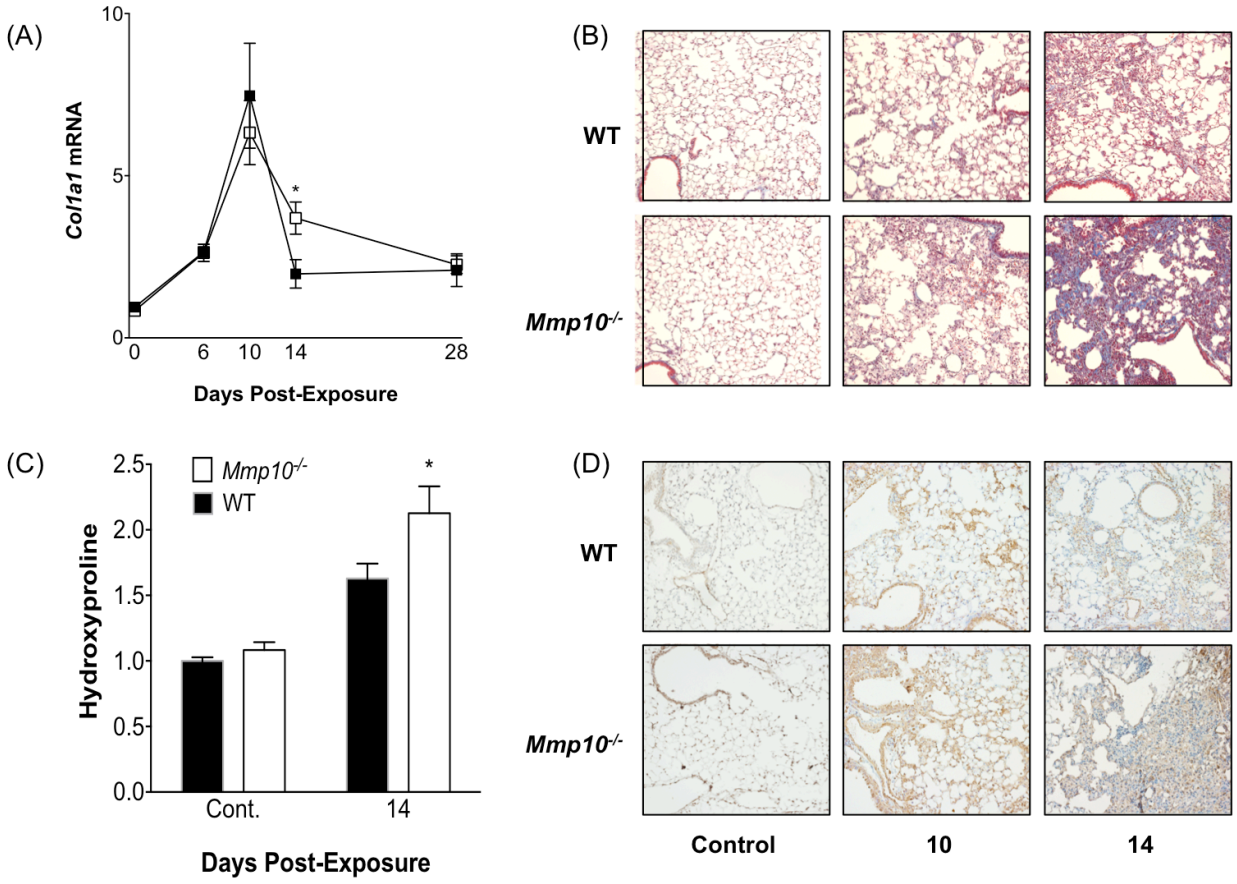

2.6. The fibrogenic response to bleomycin is exacerbated in *Mmp10*$^{-/-}$ lungs. **(A)** *Col1a1* transcript levels were assayed in whole lung homogenates of WT and *Mmp10*$^{-/-}$ animals (n = 4 to 6) post-bleomycin exposure (2.0 U/kg). **(B)** Representative images of Masson's trichrome stained sections at 10 and 14 days post exposure (10X). **(C)** Hydroxyproline content in the l. lung of bleomycin treated animals. **(D)** Representative images of αSMA IHC slides (10x). Values shown are expressed relative to untreated WT control. # significant vs. corresponding WT value. *(P<0.05)*

CHAPTER 3

Stromelysin-2 (MMP-10) Facilitates Clearance and Moderates Inflammation and Cell Death Following Lung Exposure to Long Multi-walled Carbon Nanotubes (L-MWCNT

3.1 Introduction:

Engineered carbon nanotubes (CNT) are a class of graphene cylinders of one or more layers with at least one external dimension between 1-100 nm [128]. These characteristics impart unique electrical, mechanical, and thermal properties that make CNT exceedingly valuable for a range of biomedical and commercial applications, including solar cells, adhesives, polymer composites, lithium-ion batteries, drug delivery, and medical diagnostics [96]. As a result, CNT production has increased about 10-fold since 2006 [129] to a global output of more than 2,000 tons in 2013 [130].

Concomitant with the increased production of CNT has been a growing urgency to understand the risks posed by occupational exposure to CNT [96]. Of the two major subtypes of CNT (i.e., single-walled and multi-walled), multi-walled CNT (MWCNT) represent over 99% of the global production volume [131]. In addition to the marked production disparity between CNT subtypes, evidence suggests that the toxicity of MWCNT is greater than that of single-walled CNT [132]. However, other factors also augment CNT toxicity, including the presence of residual catalyst contamination from synthesis (e.g., Ni, Fe, others) [133], surface modifications [108,134,135], and length [104]. Among these other factors, length is particularly important as longer tubes have been suggested to contribute to inflammation and fibrosis in a manner similar to asbestos fibers [136,103-107]. Thus,

understanding which cells respond to MWCNT exposure, and how, is important for assessing the potential occupational risks associated with these materials.

Matrix metalloproteinases (MMPs) comprise a family of 27 distinct, structurally-related, extracellular endopeptidases. Since the first MMP was isolated from regressing tadpole tails, they have often been assumed to function in the breakdown of extracellular matrix (ECM) [3]. However, while some MMPs do serve defined or limited roles in ECM turnover, this is far from the predominant function of these enzymes. For example, *in vivo* findings with genetically-engineered mice have shown that MMPs are critical regulators of innate immunity by controlling leukocyte influx and activation, restoration of tissue barriers, and cleavage of latent cytokines, chemokines, and antimicrobial agents, among many other processes [12,13]. Like most MMPs, *Mmp10* is not expressed in unchallenged tissues. However, in response to a variety of insults, including injury and infection, it is induced by macrophages and epithelial cells in many organs, including the lung [27,47,48,113].

Here, we report a protective role for macrophage MMP-10 in the pulmonary response to MWCNT. We found that *Mmp10* was rapidly induced in whole lung following administration of MWCNTs into the lung, and that expression was associated with both pulmonary clearance of nanoparticles, and mononuclear cell survival. Using bone marrow-derived macrophages (BMDMs), we demonstrate that macrophages respond to MWCNT exposure in culture by initiating pro-inflammatory and apoptotic responses that were moderated by MMP-10.

3.2. Results: *See Chapter 6 for detailed methods.*

MWCNT Induce Expression of MMP-10

To elucidate the impact of MMP-10 on the pulmonary response to MWCNT, wildtype and *Mmp10*$^{-/-}$ mice on a C57BL/6 genetic background were treated with 80 μg L-MWCNT by OPA, or with an equivalent volume of dispersion medium (DM) (Table 3.1). Lungs were collected 24 hours later and processed for mRNA analysis. In lungs from unchallenged wildtype mice (i.e., no MWCNT, no DM alone), we detected a Ct range for *Mmp10* mRNA of between 36-37 (data not shown) indicating essentially no or very low levels of expression, consistent with earlier observations [48]. Expression of *Mmp10* was modestly induced by administration of DM indicating that the treatment procedure caused a mild lung injury (which is quite common among treatment methods that involve direct instillation into the lung). However, when exposed to MWCNT, expression of *Mmp10* mRNA was stimulated >3-fold above DM-control levels (Figure 3.1A). As expected, *Mmp10* mRNA was not detected in *Mmp10*$^{-/-}$ samples (data not shown).

Impact on Inflammatory Cells

Total cells in BAL did not differ between unchallenged wildtype and *Mmp10*$^{-/-}$ mice (Figure 3.1B) and the bulk of these (>90%) were macrophages (Figure 3.1C). In response to DM, total cells in BAL did increase modestly but still did not differ significantly between genotypes. However, when treated with MWCNT, the total cell count was reduced relative to the controls, and was

significantly lower in *Mmp10*$^{-/-}$ samples (Figure 3.1B). Differential cell counts revealed no significant differences in the percent or total numbers of lymphocytes between genotypes and treatments. In contrast, we found reduced percent and numbers of macrophages and a higher percent of neutrophils in MWCNT-treated *Mmp10*$^{-/-}$ samples compared to wildtype BALs (Figure 3.1C,D). However, though elevated by MWCNT, the total numbers of neutrophils did not differ significantly between wildtype and *Mmp10*$^{-/-}$ mice (Figure 3.1C). Similarly, we assayed whole lung expression levels of *Cxcl1* (Figure 3.2A), which encodes KC, the murine orthologue of IL-8 and a critical acute phase neutrophil chemokine. Consistent with our neutrophil estimates (Figure 3.1C,D) we found that MWCNT treatment stimulated increased *Cxcl1* expression, and that this increase showed only a mild trend towards being greater in *Mmp10*$^{-/-}$ mice.

We also assessed if reduced chemokine expression contributed to lowered macrophage numbers in *Mmp10*$^{-/-}$ mice. As with *Cxcl1*, *Ccl2* levels increased significantly with MWCNT treatment, but did not differ between the genotypes (Figure 3.2B). These findings suggest that the reduced macrophage numbers in MWCNT-treated *Mmp10*$^{-/-}$ mice are due to a loss of cells rather than impaired recruitment. Overall, these findings indicate that MWCNTs mediate a pro-inflammatory response that is manifested by both an increase in neutrophil numbers as well as a reduction in macrophages. While both of these observations were exaggerated in *Mmp10*$^{-/-}$ mice, only the reduction of macrophages was statistically significant.

MWCNT Induce Production of Pro-inflammatory Factors

Many groups have demonstrated that L-MWCNTs induce a robust pro-inflammatory response following direct instillation into the lung, including increases in the expression of *Il1b Il6, Tnfa* [137], and *Nos2* mRNAs [138]. Therefore, we assessed each of these transcripts in the lungs of our mice (Figure 3.3A). We found that with the exception of *Tnfa,* each of these transcripts showed an increase in MWCNT mice, but that aside from a trend in *Il1b*, none of these values differed between the genotypes.

Given that the most prominent difference in our cell counts was a reduction in macrophage numbers, we hypothesized that total lung transcripts might be masking an underlying pro-inflammatory phenotype in macrophages. Therefore, we used bone marrow-derived macrophages (BMDM) from wildtype and *Mmp10*$^{-/-}$ mice to assess if the *in vivo* responses to MWCNTs could be attributed to macrophages. Mirroring what we observed *in vivo*, treatment of BMDMs for 2 hours with between 10 and 100 μg/ml (a dose range similar to other studies [139,140]) resulted in a statistically significant increase in *Mmp10* mRNA versus DM control (Figure 3.4A). (In all BMDM experiments, we added 10 μg/ml of PmB to control for possible endotoxin contamination.) In addition, we found that MWCNTs stimulated elevated expression of mRNAs for *Il1b*, *Il6*, *Il12a,* and *Tnfa* relative to WT (Figure 3.4B). Release of active IL-1β protein was also found to be induced by MWCNTs, but not by dispersion medium, and was significantly increased in *Mmp10*$^{-/-}$ macrophages (Figure 3.4C).

MMP-10 Facilitates Clearance of MWCNT.

As macrophages are critical for clearing inhaled particles, we assessed if reduced macrophages in *Mmp10*$^{-/-}$ mice impacted retention of MWCNTs. Indeed, in lung homogenates we observed more MWCNTs particles in *Mmp10*$^{-/-}$ lysate pellets compared to wildtype samples (Figure 3.5A), and in lung sections of *Mmp10*$^{-/-}$ mice we observed accumulations of particles in alveolar macrophages (Figure 3.5B). Via both our own internal counts (Figure 3.5A), as well as blinded morphometric analysis (Figure 3.5C,D), we measured significantly more (about 2.5-fold) retained particles (Figure 3.5D) and a greater percent of total tissue occupied by MWCNT (Figure 3.5E) in sections of *Mmp10*$^{-/-}$ lungs compared to wildtype tissues. A large percentage of the particles in these assay appeared to be cell-associated, and no particle signal was visible (Figure 4B) or detected in the DM-control lung (data not shown).

Despite an overall increase in retained particles in whole lung, we did not find a difference in either the percentage of MWCNT-containing macrophages (Figure 3.6B), or average MWCNT-occupied area in endocytic vacuoles between the genotypes (Figure 3.6C). However, we did find a negative relationship in both genotypes between macrophage numbers and the percentage of MWCNT-positive macrophages that was much stronger in the *Mmp10*$^{-/-}$ samples (Figure 3.6D). These data suggest that MMP-10 is involved in mediating both protection against macrophage cell death, as well as particle clearance from the lung post MWCNT exposure.

MMP-10 Protects Against MWCNT-mediated Apoptosis

As the number of resident macrophages did not differ between unchallenged wildtype and *Mmp10*$^{-/-}$ mice (Figure 3.1C,D), we assessed if the reduction of macrophages in *Mmp10*$^{-/-}$ mice was due to MWCNT-induced apoptosis. Caspase-3 activity in lung lysates was not affected by MWCNT and did not differ between genotypes (Figure 3.7A). However, we saw about a 2-fold increase in caspase-3 activity in BAL from MWCNT-treated *Mmp10*$^{-/-}$ mice compared to wildtypes (Figure 3.7B). We assessed if macrophages were responsible for the robust increase in caspase-3 activity detected in cellular *Mmp10*$^{-/-}$ BAL, and in agreement with our *in vivo* findings, we found that while the number of MWCNT-positive macrophages didn't differ between the genotypes (Figure 3.8A), MWCNTs mediated a significantly greater increase of caspase-3 activity in *Mmp10*$^{-/-}$ BMDM (Figure 3.8B). These data suggest that MMP-10 protects macrophages from MWCNT-induced apoptosis.

3.3 Discussion:

Despite their growing usage, much uncertainty still exists regarding the risk associated with respiratory CNT exposure. This is particularly true of occupational exposures during transfer, weighing, and blending [96], but the stability of these particles suggests that environmental CNT exposures will also become more important as the CNT market continues to transition from R&D to high-volume production [56,102,141,142]. Importantly, while the dosages utilized here are generally greater than what might be expected in an occupational setting [143], they are consistent with other high dose studies meant to uncover the mechanisms that augment MWCNT toxicity.

In keeping with other studies, we found that oropharyngeal aspiration OPA) of 80 μg/mouse of L-MWCNTs initiated an immediate, and robust inflammatory response [140,144, 145, 146]. Compared to DM controls, MWCNT-treated mice exhibited enhanced pulmonary edema, neutrophilia, and macrophage cell death, as well as accumulations of MWCNT in BAL macrophages at 24 hours post-exposure. In addition, mRNA analyses of whole lung revealed an up-regulation of multiple pro-inflammatory transcripts including *Il6*, *iNOS*, and notably, *Il1b*, which is known to be important in the initiation of fibrosis [107]. Interestingly, *Mmp10* was also found to be present in this milieu.

Further analysis, including BAL cell counts and independent analysis by the Cedars-Sinai BTRC revealed that *in vivo Mmp10* ablation was associated with enhanced mononuclear cell death and a 2 to 3-fold impairment in pulmonary clearance. Given the known role of endocytosis in mediating pulmonary clearance from the distal lung [147], we investigated whether a disparity in phagocytic potential between the genotypes could explain the difference in clearance. However, both *in vivo* and *in vitro* analysis with BMDMs indicated that no such difference exists. In addition, though we observed a trending increase in neutrophil recruitment into the lung, we did not observe the presence of these particles in PMN. This finding is relevant as MPO has been posited to mediate CNT breakdown [148].

One possible explanation for these results is that the difference in clearance is mediated not by enhanced endocytosis, but by an increase in *Mmp10*$^{-/-}$ sensitivity, which leads pulmonary macrophages from these animals to die before they are able to completely eliminate the particle. However, this seems

unlikely given the relatively short period of time and breakdown is thought to be secondary to mucocillary clearance processes during this period [147].

A secondary explanation is that an additional cell type(s), mostly likely the airway epithelium, is responsible for the clearance disparity. Several points of evidence support this conclusion. For instance, while we did observe an overall increase in inflammatory transcripts in whole lung with MWCNT treatment, we didn't observe any difference between the genotypes. The minority of macrophages in whole lung is a likely explanation for these results; however, we also found that whole lung *Mmp10* was up-regulated approximately 3.5 fold, and this value is consistent with the observed *in vitro* induction range. This apparent cloaking of inflammatory transcripts, but not *Mmp10* itself suggests another source of *Mmp10*. Additional support for this suggestion can be found in the caspase-3 results obtained with whole lung and cellular BAL indicating enhanced activity in *Mmp10*$^{-/-}$ mice in the later samples only. While studies of MMP-10 are limited, several studies have shown that *Mmp10* mRNA is up-regulated in epithelial cells [149, 116]. In addition, our group has previously published data indicating a protective role for MMP-10 in the epithelial response to *Pseudomonas aeruginosa*, a common nosocomial bacterium, as well as in epidermal wound repair. Interestingly, the later work describes a system whereby MMP-10 derived from alternatively activated (M2) macrophages was responsible for mediating the observed protective effects [47,48]. Further studies will be necessary to determine the contribution of MMP-10 in the epithelium with MWCNT exposure.

One of the more striking findings of this study is the clear role that macrophage MMP-10 plays in the response to MWCNTs. The *in vivo* data indicate that *Mmp10*$^{-/-}$ macrophages are more sensitive to MWCNT-induced cell death, and that this sensitivity is associated with exposure, but not enhanced

uptake. In other words, while the number of positive macrophages in BAL was not different between the genotypes, macrophage loss was more clearly associated with the number of MWCNT-positive cells in *Mmp10*$^{-/-}$ animals than WTs.

This finding was confirmed *in vitro* through the use of BMDMs, which showed that *Mmp10*$^{-/-}$ macrophages express significantly higher levels of *Il6* and *Il1b* transcripts, as well as IL-1β protein, and that this expression is associated with a dose-dependent death of these cells in culture. The conclusion that macrophages are a target of MWCNTs is consistent with other high dose exposure studies [150, 140,] and *in vitro* work with RAW 264.7 macrophages [134]. In addition, while the data presented here represent a very short-term evaluation point, it also raises further questions about the chronic and long-term impact of MWCNT exposure in *Mmp10*$^{-/-}$ mice, especially in the context of the fibrotic response to MWCNT. This response is known to be dependent upon NALP3 inflammasome-mediated activation of IL-1β [107], and while determining the nature of the inflammatory phenotype was beyond the range of this initial study, we did find that total IL-1β protein was enhanced in *Mmp10*$^{-/-}$ animals.

The data provided here indicate, for the first time, a protective role for MMP-10 in the pulmonary response to L-MWCNT. While further studies will be necessary to define the role of epithelial MMP-10, as well as clarify the mechanism underlying this response, our data indicate that macrophage MMP-10 plays an important role in orchestrating the response to MWCNT-induced lung injury.

3.4 Figures/ Tables:

MWCNT type:	OD[a]	Length[a]	Elemental Analysis[b] C	O	Ni	Fe
Stock	10 - 20 nm	10 - 30 mm	95.8 ± 0.6	3.4 ± 0.2	0.5 ± 0.5	0.3 ± 0.3

Table 3.1. Physiochemical properties of L-MWCNTs. [a] MWCNT OD and length are provided by the manufacturer, Cheap Tubes. OD = outer Diameter, [b] Catalyst residues were determined using SEM EDS by the National Cancer Institute's Nanotechnology Characterization Laboratory. Values indicate standard deviation.

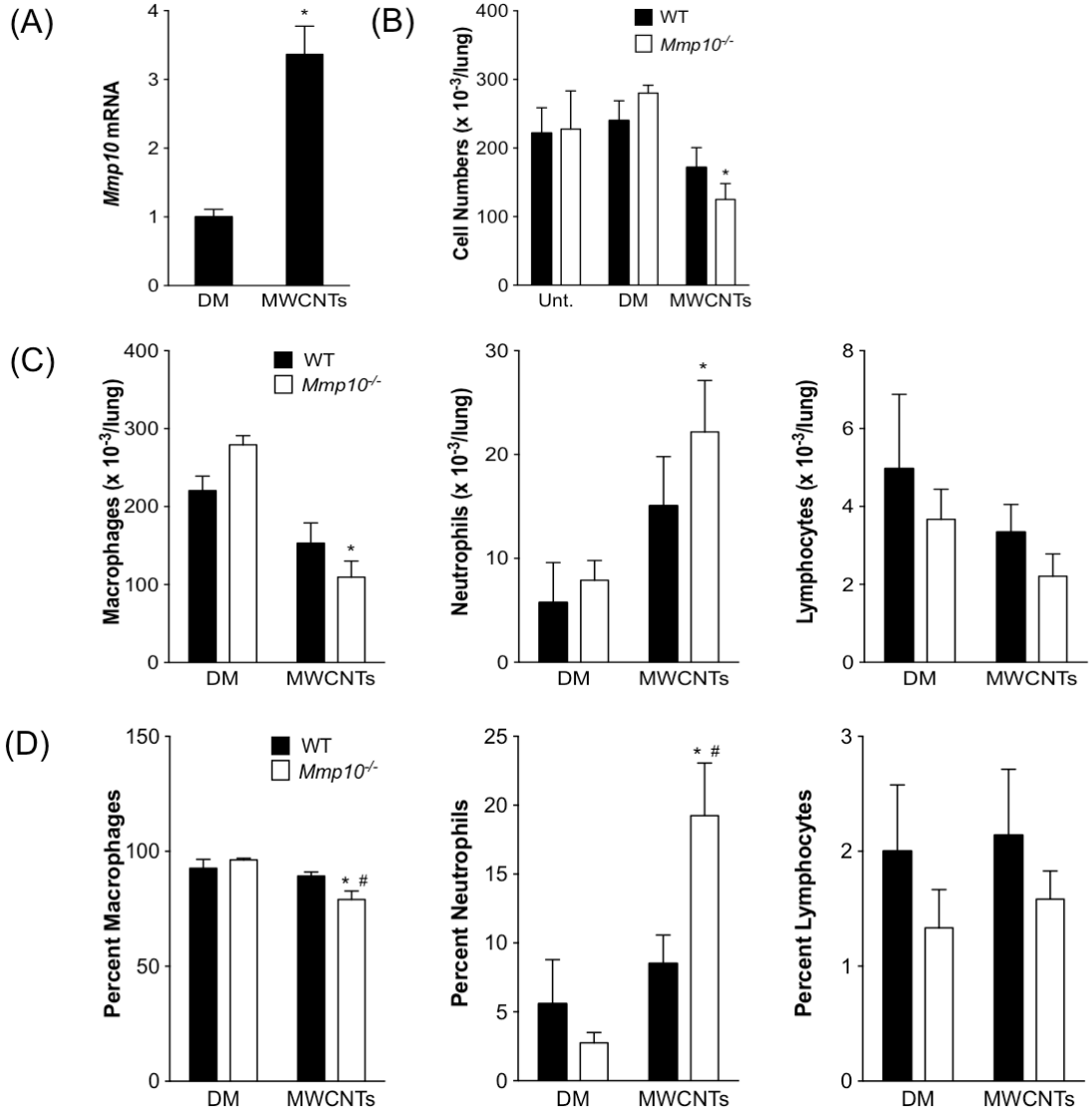

Figure 3.1. MMP10 protects against MWCNT-associated losses of BAL macrophages. WT and *Mmp10*$^{-/-}$ animals (n=6) were administered 80 μg/ml of L-MWCNTs, or an equivalent volume of DM alone (n=3), by OPA and lungs were harvested 24 hours later. (A) qPCR for *Mmp10* was performed on total RNA collected from WT l. lung homogenates. HPRT was used for an internal control and data is presented as fold change from DM mean. BAL was collected, and total cells were quantified by cell counter. (B) Cytospins were then prepared and stained with DiffQuick and (C) total and (D) percentages of macrophages, neutrophils, and lymphocytes were determined via light microscopy. * significant change relative to DM control. # change relative to WT MWCNT. *(P<0.05)*

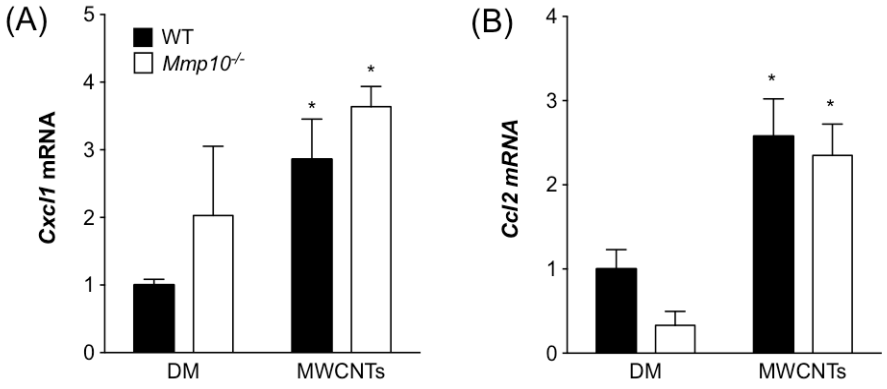

Figure 3.2: Macrophage and neutrophil recruitment is MWCNT, but not genotype dependent. Total RNA was collected from I. lung homogenates and *Cxcl1* (A) and *Ccl2* (B) transcripts were then quantified. HPRT was used as an internal control and values are expressed as a fold change from WT DM estimates. * indicates significant change relative to DM control. # significant change relative to WT MWCNT. *(P<0.05)*

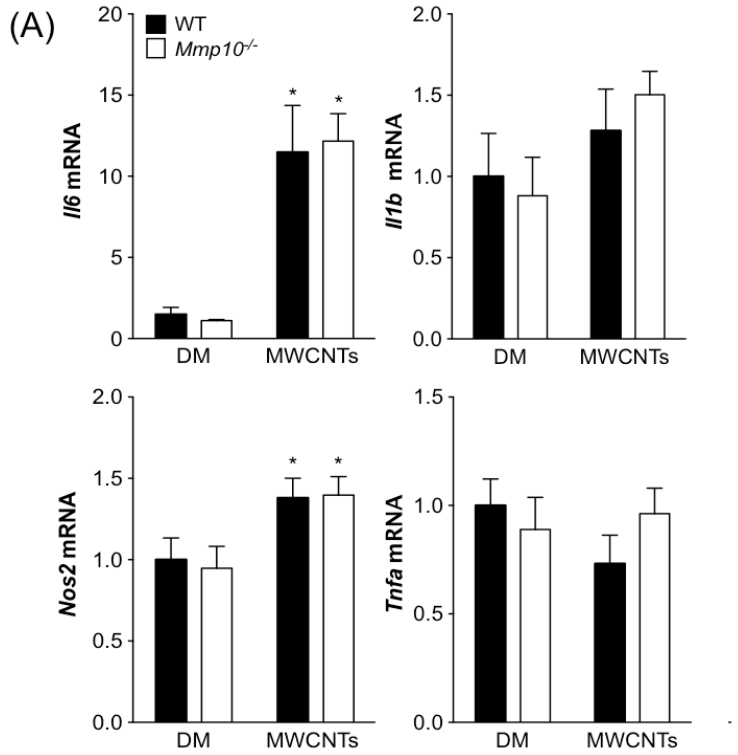

Figure 3.3. MWCNTs induce a robust inflammatory response in lungs treated with MWCNT. (**A)** *Il6, Il1b, Nos2, and Tnfa* transcripts were measured in total RNA collected from the lungs of WT and *Mmp10*$^{-/-}$ mice treated with MWCNTs or DM. Data are expressed as fold change from WT DM. * significant relative to WT DM alone. *(P<0.05)*

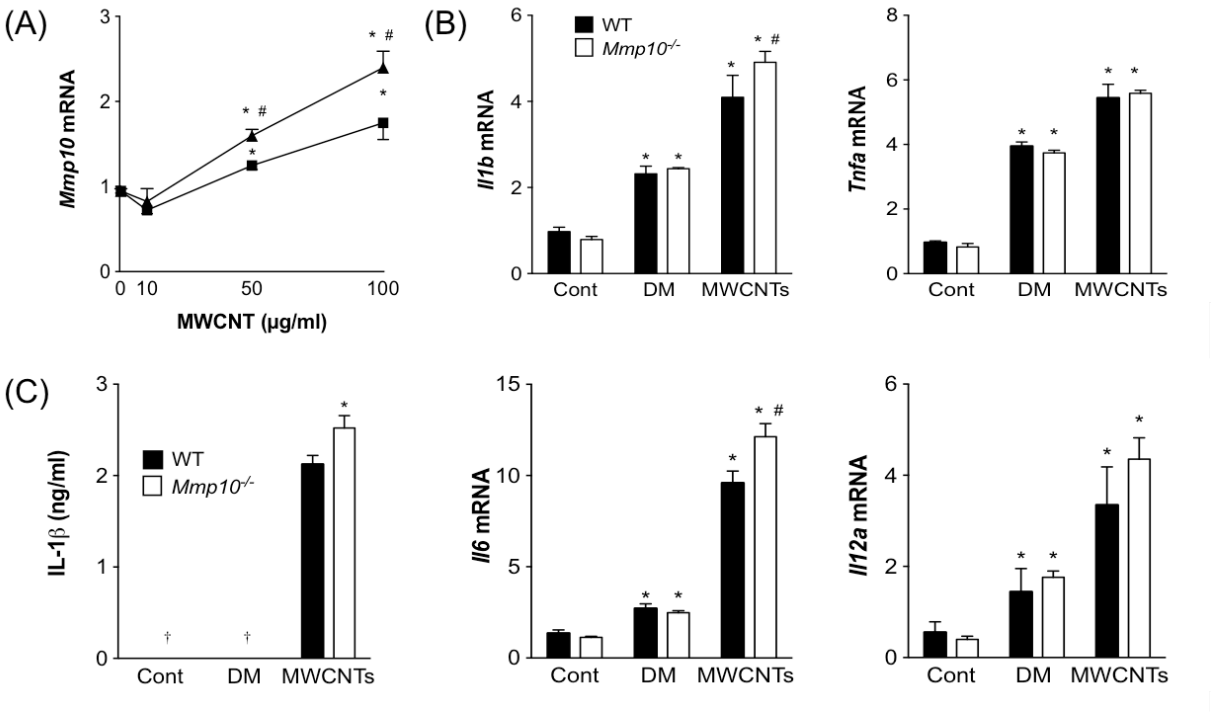

Figure 3.4: MMP10 attenuates the pro-inflammatory response to MWCNT in BMDMs. (A) Sub-confluent BMDMs (n=3) were treated with 10, 50, or 100 μg/ml of MWCNTs, or an equivalent volume of DM, for 2 hours prior to collection and *Mmp10* expression was assayed via qPCR. (B) WT and *Mmp10* deficient BMDMs were treated for 2 hours with 100 μg/ml of MWCNT or DM, and *Il1b, Tnfa, Il6, and Il12a* transcripts were assayed to determine inflammatory status. (C) Total Il-1β estimates were quantified by ELISA in pooled samples (n=3) and expressed as ng/ml. Error is expressed as standard deviation. † samples below the detection limit. * significance vs WT DM, # significance vs. WT MWCNT. All transcripts were quantified using HPRT as an internal control and values were expressed relative to untreated control. *(P<0.05)*

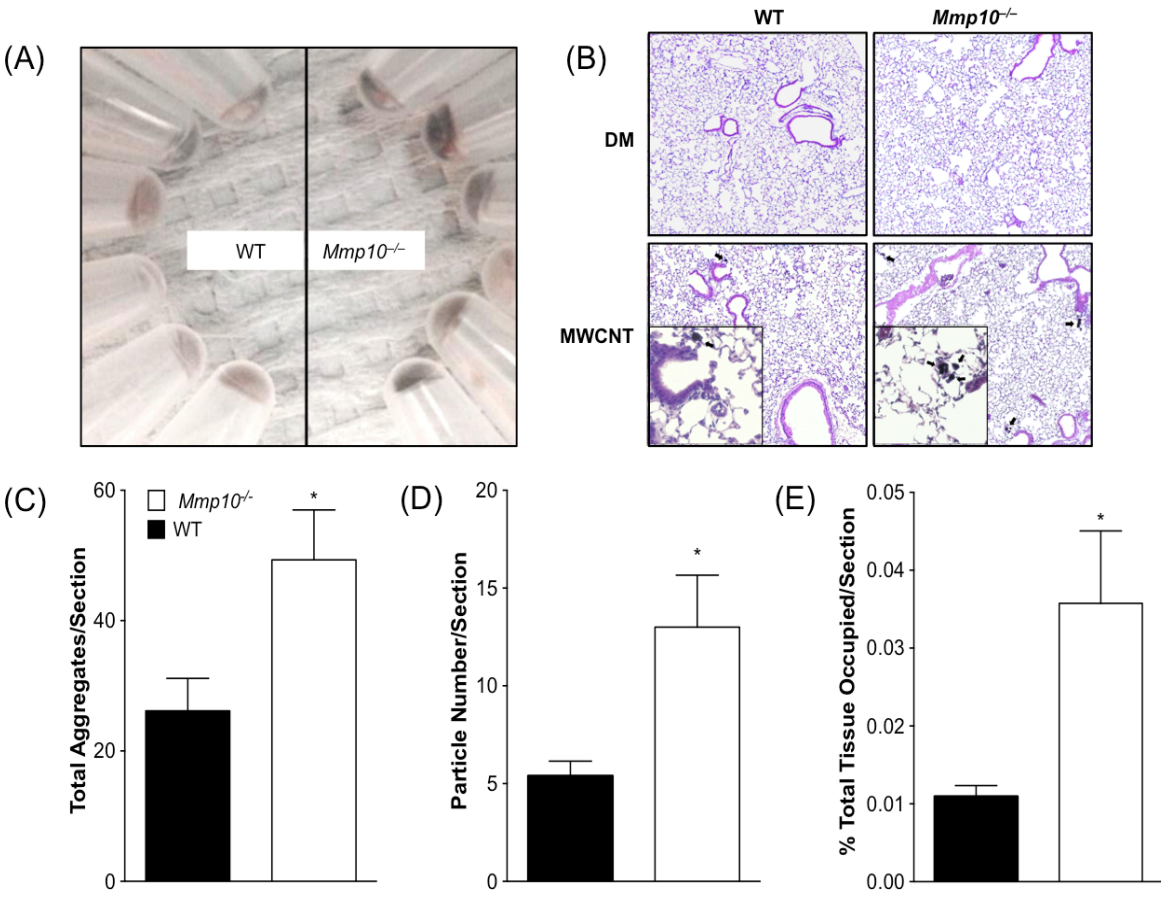

Figure 3.5. *Mmp10* deficient mice exhibit reduced clearance following exposure to MWCNTs. (A) Lysate pellets from WT and *Mmp10*$^{-/-}$ lung preparations. Samples are shown post-homogenization in RIPA buffer and centrifugation at 18,000 rcf for 10 minutes. **(B)** Right lung lobes from treated mice were formalin-fixed, embedded, sectioned, and stained with H&E. Arrows indicate the presence of MWCNT in lung sections visible at 5x and 20x magnification. **(C)** Total aggregates/right lung slide (n=6) were counted by our laboratory via light microscopy and means were plotted. Slides, each containing four r. lobe sections, were independently scanned by the CS-BTRC and total aggregates **(D)** and percentage of occupied area **(E)** were blindly quantified. * significant change relative to WT MWCNT. *(P<0.05)*

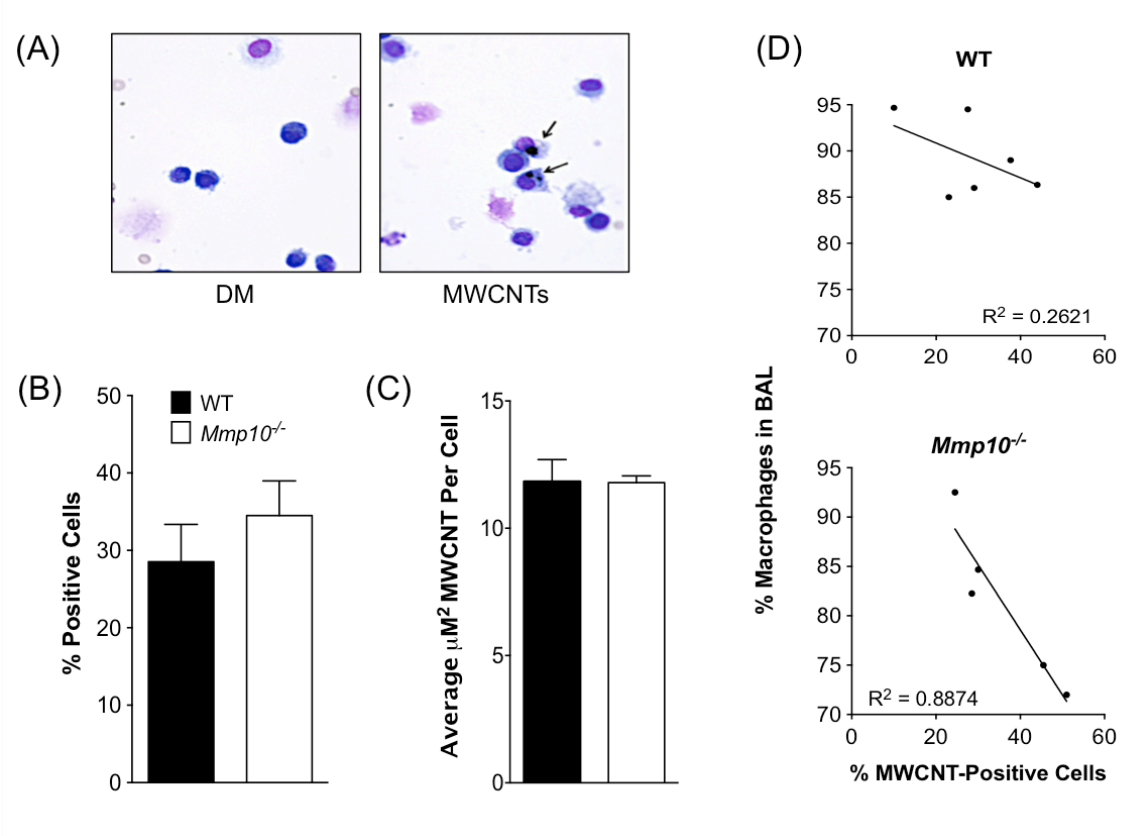

Figure 3.6. MWCNT sensitivity in *Mmp10*$^{-/-}$ animals is mediated by contact, but not enhanced endocytosis. (A) 40x image of BAL cytospins via light microscopy demonstrating the co-localization of MWCNT and macrophages. (B) Percentage estimates of MWCNT-positive cells were obtained from averages of four counts of 100 cells/ slide. (C) The average area occupied by MWCNT-positive vacuoles per cell was quantified from 30 measurements per animal utilizing Digital Image Hub software version 4.0.4. (D) Linear regression demonstrating the relationship between percentage macrophages, and MWCNT-positive cells in WT and *Mmp10*$^{-/-}$ mice. *(P<0.05)*

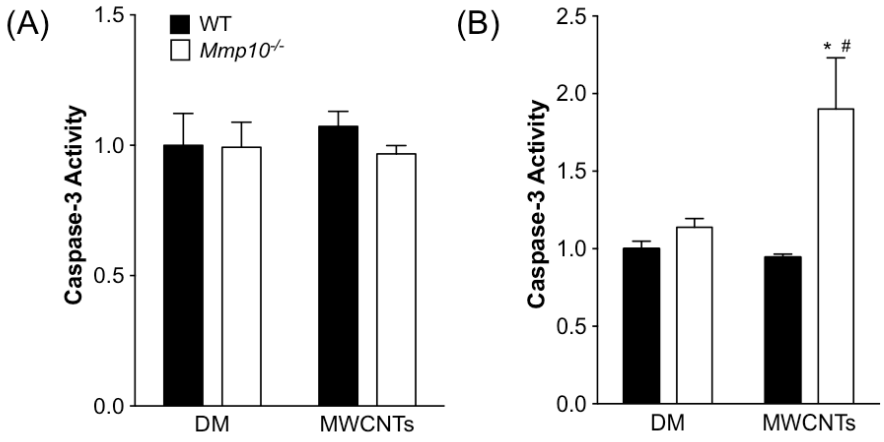

Figure 3.7. MWCNT are associated with enhanced cell death in *Mmp10*$^{-/-}$ BAL pellets, but not whole lung lysates. Caspase-3 activity was quantified in lysate sourced from either l. lung (A), or the cellular fraction of BAL at 24 h post-exposure (B). Values are expressed relative to WT DM. * significance vs. WT DM, $^{\#}$ significance vs. WT MWCNT. *(P<0.05)*

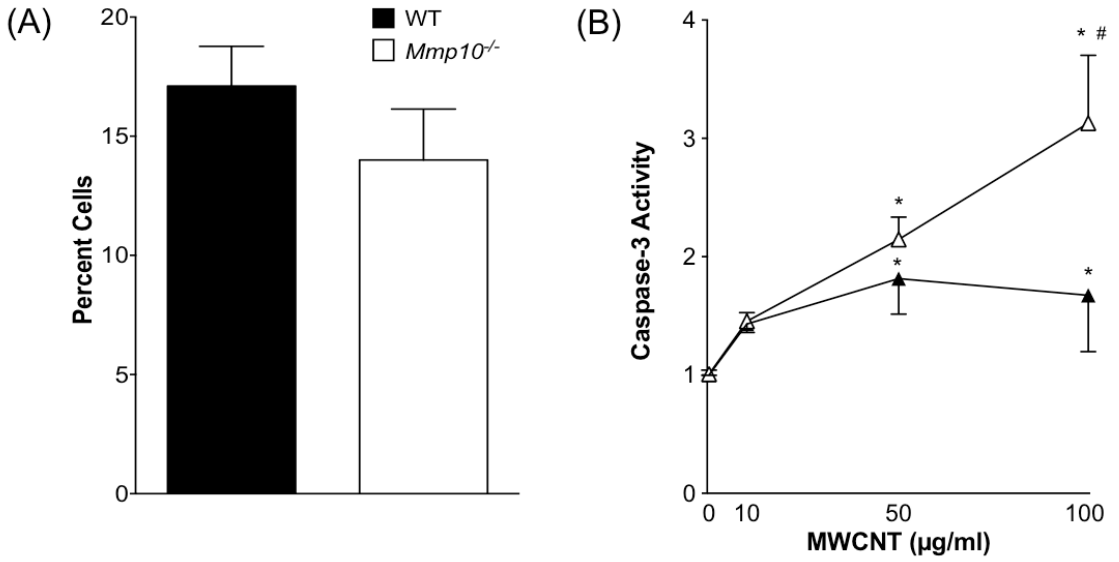

Figure 3.8. *Mmp10* ablation confers sensitivity to apoptosis in BMDMs without an increase in endocytosis. (A) WT and *Mmp10*$^{-/-}$ BMDMs (n=3) were treated with 10 µg/ml of MWNCTs for 3 hours and percentage estimates of MWCNT-positive cells were obtained from averages of four counts of 100 cells/well. (B) Caspase-3 activity was determined in WT and *Mmp10*$^{-/-}$ BMDMs following 24 hour treatment with 10, 50, and 100 mg/ml of MWCNT, or DM, and expressed as fold change relative to untreated control. * significant change from WT DM, # significant change from WT MWCNT. *(P<0.05)*

CHAPTER 4

Induction of Stromelysin-2 (MMP-10) in Macrophages Is Meditated via Diverse Signaling Pathways That Converge on NFκB

4.1 Introduction:

Macrophage responses are important for a wide range of tissue processes, including clearance of approximately $2x10^{11}$ erythrocytes each day, wound repair, and amplifying and carrying out complex activities that are essential for both host defense and immune suppression [56]. These responses are highly plastic and tissue specific, involving the rapid and precise development of distinct transcriptional responses to stimuli [57] [58] [59]. Given their versatility, it is not surprising that macrophages are present in all tissues. However, growing evidence has also demonstrated that these functions are often altered in the context of disease, necessitating further study of the mechanisms underlying these responses [151,152].

Matrix metalloproteinases are a family of 27 structurally related, extracellular endopeptidases that are largely unexpressed in unchallenged adult tissues. Nevertheless, most MMPs are induced in response to injury or infection where they serve diverse roles in growth, wound repair, immunity (leukocyte influx and activation, and cleavage of latent cytokines, chemokines, and antimicrobial agents), and more [12,13]. Unsurprisingly, regulation of these proteases is tightly controlled. This occurs to some extent through post-transcriptional mechanisms (e.g. zymogen activation, compartmentalization, inactivation via tissue inhibitors, and substrate availability), but regulation is

largely imposed at the transcriptional level through a diversity of promoter *cis*-elements (e.g. AP-1, PEA3, Sp-1, NF-kB, etc.) [15 16].

Despite having been cloned almost 20 years ago, *Mmp10* (stromelysin-2) has received substantially less attention than other MMPs, especially MMP-7, 9, and 2 [22]. Nevertheless, a growing body of research has shown an association between *Mmp10* and disease, including IPF, lung tumorigenesis and metastasis, and atherosclerosis [23-28]. *In vitro* studies have demonstrated that *Mmp10* is up-regulated by disparate stimuli (LPS, RSV, thrombin, IL-1, TGF-β1, PMA, C-reactive protein, and more [23,49,53,54,113,115,117]). Furthermore, recent data from our lab has also indicated that long multi-walled carbon nanotubes (MWCNT), a type of engineered nanotube with properties similar to asbestos, also induces *Mmp10* in bone marrow derived macrophages (BMDMs) (see Chapter 3).

These studies have implicated a number of cell surface receptors, signaling pathways, and transcript factors in controlling *Mmp10* transcription. Most notably among these are the major mitogen activate protein kinases (MAPK) (e.g. ERK, JNK, and P38), rapidly induced and highly conserved phosphorylation cascades that control a multitude of cellular events from growth and differentiation to apoptosis and survival [51,52], and transcription factors such as AP-1 and NFkB. These mechanisms have shown themselves to be highly stimulus, and to a lesser extent, cell-type specific. This last point is relevant as very few of these studies have been conducted in macrophages, and *Mmp10* has been shown to produce a distinct phenotype in macrophages [55].

In the present study, we used BMDMs to dissect the basis of *Mmp10* induction with 4 different stimuli: LPS, PMA, BAL lavage from BLM treated animals (BLM BAL), and MWCNT. We found that these stimuli differ in both their potency and temporal pattern of *Mmp10* induction, and that these differences were accompanied by unique signaling mechanisms that converge on largely redundant MAPK cascades, and ultimately, NFkB. Interestingly, we found that while LPS and MWCNT-induced transcription are TLR4-dependent (even though polymyxin B was included in all MWCNT treatments), BLM-BAL stimulated *Mmp10* is independent of TLR4. Our data suggest that dissimilar stimuli induce *Mmp10* in unique ways, and highlight the importance of NFκB in regulating macrophage *Mmp10*.

4.2. Results: *See Chapter 6 for detailed methods.*

Undifferentiated Bone Marrow Cells Up-regulate *Mmp10* During BMDM Derivation

To determine the impact of macrophage differentiation on *Mmp10* levels, BM cells were cultured for 7 days in either recombinant M-CSF or GM-CSF, which stimulate the differentiation of precursor marrow cells into macrophage and dendritic cells, respectively [153]. Lysates from either treatment were collected at 0, 1, 2, 4, and 6 days and probed for *Mmp10* levels. Analysis of these samples indicated a trend toward up-regulation in both cell types (Figure 4.1A). However, beginning at day 1 this difference was significantly greater in M-CSF differentiated cells, which peaked at more than 20-fold as of day 2. In contrast,

GM-CSF cultured cells increased only slightly during this time (~2 fold), and showed little variation over the remaining days. These data suggest that *Mmp10* is primarily induced with commitment to a macrophage lineage.

Given that *Mmp10* is undetectable in alveolar macrophages *in vivo*, we hypothesized that additional culturing might further attenuate *Mmp10* expression in these cells. Accordingly, mature BMDMs were collected at day 7, and cultured at sub-confluence for an additional 40 hours. Samples collected show a slight trend towards up-regulation at 12 hours post-plating, but confirm that *Mmp10* is significantly reduced at 40 and 48 hours (Figure 4.1B). Consequently, an additional 40-hour period of plating was adopted for subsequent studies to allow for attenuation of baseline expression of the gene.

BAL Collected Post-Bleomycin is a Surrogate For *In Vivo* Induction of Mmp10

Data from our lab has demonstrated that *Mmp10* is up-regulated in whole lung post intratracheal intubation (i.t.) of BLM, and that this induction is associated with protection against the onset of inflammation and fibrosis (chapter 2). However, we have also seen that *in vitro* exposure of BMDMs with BLM alone does not stimulate *Mmp10* expression. Given these negative findings, we then sought to determine if factors within BAL collected post-BLM administration could be used as a surrogate for *in vivo* induction.

C57BL/6 mice were treated with 2.0 U/kg of BLM by I.T. and BAL was collected at days 0 (untreated; n=3), 4 (n=4), 10 (n=5) in PBS with 1% BSA. BAL

samples (BLM BAL) from each day were pooled and concentrated 3-fold then added to wells containing slightly sub-confluent naïve BMDMs (n=3). We found that BLM BAL induced *Mmp10* in a concentration-dependent manner (Figure 4.2A), and that the potency of BLM BAL increased with time post BLM (i.e. between 1.2 and 4 fold depending upon day) (Figure 4.3A). In addition, the time-dependent increase in *Mmp10*-stimulatory activity in BLM BAL mirrored up-regulation of *Mmp10* expression seen *in vivo,* which was approximately 150 fold above baseline as of day 10 (Figure 4.3B).

Although day 10 BLM BAL resulted in the greatest *Mmp10* expression, we chose day 4 BLM BAL as a surrogate for exposure in subsequent studies to reduce confounding signals indirectly associated with subsequent, severe disease manifestations. Still, as stated, day 4 BLM BAL stimulated *Mmp10* expression about 3-fold.

To assess if endotoxin in the upper respiratory tract contributed to the inductive potential of BLM BAL, BMDMs were pretreated with 10 μg/ml of polymixin B (PmB), an LPS antagonist, for 30 minutes before the addition of BLM. Treatment with LPS was included as a positive control. PmB treatment completely blocked LPS-mediated induction of both *Mmp10* and *Il6* levels but only reduced BLM BAL stimulation by approximately 50% (Figure 4.3C, D). While these studies can't rule out a contribution of endotoxin to the signal, the reduced efficacy of the PmB, and the collection-day dependent potency of the BAL imply that BLM BAL it is a distinct source of stimulation from LPS.

Mmp10 Stimuli Initiate Transcription Via Distinct Signaling Mechanisms

To compare the temporal pattern of *Mmp10* induction with different stimuli, we treated BMDMs for 1, 2, or 4 hours with LPS, BLM BAL, or two additional stimuli: PMA, an established agonist of MMP10 induction [53], and long multi-walled carbon nanotubes (L-MWCNTs), an engineered nanomaterial that stimulates *Mmp10* expression *in vivo* (Chapter 3). PmB was included in all MWCNT samples to isolate the contribution of the tubes themselves from LPS, which can be present as contamination from synthesis.

We found that *Mmp10* mRNA was rapidly up-regulated with all stimuli at 2 hours of treatment, but that individual agents diverged in the rapidity, magnitude, and persistence of their responses (Figure 4.4A). For example, while LPS and PMA reached similar levels of magnitude, LPS was the first treatment to peak (at 1 hour), whereas PMA was the only treatment continuing to increase as of 3 hours later. Neither BLM BAL nor MWCNTs were as potent as LPS or PMA, but although both seemed to peak at 2 hours, only MWCNTs had begun to attenuate by 4 hours. Based on these data, we choose to implement a 2-hour treatment for all subsequent studies.

As PMA is a well-known activator of protein kinase C (PKC), we decided to use Bisindolymaleimide (BIS), a PKC inhibitor, to determine if any of the other stimuli utilize a similar mechanism. As shown in (Figure 4.5A), pretreatment with 360 nM of BIS significantly inhibited PMA-induced transcription. Nevertheless, inhibition in this manner had no impact on the percentage signal derived from

any of the other treatments, suggesting that they mediate their effects through a different mechanism.

Given that BLM BAL, MWCNTs, and LPS were PKC independent we next evaluated the contribution of the membrane receptor Toll-like Receptor 4 (TLR4), which is responsible for much of the signaling initiated by LPS, to *Mmp10* regulation. We generated BMDMs from WT and *Tlr4*$^{-/-}$ mice (n=3) and treated each group as before. Consistent with our hypothesis, we found that while PMA was found to be completely TLR4-independent, that the LPS signal was significantly attenuated (by approximately 75%) in the absence of TLR4 (Figure 4.6A). Similarly, although PmB was added to neutralize endotoxin during each MWCNT treatment, we found that the response to MWCNT was also modified in these cells. However, despite the observed reduction in *Il6* and *Mmp10 levels with PmB treatment (Figure 4.3.C,D)*, BLM BAL was unaffected by the loss of TLR4, suggesting that a different TLR or receptor is responsible for this signal.

Mmp10 Stimuli Utilize Largely Redundant MAPK Signaling Cascades and are NFkB-Dependent

Many groups have reported a role for MAPK signaling in the regulation of *Mmp10*, but the majority of these studies have focused on expression in endothelial cells and fibroblasts. Therefore, we used inhibitors of MEK1/2, JNK 1/2/3, and P38 (U0126, SP600125, and SB203580 respectively) to assess the contribution of each of these pathways to *Mmp10* signaling in macrophages (Figure 4.7A). As before, each sample (n=3) was pretreated for 30 minutes with

each of the inhibitors before an additional 2 hours of co-treatment with each stimulus. As has been previously reported in fibroblasts, the JNK1/2/3 inhibitor, Sp600125, was unable to significantly reduce PMA-induced *Mmp10* expression. Of the remaining treatments, we found that each was capable of reducing the percent *Mmp10* signal to varying degrees; however, only SB203580 in MWCNTs completely eliminating *Mmp10* up-regulation. These data support the finding that MAPK signaling pathways are important in the regulation of *Mmp10*, but they also suggest that they are mostly redundant.

Lastly, our group and others have reported a role for NFκB in mediating transcriptional control of *Mmp10* with LPS-treatment [113]. Therefore, we used *BMS*-345541, a potent inhibitor of IkKinase activity, to elucidate the contribution of NFκB to induction in our panel of stimuli. Surprisingly, we found that 25 and 100 nM BMS-345541 treatment was able to completely eliminate *Mmp10* induction in these cells with all stimuli (Figure 4.7B). In the majority of treatments we also observed an additional repression above and beyond the controls, suggesting that NFκB may also be contributing to the baseline *in vitro* expression of *Mmp10* in these cells. This finding is further supported by our data from treatment with each individual inhibitor alone on *Mmp10* values (Figure 4.8A), which shows a significant reduction of *Mmp10* in BMS-345541 alones, but not with any of the other 6 inhibitors.

4.3 Discussion:

Though long assumed to be functionally redundant [4,5], the last 20 years of research has demonstrated that individual MMPs serve distinct roles in injury and repair [13]. Importantly, though MMPs are known to be regulated by diverse mechanisms, control is largely thought to imposed at the transcriptional level [15] [16], necessitating further study of the signaling pathways that mediate expression. While less studied than other MMPs, MMP-10 has been the subject of increasing researched due to its demonstrated association with conditions like non-small cell cancer [25,26], cardiovascular disease [23, 24], and idiopathic pulmonary fibrosis [27,28]; however, these studies are complicated by the finding that *Mmp10* signaling events are stimulus, and to some extent cell-type specific.

Here we present the results of what we believe to be one of the most complete comparative studies of these events in macrophages. We found that *Mmp10* is slightly up-regulated in BM cells differentiated with GM-CSF or M-CSF, but that M-CSF-treated BM showed a much more robust increase (2 vs. 20 fold at day 2), suggesting that *Mmp10* is much more strongly associated with commitment to a macrophage than a dendritic cell lineage. This increase in M-CSF-treated cells gradually attenuated over time, and with 2 days of further culturing was returned almost to baseline. While the function of *Mmp10* during this time is unknown, we utilized additional culturing for all subsequent studies to maximize the response to the stimuli.

A separate finding of this study was that of a novel *Mmp10* stimulus in extracellular BAL collected post-BLM exposure. Importantly, this response was found to be collection day specific, with the potency of the BAL corresponding to

in vivo up-regulation of *Mmp10* in whole lung, and was not ablated with PmB pretreatment. These data suggest the presence of a stimulus that is distinct from LPS, which is also included in our studies of *Mmp10*. Given that the *Mmp10* expression pattern seems to increase, and not decrease well into the fibrotic response, it seems reasonable that the putative stimulus is involved with repair and/or growth processes. Several such stimuli have been suggested including TGF-β1, the extracellular domain (EDA) of fibronectin, and dermokine, but further proteomic study will be necessary to determine the exact identity of these stimuli [49,154].

One of the more striking literature findings regarding *Mmp10* is that distinct stimuli elicit unique temporal patterns of induction. This is particularly true of LPS and PMA, whose peak *in vitro* expression patterns differ by 6 or more hours [53, 113]. This conclusion was supported by our *in vitro* data, which showed that where LPS-induced expression peaked after the first hour, PMA-induced expression was still continuing to grow as of 4 hours. In contrast, both MWCNT and BLM BAL showed reduced potency, with BLM BAL neither increasing nor attenuating at the 4-hour mark, and MWCNT peaking at 2 hours and declining thereafter.

Based on their demonstrated role in *Mmp10* signaling, we evaluated the contribution of both protein kinase C (PKC) and TLR4 to *Mmp10* levels. Though PKC, which is known to be important for PMA signaling, was found to inhibit PMA-induced *Mmp10* expression, none of the other stimuli were impacted by PKC inhibition. BMDMs from TLR4 deficient mice were then tested for their ability

to respond to these agents. Paradoxically, while MWCNT and LPS signaling were found to be dependent upon these proteins, BLM BAL showed no response at all to *Tlr4* ablation. The finding that LPS is capable of inducing *Mmp10* in a TLR4 dependent manner is novel, but also consistent with findings derived from studies with other MMPs (i.e. MMP-1 and MMP-9) [155,156,157].

Although initially distinct, we found that all three of the stimuli investigated here were redundant with regard to MAPK signaling. The one exception is PMA, which, in agreement with a report by Sampieri et al., was found to be JNK-independent [53]. This conclusion is not unexpected given the diversity of components present in both MWCNT and BLM BAL, but it is particularly interesting for LPS, which is well defined. Nevertheless, it is consistent with reports indicating that LPS is capable of signaling through all three pathways in macrophages [158].

Finally, we found that in spite of the reported responsiveness of *Mmp10* to other transcription factors (i.e. CHF1/Hey2, AP-1) [159,23], all stimuli were completely inhibited by the addition of even low quantities (i.e. 25 nM) of BMS-345541, a potent IκK/NFκB inhibitor. This is compatible with the observations of Murray et al., who showed a similar, though less complete inhibition in BMDMs with LPS [113]. In addition, we found that of all the inhibitors tested, that only BMS-345541 was capable of further reducing baseline *Mmp10* expression. This is compelling as acetylation of the p65 subunit of NFκB at the K314/315 positions has been suggested to mediate baseline repression of *Mmp10* and *Mmp13* [160].

These results indicate that *Mmp10* is a well-conserved component of the macrophage response to its environment, and argue for further study of the exact mechanisms underlying transcriptional regulation of *Mmp10*.

Figures:

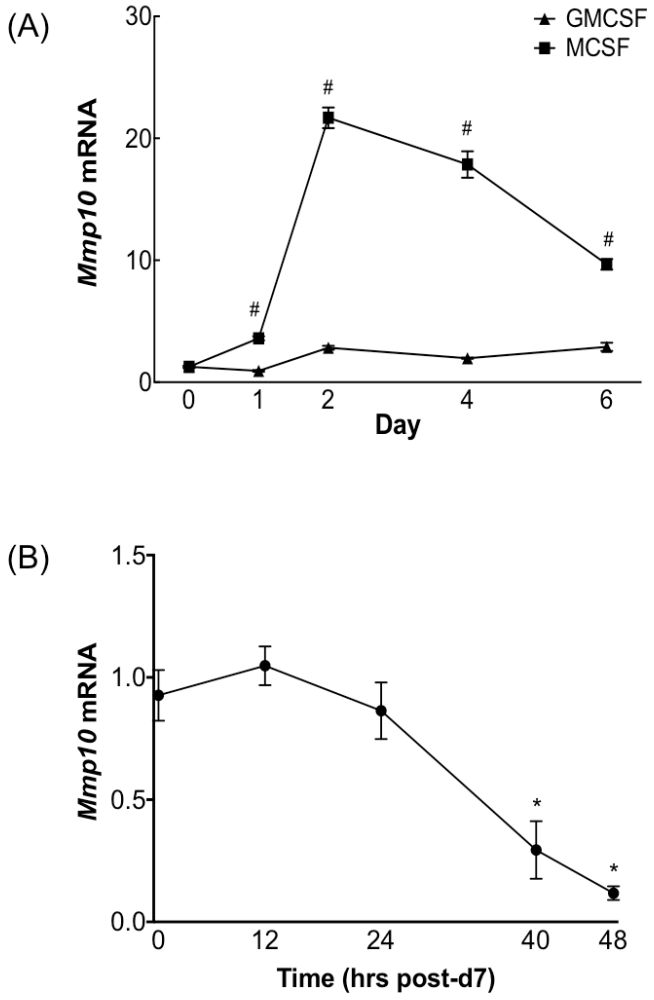

Figure 4.1. *Mmp10* is induced during *in vitro* derivation of BMDMs from bone marrow. (A) Bone marrow from WT C57BL/6 mice was isolated and plated (as described in the methods section) and maturated in media containing either recombinant mouse M-CSF or GM-CSF. Lysates were then collected and assayed for *Mmp10* transcript levels at the indicated times post-plating**. (B).** Following collection of mature BMDMs on day 7, adherent cells were counted and replated in macrophage differentiation media at sub-confluence for an additional 40 hours. Lysates were assayed at 12, 24, and 40 hours to determine the impact of additional culturing on *Mmp10*. * significant increase vs. Control. # significant decrease vs. corresponding GM-CSF value. *(P<0.05)*

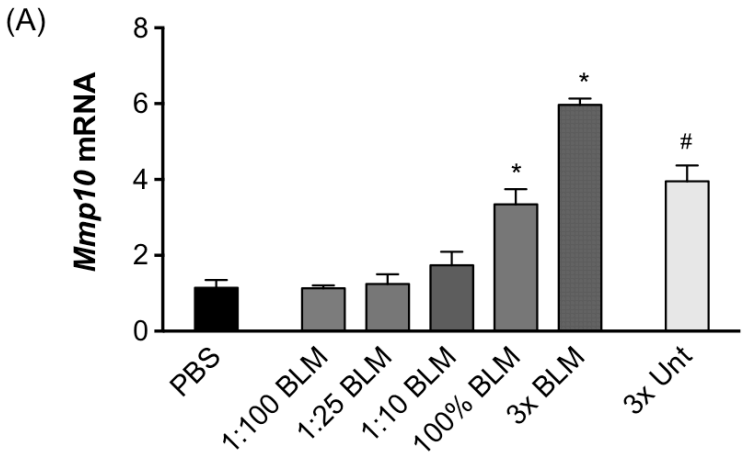

Figure 4.2. Day 4 BLM BAL shows a dose-dependent induction of *Mmp10* that is greater than untreated BAL alone. (A) Naïve BMDMs (n=3) were treated with PBS, the indicated dilutions of day 4 BLM BAL, or 3x BAL from Untreated WT animals (n=3). *significant increase vs. PBS alone. # significant decrease vs. 3x BLM BAL. *(P<0.05)*

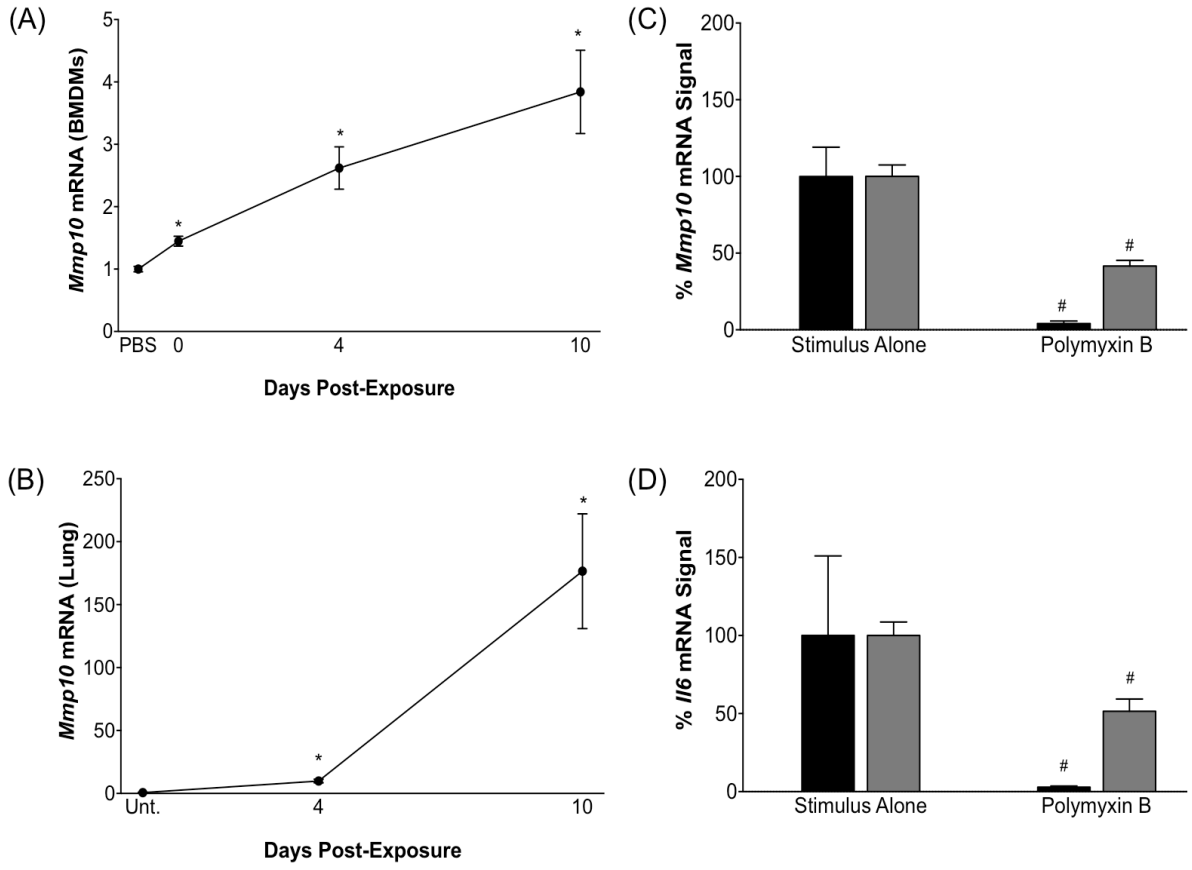

Figure 4.3. BMDM *Mmp10* is upregulated by treatment with BAL collected from BLM treated animals. Mice were treated with 2.0 U/kg of BLM via i.t. and BAL was collected at 0 (untreated; n=3), 4 (n=4), and 10 (n=5) days post-treatment in PBS + 1% BSA. Following collection, BALs were concentrated 3x and added to naïve BMDMs for 2 hours **(A). (B)** The lungs from these same animals were then homogenized and probed for *Mmp10* at each of the collection days. A 30 minute pre-treatment with 10 µg/ml PmB, followed by a 2 hour co-treatment with either day 4 BAL, or 500 ng/ml of LPS was then utilized to assess the contribution of endotoxin to the *Mmp10* **(C)** and *Il6* **(D)** responses. * significant increase vs. **(A)** PBS or **(B)** Unt. Control. # significant decrease vs. stimulus alone **(C, D).** *(P<0.05)*

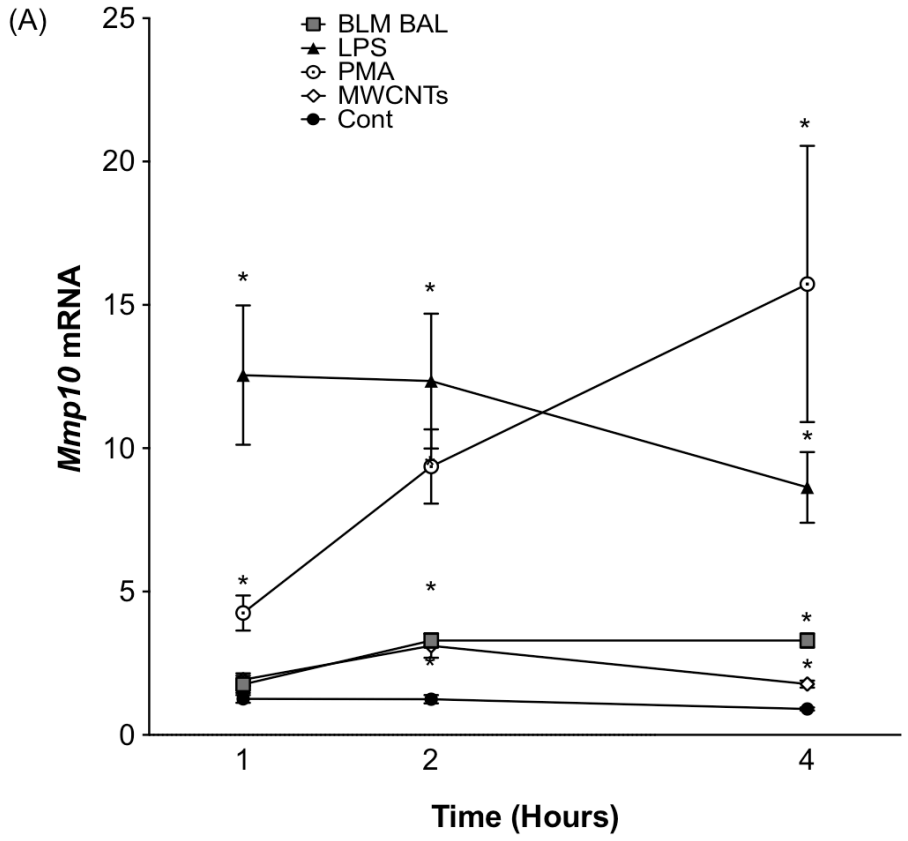

Figure 4.4. *Mmp10* stimuli show distinct temporal induction profiles in treated BMDMs. (A) Naïve BMDMs were treated with BLM BAL, 500 ng/ml LPS, 100 nM PMA, or 100 µg/ml of MWCNTs, and the fold change in *Mmp10* response from controls was assayed 1, 2, and 4 hours later. * significant increase vs. WT Cont. *(P<0.05)*

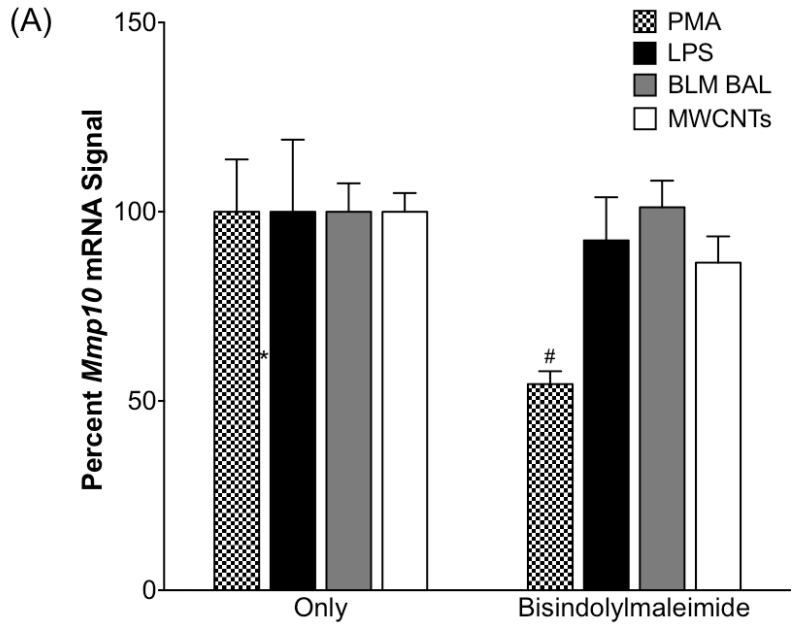

Figure 4.5. PMA, but not LPS, MWCNT, or BLM BAL signaling is protein kinase C dependent. (A) Naïve BMDMs were either treated with BLM BAL, 500 ng/ml LPS, 100 nM PMA, or 100 µg/ml of MWCNTs for 2 hours, or pretreated with 360 nM of the PKC inhibitor, Bisindolylmaleimide, for 30 minutes followed by a 2 hour concurrent treatment with each of the stimuli. # significant decrease vs. stimulus alone. *(P<0.05)*

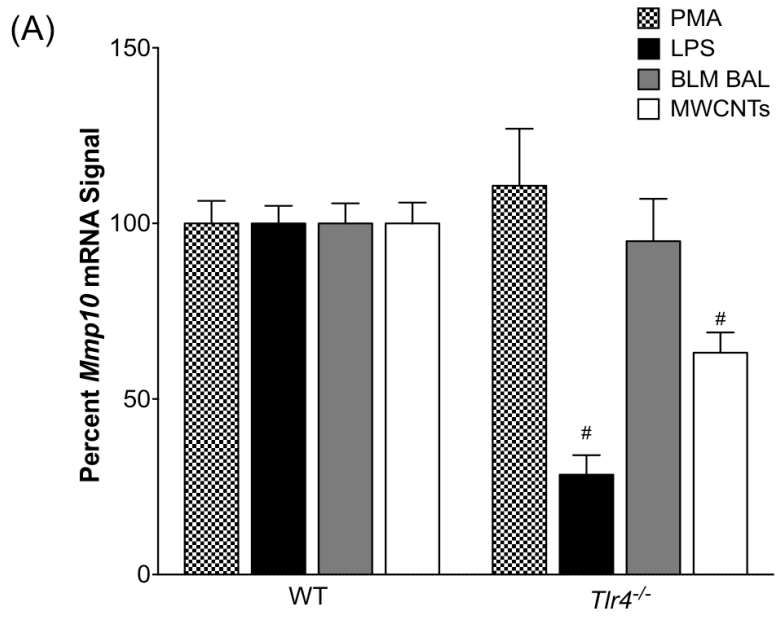

Figure 4.6. MWCNT and PMA, but not LPS or BLM BAL are modified by *Tlr4* ablation. **(A)** Naïve BMDMs, with and without *Tlr4* (n=3), were treated with BLM BAL, 500 ng/ml LPS, 100nM PMA, or 100 µg/ml of MWCNTs for 2 hours and assayed for changes in *Mmp10*. * significant increase vs. WT stimulus alone. # significant decrease vs. WT stimulus alone. *(P<0.05)*

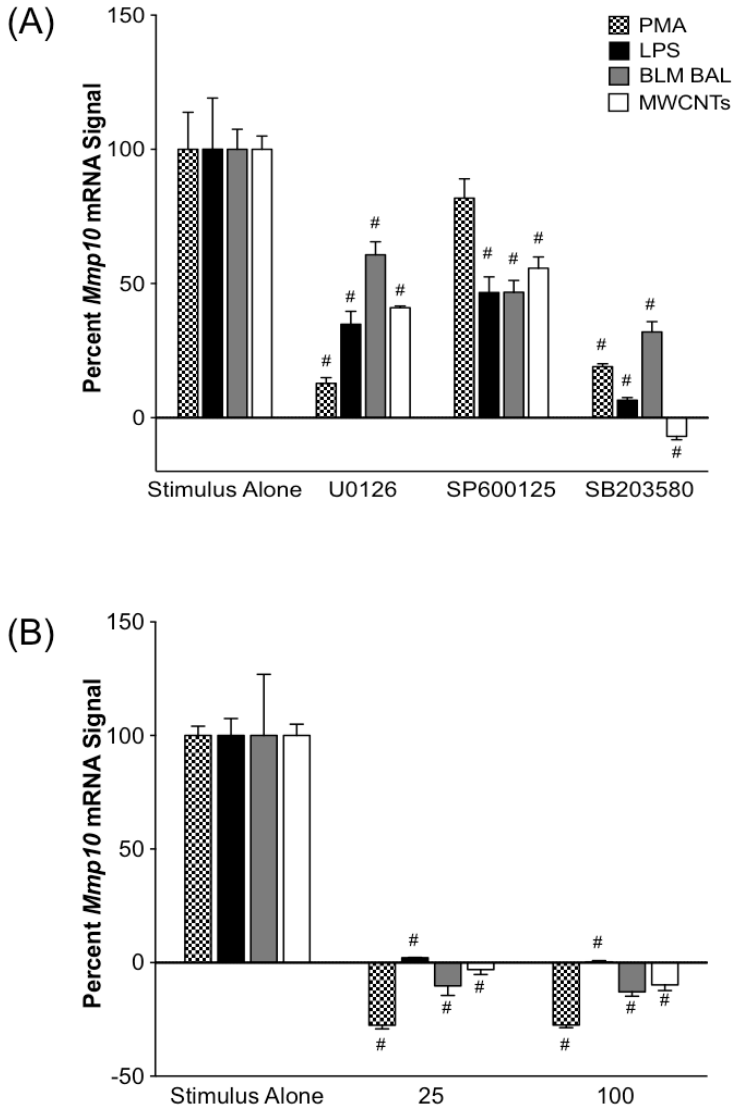

Figure 4.7. *Mmp10* stimuli utilize diverse MAPK signaling cascades that converge on NFκB. (A) Naïve BMDMs were pretreated with 10 μM of U0126, 10 μM of SP600125, or 60 μM of SB203580 (MEK1/2, JNK1/2/3, and p38 inhibitors respectively) for 30 minutes, followed by BLM BAL, 500 ng/ml LPS, 100 nM PMA, or 100 μg/ml of MWCNTs for 2 hours. The samples were then assayed for *Mmp10* and compared against stimulation alone values. **(B)** Cells were pretreated with 25 and 100 μM of the IκK inhibitor, SB203580, before 2 hour co-treatment as above. *Mmp10* values were then compared to stimulus alone. # significant decrease vs. stimulus alone. *(P<0.05)*

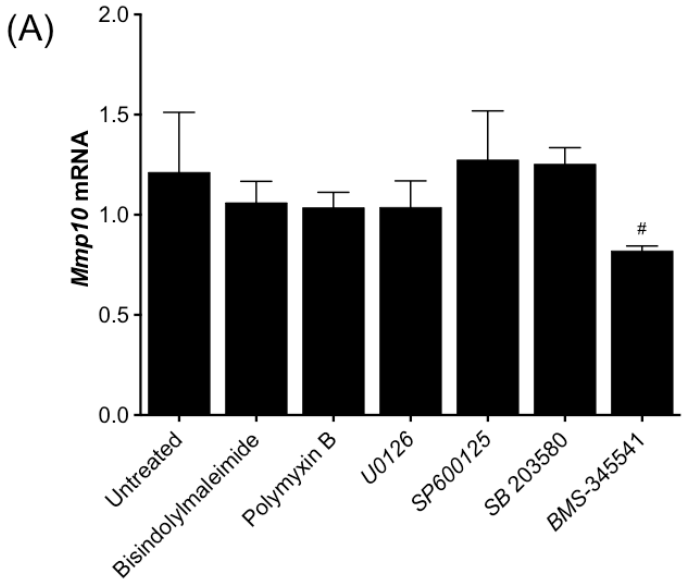

Figure 4.8. *Mmp10* signaling inhibitors have minimal or no impact on baseline Mmp10 expression. (A) Fold change in *Mmp10* induction from WT control for indicated inhibitors following 2.5 hours of treatment. # significantly decreased vs. untreated BMDMs. *(P<0.05)*

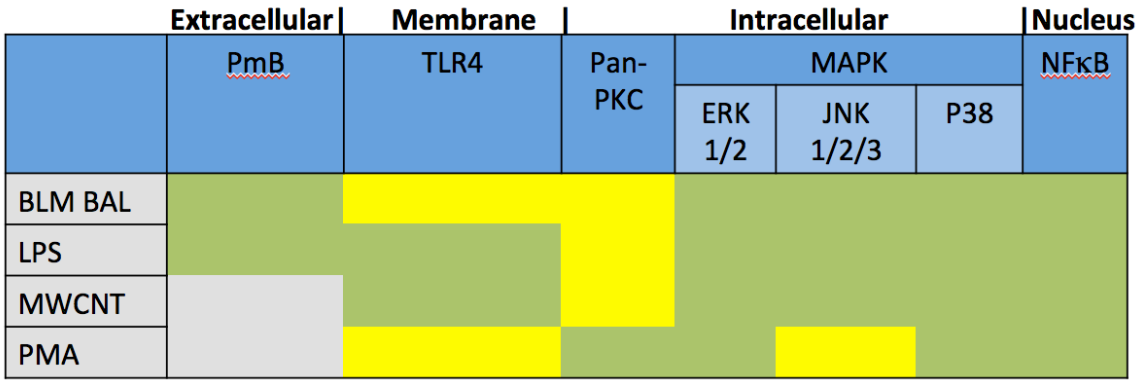

Table 4.1. Summary of results for experiments regarding *Mmp10* signaling with various stimuli. The overall results of these inhibitor and ablation studies are shown above. Yellow indicates no change in *Mmp10* mRNA, green indicates a significant reduction. Grey values are unknown. Inhibitors are presented based on the proximity of the target protein/molecule to the *Mmp10* promoter.

CHAPTER 5

Conclusions

5.1. Summary:

As of November 2015, a PubMed search of the term “matrix metalloproteinase 10” yielded only 266 results. In contrast, a search of “matrix metalloproteinase 9” returned 16,247 results. In light of this disparity, the work presented in chapters 2, 3, and 4 constitutes a valuable addition to a relatively small body of work regarding MMP-10, especially when you take into account that only 10 of the “matrix metalloproteinase 10" results also contained the term “macrophage”.

Collectively, prior research has demonstrated four things about tissue *Mmp10* expression. First, although *Mmp10* is weakly detectably/undetectable in virtually all tissues with the exception of small intestine [22], *Mmp10* is rapidly quantifiable in injured tissues, typically within 24 hours. Secondly, up-regulation modulates disease pathology in a wide range of tissues (i.e. colon tissue, liver, brain, skin, lung (unpublished observations)) and, thirdly, in a multitude of injury models [33,49,50,161,162]. Finally, while the preponderance of acute injury data indicate that *Mmp10* expression peaks and attenuates in most of these models [49,50], this increase is also sustained in chronic conditions such as Crohn’s disease and ulcerative/ischemic colitis, idiopathic pulmonary fibrosis, lung tumorigenesis and metastasis, and atherosclerosis [23-28,32].

In the present work we contribute to the state of MMP-10 research by demonstrating a role for macrophage MMP-10 in protection against the

development of BLM, and MWCNT-induced lung disease. Furthermore, our investigations into the signaling mechanisms underlying *Mmp10* expression in primary macrophages in culture (BMDMs) add several novel observations regarding the divergent and convergent nature of *Mmp10* signaling.

5.2. Macrophage *Mmp10* is a major *in vivo* mediator of the response to lung injury

Although pulmonary *Mmp10* has been shown to be up-regulated in the context of PAK-inducted infection ([48], unpublished observations), as well as in tumor initiation and metastasis [25,26], we are unaware of any studies examining its role in sterile lung damage. To that end, we carried out exposures of WT or *Mmp10*$^{-/-}$ mice to both the pro-fibrotic drug bleomycin, as well as to a particular type of engineered nanomaterial known as long multi-walled carbon nanotube (L-MWCNT).

In the context of BLM, we found that *Mmp10* protects against the pulmonary inflammation, recruitment of macrophages, and ultimately, fibrogenesis. Notably, this phenotype was present even though no difference in damage (i.e. BAL IgM) was observed between the genotypes. However we did observe that *Mmp10*$^{-/-}$ lungs expressed significantly more *Ccl2*, and displayed greater chemotactic potential for naïve BMDMs than their WT counterparts. Interestingly, not only are elevated *Ccl2* levels known to have a causative role in BLM-induced fibrosis [75,76,163], but at least three other studies have shown a similar difference in CCL2 levels between WT and *Mmp10*$^{-/-}$ mice [49,50,32].

More recently, we have observed that both BMDMs, as well as BLM-treated lung tissue display significantly increased phosphorylation of the mitogen activate protein kinase proteins known as ERK1 and 2 (data not shown). Further research into this phenotype has shown that the receptor tyrosine kinase (RTK) known as macrophage colony stimulating factor receptor (M-CSFR), which mediates signaling of the M-CSF ligand through ERK1/2, is also phosphorylated (i.e. activated) to a greater degree in *Mmp10*$^{-/-}$ BMDMs (data not shown). Finally, in chapter 3 we demonstrated that macrophages differentiated with M-CSF express increased *Mmp10* during the maturation process (Figure 3.1A). These data are important as recombinant M-CSF has been shown to induce CCL2 levels in treated BMDMs, and both CCL2 and M-CSF ablation in the BLM model attenuate fibrogenesis [76]. Together, these observations suggest that macrophage *Mmp10* is likely to directly or indirectly attenuate macrophage recruitment and fibrosis through attenuated CCL2 production.

While L-MWCNT exposure was initially employed to test the generalizability of our BLM interpretations in the context of a toxicologically relevant stimulus, we found that the phenotypic differences between the models revealed as much as the similarities. For example, in contrast to our BLM data, we found no observable difference in *Ccl2* levels in whole lung mRNA at 24 hours post-MWCNTs (which is not entirely surprising given the timeframe). Furthermore, though we observed a statistically significant increase in fibrogenesis between WT and *Mmp10*$^{-/-}$ mice treated with BLM, no difference was observed at 28 days post-treatment with L-MWCNT (data not shown),

suggesting that the fibrotic difference in the BLM model may be an indirect impact of MMP-10—possibly due to inflammation resulting from enhanced macrophage recruitment. Finally, our use of L-MWCNT also uncovered a previously unreported role for *Mmp10* in pulmonary clearance, though the role of macrophage *Mmp10* in this phenotype is still unclear.

However, we also found striking similarities between these models, including the development of enhanced inflammation in the lungs of *Mmp10*$^{-/-}$ mice treated with either agent. Interestingly, measurements of BAL IgM, as well as multiple indices of endocytosis (with L-MWCNT treatment) showed that this difference is not a result of enhanced damage or particle uptake, but instead it results from enhanced sensitivity. The distinction between the two points is important as it indicates that *Mmp10* is important for the injury response, and not necessary the insult itself. Overall, the data presented here are consistent with our PAK data suggesting that macrophage *Mmp10* is a major mediator of the response to lung injury.

5.3. Macrophage *Mmp10* orchestrates inflammation via distinct but conserved mechanisms *in vitro*

Chapter 4, as well as the *in vitro* components of Chapter 3, provide strong evidence for a causal relationship between macrophage *Mmp10* and the phenotypes observed *in vivo*. In the L-MWCNT model we found that BAL cells from *Mmp10*$^{-/-}$ mice contained significantly more caspase-3 activity than WTs, which is indicative of enhanced intrinsic and extrinsic apoptotic pathway

activation [164]. Notably, no difference was observed in whole lung lysates. In addition, we observed a decrease in macrophage counts (and only macrophage counts) with L-MWCNT exposure that was further exacerbated by the loss of *Mmp10*, suggesting the *Mmp10* deficient macrophages were more susceptible to apoptosis post-treatment. Using BMDMs we demonstrated that macrophages selectively up-regulate *Mmp10* following MWCNT exposure, which then protects against both inflammation and cell death, potentially through NALP3 inflammasome-mediated IL-1β production.

The propensity for *Mmp10* to be both a component of, as well as a important feature during the inflammatory response was supported by the finding that even low quantities of an IκK inhibitor (BMS-345541), which prevents NFκB-induced transcript by inhibiting its dissociation from IκBα [165], were able to completely inhibit *Mmp10* induction with all stimuli investigated. In addition, we found that instead of utilizing a single MAPK signaling pathway to induce NFκB transcription, that these pathways appeared somewhat redundant. While it is possible that compensatory mechanisms, and not just parallel signaling could explain some or all of these results, this redundancy implies that *Mmp10* expression is well conserved in macrophages.

Despite the fact that *Mmp10* signaling appeared to converge as it approached the transcriptional level, the data presented in Chapter 3 also indicated that these signals are initially quite distinct, with different temporal patterns, potency, and early signaling components. For example, whereas LPS and PMA elicited the same magnitude of induction, their signals peaked at

distinctly different times (1 hour vs 4 hours). In contrast, MWCNTs and BLM BAL were far less potent than LPS or PMA, and their peaks of *Mmp10* mRNA were observed at 2 hours.

These differences were also readily apparent following both protein kinase C (PKC) inhibition, and in TLR knockout BMDMs. Consistent with other studies [53], we found that PMA-mediated induction was effectively inhibited in the presence of a PKC inhibitor; however, none of the other stimuli appeared to be PKC dependent. Likewise, we correctly hypothesized that TLR4 ablation would inhibit LPS signaling, which is also consistent with reports from other MMP studies (i.e. MMP-1 and MMP-9) [155,156,157]. Nevertheless, we observed that BLM BAL was not inhibited in the absence of TLR4, suggesting that it mediates induction via another mechanism, potentially a different TLR, or a receptor tyrosine kinase.

A separate finding was that, similar to LPS, L-MWCNT-induced expression was TLR4 dependent. This is particular interesting as PmB was included in all treatments to prevent any contribution of endotoxin-derived from synthesis (which is, obviously, also a stimulus for *Mmp10*). Of note is the fact that this concentration was capable of completely eliminating the *Mmp10* signal derived with 500 ng/ml of LPS. This result could indicate that L-MWCNT is capable of serving as damage associated molecular pattern (DAMP) to initiate transcription via TLR4. This conclusion is supported by a recent finding that CNT-related inflammation in alveolar macrophages is MyD88 dependent [166].

While our survey also yielded several other interesting observations, an inescapable conclusion of this work is that *Mmp10* signaling is important for organizing the inflammatory response to many different classes of molecules. Future studies will focus on the mechanism(s) underling the observed protective role of *Mmp10* in macrophages.

CHAPTER 6

Materials and Methods

The Institutional Animal Care and Use Committees at the University of Washington (Seattle, WA), and Cedars-Sinai Medical Center (Los Angeles, CA), approved all animal experiments.

CHAPTER 2:

RT-qPCR: Total RNA purification, cDNA purification and qPCR was performed with the RNeasy Plus Mini Kit (Qiagen; Germantown, MD), High Capacity cDNA RT Kit (Applied Biosystems; Foster City, California), and SensiMix Probe Kit (Bioline; Taunton, MA). Probes were also from Applied Biosystems. Data was normalized to HPRT and calibrated to WT control values.

IgM ELISA: IgM ELISA Quantification Kit (Bethyl Laboratories; Montgomery, TX) was used to quantify IgM in BAL according to the manufacturer's specifications.

Dot Blot: Dot blots were performed for F4/80 (MCA497R, Abd Serotec, Raleigh, NC) using 80 μl of BAL collected at day 10 post-exposure. Densitometry analysis was conducted utilizing ImageJ software Ver. 1.46r (National Institutes of Health, USA)

Tissue Staining and IHC: Masson's trichrome and H&E staining was conducted by the UW's Histology and Imaging Core. IHC for αSMA was performed utilizing an antibody from Sigma Aldrich (St. Louis, MO).

Hydroxyproline content: Hydroxyproline content was quantified in left lung lobes using the Hydroxyproline Colorimetric Assay Kit from Biovision (Milpitas, CA) according to their specifications. Left lungs were weighed prior to the assay and homogenates were normalized to 10 μl of ddh_20 per mg of tissue. Total hydroxproline per lung was back-calculated based on this information.

***In vivo* bleomycin exposures:** All experiments involved intratracheal intubation of mixed gender WT and *Mmp10*$^{-/-}$ C57BL/6 mice between 6 and 12 weeks of age. *Mmp10* null mice were generated previously through the targeted deletion of exons 3 to 5 of the *Mmp10* gene (also see Figure 1.1), which includes the catalytic domain [48]. These mice had been backcrossed for 11 or more generations at the time of these experiments. Animals were monitored for signs of distress following exposure and weight loss was recorded daily.

Bleomycin dosage: mortality data was derived with 0.08 U or bleomycin per mouse (~3.6 U/kg), fibrogenesis (i.e. collagen and αSMA endpoints) utilized 2.0 U/kg of bleomycin, and a dose of 1.2 U/kg was used to study acute lung injury (cell counts, inflammatory transcripts, etc.)

BLM Tissue Collection: Lung tissue was perfused and the left lung was occluded, removed, and flash frozen in liquid nitrogen. The right lung was lavaged with 1x 0.6 ml, and 2x 0.5 ml of sterile PBS before being inflated with formalin O/N. The following day the lungs were washed in PBS and transferred to 70% EtOH for storage at 4° C.

BAL cell counts: BAL was collected at the indicated days in 3 washes of (0.6, 0.5, and 0.5 mls) of ice cold PBS and total cells were counted via automated cell counter. 50 $x10^3$ cells from each animal were used to generat cytospins (5 minutes at 700 rpm), which were subsequently stained with DiffQuick. The percent macrophages, neutrophils, and lymphocytes were quantified via microscopy by averages of 4 counts of 100 cells per animal, and the total number of each cell type was back-calculated using the total cell numbers.

Statistics. Statistical analyses included either T-test or two-way ANOVA where appropriate utilizing Prism 5 (GraphPad Software, La Jolla, CA). Bonferroni post-test was used account for multiple comparisons. All data are presented as mean ± SEM, except where indicated, and a P-value of >0.05 was considered significant.

CHAPTER 3:

Animals. *Mmp10*$^{-/-}$ mice (C57BL/6J) [48] and wildtype littermates (male and female, 8-12 week old) were used for these studies.

MWCNT. MWCNT were purchased from CheapTubes, Inc. (Cambridgeport, VT) by the University of Washington's Nanotoxicology Center as part of the NIEHS Centers for Nanotechnology Health Implications Research (NCNHIR) Consortia. Tube preparation for both *in vivo* and *in vitro* work consisted of suspension in dispersion medium (DM) that contained 0.6 mg/ml mouse serum albumin, 10 μg/ml 1,2-dipalmitoyl-sn-glycero-3-phosphocholine, and 0.1% ethanol (v/v) in PBS. Stock aliquots of MWCNT (1.6 μg/μl) were sonicated during both preparation and immediately before treatments. The manufacturer's product data specified an outer diameter of 10-20 nm and a length of 10-30 mm. Scanning electron microscopy with energy dispersive x-ray spectroscopy analysis (SEM-EDS), conducted by the National Cancer Institute Nanotechnology Characterization Laboratory, confirmed an elemental composition of 95.8% ± 0.6 (SD) carbon and 3.4% ± 0.2 oxygen and the presence of trace remains of Ni (0.5% ± 0.5) and Fe (0.3% ± 0.3). These values are consistent with composition determined by Pulskamp *et al.* [133].

Exposures and Tissue Harvest. Mice (6/group/genotype) were treated with a single 50-μl OPA of DM or an equivalent volume containing 80 μg MWCNT. Mice were sacrificed 24 h later, and the left lung was occluded, flash frozen, and homogenized in either RIPA, or RLT buffer (Qiagen, Valencia, CA) for protein and RNA analysis. BAL was collected from the right lungs, and total cells were identified and counted via automated cell counter. The right lung was then inflated with 600 ml of 10% formalin and prepared for histology as described [167].

MWCNT Clearance. Fixed lungs were paraffin-embedded, sectioned, and stained with H&E by CS-BTRC. Using these images, the CS-BTRC then set a threshold value with DM alone sections to eliminate artifacts, and blindly

assessed both the MWCNT aggregate count, as well as the percentage of area occupied (in pixels) in each treated lung section (n=6). These findings were supported by our own counts obtained with microscopy (10x).

Macrophage Cell Culture. Bone marrow-derived macrophages (BMDMs) were isolated and differentiated for 7 days in CSF-1-containing medium as described [168]. Polymyxin B sulfate salt was included (10 μg/ml; Sigma-Aldrich, St. Louis, MO) to control for potential endotoxin contamination.

Particle Uptake. *In vivo* estimates of endocytosis were calculated from BAL cytospin slides. MWCNT-positive cells were identified by light microscopy, and percentages were determined from averages of four separate counts of 100 cells. Total positive cells were back-calculated from total cell estimates. *In vitro* endocytosis was determined in a similar manner following 3 hours of exposure. The average area occupied by MWCNT-positive vacuoles per cell was quantified from 30 measurements per animal at 80x utilizing Digital Image Hub software version 4.0.4. (*Leica* Microsystems GmbH, Buffalo Grove, IL).

Assays. Caspase-3 activity in whole lung and cell lysates was assayed using a Caspase-3 Colorimetric Assay Kit (Biovision, Milpitas, CA) according to manufacturer instructions. Total RNA was isolated from whole lung and cultured macrophages. Total RNA was isolated (Qiagen, Valencia, CA) and specific transcripts were quantified by real-time PCR using TaqMan FAM-labeled probes (Applied Biosystems, Foster City, CA) as described [169]. Total IL-1β levels were measured using the Mouse IL-1β ELISA Ready-SET-Go! Kit (eBiosciences, San Diego, CA).

Statistics. Statistical analyses included either T-test or two-way ANOVA where appropriate utilizing Prism 5 (GraphPad Software, La Jolla, CA). Bonferroni post-test was used account for multiple comparisons. All data are presented as mean ± SEM, except where indicated, and a P-value of >0.05 was considered significant.

CHAPTER 4:

Macrophage culture and migration assay: BMDMs were generated as previously described [153] [14]. Tibias and femurs of WT, and *Tlr4*$^{-/-}$ C57BL/6 mice were collected and centrifuged (1,500 rcf for 2 min), treated with RBC lysis buffer, and cultured overnight in recombinant GM-CSF, M-CSF, or Mac Media (RPMI 1640 with glutamine, 1% penicillin/streptomycin, 10% heat-inactivated fetal bovine serum (FBS) and 20% L929 cell supernatant). Non-adherent cells were then collected and replated for an additional 6 days.

For the recombinant M-CSF and GM-CSF studies, RNA was collected at 0, 1, 2, 4, and 6 days. For all other studies, day 7 cells were collected and replated in sub-confluence for an additional culture period of 40 hours prior to use.

In vivo **bleomycin exposures:** WT and *Mmp10*$^{-/-}$ C57BL/6 mice between 6 and 12 weeks of age (n=3 to 6) were administered 2.0 U/kg of bleomycin by i.t. *Mmp10* null mice were generated previously through the targeted deletion of exons 3 to 5 of the *Mmp10* gene (also see Figure 1.2), which includes the catalytic domain [48]. These mice had been backcrossed for 11 or more generations at the time of these experiments. Animals were monitored for signs

of distress and sacrificed at 0 (untreated), 4, or 10 days post-BLM. BAL was collected in 3 washes of (0.6, 0.5, and 0.5 mls) of ice cold PBS, centrifuged at 500 rcf for 5 minutes, and the extracellular fraction was isolated. The left lungs of these animals were occluded, homogenized in RLT buffer (Qiagen, Valencia, CA), and *Mmp10* mRNA was quantified.

***In vitro* BAL preparation:** Depending up the experiment, this fraction was either diluted in media, or concentrated 3x with an Amicon Ultra-2 Centrifugal Filter Unit with Ultracel-3 membrane (MWCO: 3 kD) (EMD Milipore, Temecula, CA).

Macrophage induction stimuli: Unless otherwise noted, all induction experiments consisted of a 40-hour post-day 7 plating protocol, followed by a 2-hour exposure. Stimulus concentrations were: 3 fold diluted BLM BAL, 500 ng/ml of LPS, 100 nM of PMA, and 100 μg/ml of MWCNTs.

Macrophage inhibitors: All inhibitor experiments involved a 30 minute pretreatment, followed by a 2 hour co-treatment with the indicated stimuli (except where indicated). Inhibitors: 360 nM bisindolylmaleimide (Cayman Chemical, Ann Arbor, MI) 10 μg/ml polymyxin B (Sigma Aldrich, St. Louis, MO) 10 μM U0126 (Calbiochem, Billerica, MA) , 20 μM SP600125 (Cell Signaling, Danvers, MA), 60 μM SB203580 (Tocris, Minneapois, MN) 25 or 100 nM BMS34551 (Sigma Aldrich, St. Louis, MO).

REFERENCES

1 Turk, V. *et al.* Cysteine cathepsins: from structure, function and regulation to new frontiers. *Biochim Biophys Acta* **1824**, 68-88, doi:10.1016/j.bbapap.2011.10.002 (2012).

2 Manase, K. *et al.* Coordinated elevation of membrane type 1-matrix metalloproteinase and matrix metalloproteinase-2 expression in rat uterus during postpartum involution. *Reprod Biol Endocrinol* **4**, 32, doi:10.1186/1477-7827-4-32 (2006).

3 Gross, J. & Lapiere, C. M. Collagenolytic activity in amphibian tissues: a tissue culture assay. *Proc Natl Acad Sci U S A* **48**, 1014-1022 (1962).

4 Greenlee, K. J., Werb, Z. & Kheradmand, F. Matrix metalloproteinases in lung: multiple, multifarious, and multifaceted. *Physiol Rev* **87**, 69-98, doi:10.1152/physrev.00022.2006 (2007).

5 Hu, J., Van den Steen, P. E., Sang, Q. X. & Opdenakker, G. Matrix metalloproteinase inhibitors as therapy for inflammatory and vascular diseases. *Nat Rev Drug Discov* **6**, 480-498, doi:10.1038/nrd2308 (2007).

6 Zhou, Z. *et al.* Impaired endochondral ossification and angiogenesis in mice deficient in membrane-type matrix metalloproteinase I. *Proc Natl Acad Sci U S A* **97**, 4052-4057, doi:10.1073/pnas.060037197 (2000).

7 Giannandrea, M. & Parks, W. C. Diverse functions of matrix metalloproteinases during fibrosis. *Dis Model Mech* **7**, 193-203, doi:10.1242/dmm.012062 (2014).

8 Loffek, S., Schilling, O. & Franzke, C. W. Biological role of matrix metalloproteinases: a critical balance. *Eur Respir J* **38**, 191-208, doi:10.1183/09031936.00146510 (2011).

9 Kessenbrock, K., Plaks, V. & Werb, Z. Matrix metalloproteinases: regulators of the tumor microenvironment. *Cell* **141**, 52-67, doi:10.1016/j.cell.2010.03.015 (2010).

10 Tocchi, A. & Parks, W. C. Functional interactions between matrix metalloproteinases and glycosaminoglycans. *FEBS J* **280**, 2332-2341, doi:10.1111/febs.12198 (2013).

11 Li, Q., Park, P. W., Wilson, C. L. & Parks, W. C. Matrilysin shedding of syndecan-1 regulates chemokine mobilization and transepithelial efflux of neutrophils in acute lung injury. *Cell* **111**, 635-646 (2002).

12 Chen, P. & Parks, W. C. Role of matrix metalloproteinases in epithelial migration. *J Cell Biochem* **108**, 1233-1243, doi:10.1002/jcb.22363 (2009).

13 Parks, W. C., Wilson, C. L. & Lopez-Boado, Y. S. Matrix metalloproteinases as modulators of inflammation and innate immunity. *Nat Rev Immunol* **4**, 617-629 (2004).

14 Weischenfeldt, J. & Porse, B. Bone Marrow-Derived Macrophages (BMM): Isolation and Applications. *CSH Protoc* **2008**, pdb prot5080, doi:10.1101/pdb.prot5080 (2008).

15 Fanjul-Fernandez, M., Folgueras, A. R., Cabrera, S. & Lopez-Otin, C. Matrix metalloproteinases: evolution, gene regulation and functional analysis in mouse models. *Biochim Biophys Acta* **1803**, 3-19, doi:10.1016/j.bbamcr.2009.07.004 (2010).

16 Ra, H. J. & Parks, W. C. Control of matrix metalloproteinase catalytic activity. *Matrix Biol* **26**, 587-596, doi:10.1016/j.matbio.2007.07.001 (2007).
17 Van Wart, H. E. & Birkedal-Hansen, H. The cysteine switch: a principle of regulation of metalloproteinase activity with potential applicability to the entire matrix metalloproteinase gene family. *Proc Natl Acad Sci U S A* **87**, 5578-5582 (1990).
18 Gasson, J. C. *et al.* Molecular characterization and expression of the gene encoding human erythroid-potentiating activity. *Nature* **315**, 768-771 (1985).
19 Docherty, A. J. *et al.* Sequence of human tissue inhibitor of metalloproteinases and its identity to erythroid-potentiating activity. *Nature* **318**, 66-69 (1985).
20 Jacobsen, J. A., Major Jourden, J. L., Miller, M. T. & Cohen, S. M. To bind zinc or not to bind zinc: an examination of innovative approaches to improved metalloproteinase inhibition. *Biochim Biophys Acta* **1803**, 72-94, doi:10.1016/j.bbamcr.2009.08.006 (2010).
21 Khokha, R., Murthy, A. & Weiss, A. Metalloproteinases and their natural inhibitors in inflammation and immunity. *Nat Rev Immunol* **13**, 649-665, doi:10.1038/nri3499 (2013).
22 Madlener, M. & Werner, S. cDNA cloning and expression of the gene encoding murine stromelysin-2 (MMP-10). *Gene* **202**, 75-81 (1997).
23 Orbe, J. *et al.* Matrix metalloproteinase-10 is upregulated by thrombin in endothelial cells and increased in patients with enhanced thrombin generation. *Arterioscler Thromb Vasc Biol* **29**, 2109-2116, doi:10.1161/ATVBAHA.109.194589 (2009).
24 Rodriguez, J. A. *et al.* Metalloproteinases and atherothrombosis: MMP-10 mediates vascular remodeling promoted by inflammatory stimuli. *Front Biosci* **13**, 2916-2921 (2008).
25 Justilien, V. *et al.* Matrix metalloproteinase-10 is required for lung cancer stem cell maintenance, tumor initiation and metastatic potential. *PLoS One* **7**, e35040, doi:10.1371/journal.pone.0035040 (2012).
26 Regala, R. P. *et al.* Matrix metalloproteinase-10 promotes Kras-mediated bronchio-alveolar stem cell expansion and lung cancer formation. *PLoS One* **6**, e26439, doi:10.1371/journal.pone.0026439 (2011).
27 Konishi, K. *et al.* Gene expression profiles of acute exacerbations of idiopathic pulmonary fibrosis. *Am J Respir Crit Care Med* **180**, 167-175, doi:10.1164/rccm.200810-1596OC (2009).
28 Sokai, A. *et al.* Matrix metalloproteinase-10: a novel biomarker for idiopathic pulmonary fibrosis. *Respir Res* **16**, 120, doi:10.1186/s12931-015-0280-9 (2015).
29 Nuttall, R. K. *et al.* Expression analysis of the entire MMP and TIMP gene families during mouse tissue development. *FEBS Lett* **563**, 129-134 (2004).
30 Kerkela, E. *et al.* Differential patterns of stromelysin-2 (MMP-10) and MT1-MMP (MMP-14) expression in epithelial skin cancers. *Br J Cancer* **84**, 659-669 (2001).
31 Saarialho-Kere, U. K., Kovacs, S. O., Pentland, A. P., Parks, W. C. & Welgus, H. G. Distinct populations of keratinocytes express stromelysin-1 and -2 in chronic wounds. *J. Clin. Invest.* **94**, 79-88 (1994).

32 Vaalamo, M., Karjalainen-Lindsberg, M. L., Puolakkainen, P., Kere, J. & Saarialho-Kere, U. Distinct expression profiles of stromelysin-2 (MMP-10), collagenase-3 (MMP-13), macrophage metalloelastase (MMP-12), and tissue inhibitor of metalloproteinases-3 (TIMP-3) in intestinal ulcerations. *Am J Pathol* **152**, 1005-1014 (1998).
33 Rechardt, O. *et al.* Stromelysin-2 is upregulated during normal wound repair and is induced by cytokines. *J Invest Dermatol* **115**, 778-787, doi:10.1046/j.1523-1747.2000.00135.x (2000).
34 Saghizadeh, M. *et al.* Overexpression of matrix metalloproteinase-10 and matrix metalloproteinase-3 in human diabetic corneas: a possible mechanism of basement membrane and integrin alterations. *Am J Pathol* **158**, 723-734 (2001).
35 Daniels, J. T. *et al.* Temporal and spatial expression of matrix metalloproteinases during wound healing of human corneal tissue. *Exp Eye Res* **77**, 653-664 (2003).
36 Kabosova, A. *et al.* Human diabetic corneas preserve wound healing, basement membrane, integrin and MMP-10 differences from normal corneas in organ culture. *Exp Eye Res* **77**, 211-217 (2003).
37 Salmela, M. T. *et al.* Collagenase-1 (MMP-1), matrilysin-1 (MMP-7), and stromelysin-2 (MMP-10) are expressed by migrating enterocytes during intestinal wound healing. *Scand J Gastroenterol* **39**, 1095-1104 (2004).
38 Ljumovic, D., Diamantis, I., Alegakis, A. K. & Kouroumalis, E. A. Differential expression of matrix metalloproteinases in viral and non-viral chronic liver diseases. *Clin Chim Acta* **349**, 203-211 (2004).
39 Gill, J. H. *et al.* MMP-10 is overexpressed, proteolytically active, and a potential target for therapeutic intervention in human lung carcinomas. *Neoplasia* **6**, 777-785 (2004).
40 Cho, N. H. *et al.* MMP expression profiling in recurred stage IB lung cancer. *Oncogene* **23**, 845-851 (2004).
41 Martorana, A. M., Zheng, G., Crowe, T. C., O'Grady, R. L. & Lyons, J. G. Epithelial cells up-regulate matrix metalloproteinases in cells within the same mammary carcinoma that have undergone an epithelial-mesenchymal transition. *Cancer Res* **58**, 4970-4979 (1998).
42 Bodey, B., Bodey, B., Jr., Siegel, S. E. & Kaiser, H. E. Matrix metalloproteinases in neoplasm-induced extracellular matrix remodeling in breast carcinomas. *Anticancer Res* **21**, 2021-2028 (2001).
43 Bodey, B., Bodey, B., Jr., Siegel, S. E. & Kaiser, H. E. Immunocytochemical detection of MMP-3 and -10 expression in hepatocellular carcinomas. *Anticancer Res* **20**, 4585-4590 (2000).
44 Mathew, R. *et al.* Stromelysin-2 overexpression in human esophageal squamous cell carcinoma: potential clinical implications. *Cancer Detect Prev* **26**, 222-228 (2002).
45 Martinez, C., Bhattacharya, S., Freeman, T., Churchman, M. & Ilyas, M. Expression profiling of murine intestinal adenomas reveals early deregulation of multiple matrix metalloproteinase (Mmp) genes. *J Pathol* **206**, 100-110 (2005).
46 Seargent, J. M. *et al.* Expression of matrix metalloproteinase-10 in human bladder transitional cell carcinoma. *Urology* **65**, 815-820 (2005).

47 Rohani, M. G. *et al.* MMP-10 Regulates Collagenolytic Activity of Alternatively Activated Resident Macrophages. *J Invest Dermatol* **135**, 2377-2384, doi:10.1038/jid.2015.167 (2015).
48 Kassim, S. Y. *et al.* Individual matrix metalloproteinases control distinct transcriptional responses in airway epithelial cells infected with Pseudomonas aeruginosa. *Infect Immun* **75**, 5640-5650, doi:10.1128/IAI.00799-07 (2007).
49 Garcia-Irigoyen, O. *et al.* Matrix metalloproteinase-10 expression is induced during hepatic injury and plays a fundamental role in liver tissue repair. *Liver Int* **34**, e257-270, doi:10.1111/liv.12337 (2014).
50 Koller, F. L. *et al.* Lack of MMP10 exacerbates experimental colitis and promotes development of inflammation-associated colonic dysplasia. *Lab Invest* **92**, 1749-1759, doi:10.1038/labinvest.2012.141 (2012).
51 Cargnello, M. & Roux, P. P. Activation and function of the MAPKs and their substrates, the MAPK-activated protein kinases. *Microbiol Mol Biol Rev* **75**, 50-83, doi:10.1128/MMBR.00031-10 (2011).
52 Raman, M., Chen, W. & Cobb, M. H. Differential regulation and properties of MAPKs. *Oncogene* **26**, 3100-3112, doi:10.1038/sj.onc.1210392 (2007).
53 Sampieri, C. L. *et al.* Activation of p38 and JNK MAPK pathways abrogates requirement for new protein synthesis for phorbol ester mediated induction of select MMP and TIMP genes. *Matrix Biol* **27**, 128-138, doi:10.1016/j.matbio.2007.09.004 (2008).
54 Hirakawa, S. *et al.* Marked induction of matrix metalloproteinase-10 by respiratory syncytial virus infection in human nasal epithelial cells. *J Med Virol* **85**, 2141-2150, doi:10.1002/jmv.23718 (2013).
55 Treiber, M. *et al.* Myeloid, but not pancreatic, RelA/p65 is required for fibrosis in a mouse model of chronic pancreatitis. *Gastroenterology* **141**, 1473-1485, 1485 e1471-1477, doi:10.1053/j.gastro.2011.06.087 (2011).
56 Mosser, D. M. & Edwards, J. P. Exploring the full spectrum of macrophage activation. *Nat Rev Immunol* **8**, 958-969, doi:10.1038/nri2448 (2008).
57 Das, A. *et al.* Monocyte and Macrophage Plasticity in Tissue Repair and Regeneration. *Am J Pathol* **185**, 2596-2606, doi:10.1016/j.ajpath.2015.06.001 (2015).
58 Sica, A. & Mantovani, A. Macrophage plasticity and polarization: in vivo veritas. *J Clin Invest* **122**, 787-795, doi:10.1172/JCI59643 (2012).
59 Davies, L. C. & Taylor, P. R. Tissue-resident macrophages: then and now. *Immunology* **144**, 541-548, doi:10.1111/imm.12451 (2015).
60 Gordon, S. Alternative activation of macrophages. *Nat Rev Immunol* **3**, 23-35, doi:10.1038/nri978 (2003).
61 Lumeng, C. N., Bodzin, J. L. & Saltiel, A. R. Obesity induces a phenotypic switch in adipose tissue macrophage polarization. *J Clin Invest* **117**, 175-184, doi:10.1172/JCI29881 (2007).
62 Gordon, S. & Taylor, P. R. Monocyte and macrophage heterogeneity. *Nat Rev Immunol* **5**, 953-964 (2005).
63 Laskin, D. L., Weinberger, B. & Laskin, J. D. Functional heterogeneity in liver and lung macrophages. *J Leukoc Biol* **70**, 163-170 (2001).

64 Benoit, M., Desnues, B. & Mege, J. L. Macrophage polarization in bacterial infections. *J Immunol* **181**, 3733-3739 (2008).
65 Wang, N., Liang, H. & Zen, K. Molecular mechanisms that influence the macrophage m1-m2 polarization balance. *Front Immunol* **5**, 614, doi:10.3389/fimmu.2014.00614 (2014).
66 Mills, C. D. M1 and M2 Macrophages: Oracles of Health and Disease. *Crit Rev Immunol* **32**, 463-488 (2012).
67 Popovic, P. J., Zeh, H. J., 3rd & Ochoa, J. B. Arginine and immunity. *J Nutr* **137**, 1681S-1686S (2007).
68 Rath, M., Muller, I., Kropf, P., Closs, E. I. & Munder, M. Metabolism via Arginase or Nitric Oxide Synthase: Two Competing Arginine Pathways in Macrophages. *Front Immunol* **5**, 532, doi:10.3389/fimmu.2014.00532 (2014).
69 Murray, P. J. *et al.* Macrophage activation and polarization: nomenclature and experimental guidelines. *Immunity* **41**, 14-20, doi:10.1016/j.immuni.2014.06.008 (2014).
70 Kratz, M. *et al.* Metabolic dysfunction drives a mechanistically distinct proinflammatory phenotype in adipose tissue macrophages. *Cell Metab* **20**, 614-625, doi:10.1016/j.cmet.2014.08.010 (2014).
71 Lichtnekert, J., Kawakami, T., Parks, W. C. & Duffield, J. S. Changes in macrophage phenotype as the immune response evolves. *Curr Opin Pharmacol* **13**, 555-564, doi:10.1016/j.coph.2013.05.013 (2013).
72 Wynn, T. A. & Barron, L. Macrophages: master regulators of inflammation and fibrosis. *Semin. Liver Dis.* **30**, 245-257, doi:10.1055/s-0030-1255354 (2010).
73 Gharib, S. A. *et al.* MMP28 promotes macrophage polarization toward M2 cells and augments pulmonary fibrosis. *J Leukoc Biol* **95**, 9-18, doi:10.1189/jlb.1112587 (2014).
74 Duffield, J. S., Lupher, M., Thannickal, V. J. & Wynn, T. A. Host responses in tissue repair and fibrosis. *Annu. Rev. Pathol.* **8**, 241-276, doi:10.1146/annurev-pathol-020712-163930 (2013).
75 Wynn, T. A. & Barron, L. Macrophages: master regulators of inflammation and fibrosis. *Semin Liver Dis* **30**, 245-257, doi:10.1055/s-0030-1255354 (2010).
76 Baran, C. P. *et al.* Important roles for macrophage colony-stimulating factor, CC chemokine ligand 2, and mononuclear phagocytes in the pathogenesis of pulmonary fibrosis. *Am J Respir Crit Care Med* **176**, 78-89, doi:10.1164/rccm.200609-1279OC (2007).
77 Gharaee-Kermani, M., McCullumsmith, R. E., Charo, I. F., Kunkel, S. L. & Phan, S. H. CC-chemokine receptor 2 required for bleomycin-induced pulmonary fibrosis. *Cytokine* **24**, 266-276 (2003).
78 Okuma, T. *et al.* C-C chemokine receptor 2 (CCR2) deficiency improves bleomycin-induced pulmonary fibrosis by attenuation of both macrophage infiltration and production of macrophage-derived matrix metalloproteinases. *J Pathol* **204**, 594-604, doi:10.1002/path.1667 (2004).
79 Lucas, T. *et al.* Differential roles of macrophages in diverse phases of skin repair. *J Immunol* **184**, 3964-3977, doi:10.4049/jimmunol.0903356 (2010).
80 Goren, I. *et al.* A transgenic mouse model of inducible macrophage depletion: effects of diphtheria toxin-driven lysozyme M-specific cell lineage ablation on

wound inflammatory, angiogenic, and contractive processes. *Am J Pathol* **175**, 132-147, doi:10.2353/ajpath.2009.081002 (2009).
81 Duffield, J. S. *et al.* Selective depletion of macrophages reveals distinct, opposing roles during liver injury and repair. *J Clin Invest* **115**, 56-65 (2005).
82 Ramachandran, P. *et al.* Differential Ly-6C expression identifies the recruited macrophage phenotype, which orchestrates the regression of murine liver fibrosis. *Proc Natl Acad Sci USA* **109**, E3186-3195, doi:10.1073/pnas.1119964109 (2012).
83 Cutting, G. R. Cystic fibrosis genetics: from molecular understanding to clinical application. *Nat Rev Genet* **16**, 45-56, doi:10.1038/nrg3849 (2015).
84 Li, Z. *et al.* Longitudinal development of mucoid Pseudomonas aeruginosa infection and lung disease progression in children with cystic fibrosis. *JAMA* **293**, 581-588, doi:10.1001/jama.293.5.581 (2005).
85 Speert, D. P. *et al.* Epidemiology of Pseudomonas aeruginosa in cystic fibrosis in British Columbia, Canada. *Am J Respir Crit Care Med* **166**, 988-993 (2002).
86 Hyde, D. M., Hamid, Q. & Irvin, C. G. Anatomy, pathology, and physiology of the tracheobronchial tree: emphasis on the distal airways. *J Allergy Clin Immunol* **124**, S72-77, doi:10.1016/j.jaci.2009.08.048 (2009).
87 Rosenthal, N. & Brown, S. The mouse ascending: perspectives for human-disease models. *Nat Cell Biol* **9**, 993-999, doi:10.1038/ncb437 (2007).
88 Peters, L. L. *et al.* The mouse as a model for human biology: a resource guide for complex trait analysis. *Nat Rev Genet* **8**, 58-69, doi:10.1038/nrg2025 (2007).
89 Baron, R. M., Choi, A. J., Owen, C. A. & Choi, A. M. Genetically manipulated mouse models of lung disease: potential and pitfalls. *Am J Physiol Lung Cell Mol Physiol* **302**, 485-497, doi:10.1152/ajplung.00085.2011 (2012).
90 Sharma, S. Acute respiratory distress syndrome. *BMJ Clin Evid* **2010** (2010).
91 Saguil, A. & Fargo, M. Acute respiratory distress syndrome: diagnosis and management. *Am Fam Physician* **85**, 352-358 (2012).
92 Wilson, M. S. & Wynn, T. A. Pulmonary fibrosis: pathogenesis, etiology and regulation. *Mucosal Immunol* **2**, 103-121, doi:10.1038/mi.2008.85 (2009).
93 Wuyts, W. A. *et al.* The pathogenesis of pulmonary fibrosis: a moving target. *Eur Respir J* **41**, 1207-1218, doi:10.1183/09031936.00073012 (2013).
94 Kim, H. J., Perlman, D. & Tomic, R. Natural history of idiopathic pulmonary fibrosis. *Respir Med*, doi:10.1016/j.rmed.2015.02.002 (2015).
95 American Thoracic, S. & European Respiratory, S. American Thoracic Society/European Respiratory Society International Multidisciplinary Consensus Classification of the Idiopathic Interstitial Pneumonias. This joint statement of the American Thoracic Society (ATS), and the European Respiratory Society (ERS) was adopted by the ATS board of directors, June 2001 and by the ERS Executive Committee, June 2001. *Am J Respir Crit Care Med* **165**, 277-304, doi:10.1164/ajrccm.165.2.ats01 (2002).
96 NIOSH. Current Intelligence Bulletin 65 Occupational Exposure to Carbon Nanotubes and Nanofibers. (ed Department of Health and Human Services) 1 - 184 (2013).
97 Mortality, G. B. D. & Causes of Death, C. Global, regional, and national age-sex specific all-cause and cause-specific mortality for 240 causes of death, 1990-

2013: a systematic analysis for the Global Burden of Disease Study 2013. *Lancet* **385**, 117-171, doi:10.1016/S0140-6736(14)61682-2 (2015).
98 Mouratis, M. A. & Aidinis, V. Modeling pulmonary fibrosis with bleomycin. *Curr Opin Pulm Med* **17**, 355-361, doi:10.1097/MCP.0b013e328349ac2b (2011).
99 Moeller, A., Ask, K., Warburton, D., Gauldie, J. & Kolb, M. The bleomycin animal model: a useful tool to investigate treatment options for idiopathic pulmonary fibrosis? *Int J Biochem Cell Biol* **40**, 362-382, doi:10.1016/j.biocel.2007.08.011 (2008).
100 Myllärniemi, M. & Kaarteenaho, R. Pharmacological treatment of idiopathic pulmonary fibrosis – preclinical and clinical studies of pirfenidone, nintedanib, and N-acetylcysteine. *European Clinical Respiratory Journal* **2**, doi:10.3402/ecrj.v2.26385 (2015).
101 Reinert, T., Baldotto, C. S. d. R., Nunes, F. A. P. & Scheliga, A. A. d. S. Bleomycin-Induced Lung Injury. *Journal of Cancer Research* **2013**, 1-9, doi:10.1155/2013/480608 (2013).
102 Lam, C. W., James, J. T., McCluskey, R., Arepalli, S. & Hunter, R. L. A review of carbon nanotube toxicity and assessment of potential occupational and environmental health risks. *Crit Rev Toxicol* **36**, 189-217 (2006).
103 van Berlo, D. *et al.* Apoptotic, inflammatory, and fibrogenic effects of two different types of multi-walled carbon nanotubes in mouse lung. *Arch Toxicol* **88**, 1725-1737, doi:10.1007/s00204-014-1220-z (2014).
104 Chen, T. *et al.* Epithelial-mesenchymal transition involved in pulmonary fibrosis induced by multi-walled carbon nanotubes via TGF-beta/Smad signaling pathway. *Toxicol Lett* **226**, 150-162, doi:10.1016/j.toxlet.2014.02.004 (2014).
105 Hussain, S. *et al.* Inflammasome activation in airway epithelial cells after multi-walled carbon nanotube exposure mediates a profibrotic response in lung fibroblasts. *Part Fibre Toxicol* **11**, 28, doi:10.1186/1743-8977-11-28 (2014).
106 Mercer, R. R. *et al.* Pulmonary fibrotic response to aspiration of multi-walled carbon nanotubes. *Part Fibre Toxicol* **8**, 21, doi:10.1186/1743-8977-8-21 (2011).
107 Sun, B. *et al.* NADPH Oxidase-Dependent NLRP3 Inflammasome Activation and its Important Role in Lung Fibrosis by Multiwalled Carbon Nanotubes. *Small*, doi:10.1002/smll.201402859 (2015).
108 Liu, Z., Liu, Y. & Peng, D. Hydroxylation of multi-walled carbon nanotubes reduces their cytotoxicity by limiting the activation of mitochondrial mediated apoptotic pathway. *J Mater Sci Mater Med* **25**, 1033-1044, doi:10.1007/s10856-013-5128-6 (2014).
109 Girtsman, T. A., Beamer, C. A., Wu, N., Buford, M. & Holian, A. IL-1R signalling is critical for regulation of multi-walled carbon nanotubes-induced acute lung inflammation in C57Bl/6 mice. *Nanotoxicology* **8**, 17-27, doi:10.3109/17435390.2012.744110 (2014).
110 Muhl, H. & Pfeilschifter, J. Anti-inflammatory properties of pro-inflammatory interferon-gamma. *Int Immunopharmacol* **3**, 1247-1255, doi:10.1016/S1567-5769(03)00131-0 (2003).
111 Guo, H., Callaway, J. B. & Ting, J. P. Inflammasomes: mechanism of action, role in disease, and therapeutics. *Nat Med* **21**, 677-687, doi:10.1038/nm.3893 (2015).

112 Sims, J. E. & Smith, D. E. The IL-1 family: regulators of immunity. *Nat Rev Immunol* **10**, 89-102, doi:10.1038/nri2691 (2010).
113 Murray, M. Y. *et al.* Macrophage migration and invasion is regulated by MMP10 expression. *PLoS One* **8**, e63555, doi:10.1371/journal.pone.0063555 (2013).
114 Lisboa, R. A., Andrade, M. V. & Cunha-Melo, J. R. Toll-like receptor activation and mechanical force stimulation promote the secretion of matrix metalloproteinases 1, 3 and 10 of human periodontal fibroblasts via p38, JNK and NF-kB. *Arch Oral Biol* **58**, 731-739, doi:10.1016/j.archoralbio.2012.12.009 (2013).
115 Huang, W. C., Sala-Newby, G. B., Susana, A., Johnson, J. L. & Newby, A. C. Classical macrophage activation up-regulates several matrix metalloproteinases through mitogen activated protein kinases and nuclear factor-kappaB. *PLoS One* **7**, e42507, doi:10.1371/journal.pone.0042507 (2012).
116 Oona Rechardt, O. E., Maarit Vaalamo, Kati Pääkkönen, Tiina Jahkola, Johanna Höök-Nikanne, Rosalind M Hembry, Lari Häkkinen, Juha Kere and Ulpu Saarialho-Kere. Stromelysin-2 is Upregulated During Normal Wound Repair and is Induced by Cytokines. *Journal of Investigative Dermatology* **115**, 778–787 (2000).
117 Cui, C. *et al.* CRP promotes MMP-10 expression via c-Raf/MEK/ERK and JAK1/ERK pathways in cardiomyocytes. *Cell Signal* **24**, 810-818, doi:10.1016/j.cellsig.2011.11.019 (2012).
118 Zhang, J. J. *et al.* Yin Yang-1 suppresses invasion and metastasis of pancreatic ductal adenocarcinoma by downregulating MMP10 in a MUC4/ErbB2/p38/MEF2C-dependent mechanism. *Mol Cancer* **13**, 130, doi:10.1186/1476-4598-13-130 (2014).
119 Batchelor, C. L. & Winder, S. J. Sparks, signals and shock absorbers: how dystrophin loss causes muscular dystrophy. *Trends Cell Biol* **16**, 198-205, doi:10.1016/j.tcb.2006.02.001 (2006).
120 Moore, B. B. *et al.* Animal models of fibrotic lung disease. *Am J Respir Cell Mol Biol* **49**, 167-179, doi:10.1165/rcmb.2013-0094TR (2013).
121 Rosenbloom, J., Mendoza, F. A. & Jimenez, S. A. Strategies for anti-fibrotic therapies. *Biochim Biophys Acta* **1832**, 1088-1103, doi:10.1016/j.bbadis.2012.12.007 (2013).
122 Chong, S. *et al.* Pneumoconiosis: comparison of imaging and pathologic findings. *Radiographics* **26**, 59-77, doi:10.1148/rg.261055070 (2006).
123 Wynn, T. A. Integrating mechanisms of pulmonary fibrosis. *J Exp Med* **208**, 1339-1350, doi:10.1084/jem.20110551 (2011).
124 Izbicki, G., Segel, M. J., Christensen, T. G., Conner, M. W. & Breuer, R. Time course of bleomycin-induced lung fibrosis. *Int J Exp Pathol* **83**, 111-119 (2002).
125 Hold, G. L., Untiveros, P., Saunders, K. A. & El-Omar, E. M. Role of host genetics in fibrosis. *Fibrogenesis Tissue Repair* **2**, 6, doi:10.1186/1755-1536-2-6 (2009).
126 Schupp, J. C. *et al.* Macrophage activation in acute exacerbation of idiopathic pulmonary fibrosis. *PLoS One* **10**, e0116775, doi:10.1371/journal.pone.0116775 (2015).

127 Mora, A. L. *et al.* Activation of alveolar macrophages via the alternative pathway in herpesvirus-induced lung fibrosis. *Am J Respir Cell Mol Biol* **35**, 466-473, doi:10.1165/rcmb.2006-0121OC (2006).
128 FDA. Guidance for Industry Considering Whether an FDA-Regulated Product Involves the Application of Nanotechnology. (2014).
129 De Volder, M. F., Tawfick, S. H., Baughman, R. H. & Hart, A. J. Carbon nanotubes: present and future commercial applications. *Science* **339**, 535-539, doi:10.1126/science.1222453 (2013).
130 Manke, A., Luanpitpong, S. & Rojanasakul, Y. Potential Occupational Risks Associated with Pulmonary Toxicity of Carbon Nanotubes. *Occup Med Health Aff* **2**, doi:10.4172/2329-6879.1000165 (2014).
131 Nanotech. Nanotubes hanging in there... *Nanotech Magazine*, 4-5 (2013).
132 Pacurari, M., Castranova, V. & Vallyathan, V. Single- and multi-wall carbon nanotubes versus asbestos: are the carbon nanotubes a new health risk to humans? *J Toxicol Environ Health A* **73**, 378-395, doi:10.1080/15287390903486527 (2010).
133 Pulskamp, K., Diabate, S. & Krug, H. F. Carbon nanotubes show no sign of acute toxicity but induce intracellular reactive oxygen species in dependence on contaminants. *Toxicol Lett* **168**, 58-74, doi:10.1016/j.toxlet.2006.11.001 (2007).
134 Jiang, Y. *et al.* Modulation of apoptotic pathways of macrophages by surface-functionalized multi-walled carbon nanotubes. *PLoS One* **8**, e65756, doi:10.1371/journal.pone.0065756 (2013).
135 Hamilton, R. F., Jr., Wu, Z., Mitra, S., Shaw, P. K. & Holian, A. Effect of MWCNT size, carboxylation, and purification on in vitro and in vivo toxicity, inflammation and lung pathology. *Part Fibre Toxicol* **10**, 57, doi:10.1186/1743-8977-10-57 (2013).
136 Donaldson, K. *et al.* Pulmonary toxicity of carbon nanotubes and asbestos - similarities and differences. *Adv Drug Deliv Rev* **65**, 2078-2086, doi:10.1016/j.addr.2013.07.014 (2013).
137 Dong, J. *et al.* Pathologic and molecular profiling of rapid-onset fibrosis and inflammation induced by multi-walled carbon nanotubes. *Arch Toxicol* **89**, 621-633, doi:10.1007/s00204-014-1428-y (2015).
138 Pacurari, M. *et al.* Multi-walled carbon nanotube-induced gene expression in the mouse lung: association with lung pathology. *Toxicol Appl Pharmacol* **255**, 18-31, doi:10.1016/j.taap.2011.05.012 (2011).
139 Chen, B. *et al.* In vitro evaluation of cytotoxicity and oxidative stress induced by multiwalled carbon nanotubes in murine RAW 264.7 macrophages and human A549 lung cells. *Biomed Environ Sci* **24**, 593-601, doi:10.3967/0895-3988.2011.06.002 (2011).
140 Taylor, A. J. *et al.* Atomic layer deposition coating of carbon nanotubes with aluminum oxide alters pro-fibrogenic cytokine expression by human mononuclear phagocytes in vitro and reduces lung fibrosis in mice in vivo. *PLoS One* **9**, e106870, doi:10.1371/journal.pone.0106870 (2014).
141 Invernizzi, N. Nanotechnology between the lab and the shop floor: what are the effects on labor? *J Nanopart Res* **13(6)**, 2249-2268, doi:10.1007/s11051-011-0333-z (2011).

142 Yang, S. T., Luo, J., Zhou, Q. & Wang, H. Pharmacokinetics, metabolism and toxicity of carbon nanotubes for biomedical purposes. *Theranostics* **2**, 271-282, doi:10.7150/thno.3618 (2012).
143 Erdely, A. *et al.* Carbon nanotube dosimetry: from workplace exposure assessment to inhalation toxicology. *Part Fibre Toxicol* **10**, 53, doi:10.1186/1743-8977-10-53 (2013).
144 Poulsen, S. S. *et al.* MWCNTs of different physicochemical properties cause similar inflammatory responses, but differences in transcriptional and histological markers of fibrosis in mouse lungs. *Toxicol Appl Pharmacol* **284**, 16-32, doi:10.1016/j.taap.2014.12.011 (2015).
145 Han, S. G., Andrews, R. & Gairola, C. G. Acute pulmonary response of mice to multi-wall carbon nanotubes. *Inhal Toxicol* **22**, 340-347, doi:10.3109/08958370903359984 (2010).
146 Porter, D. W. *et al.* Mouse pulmonary dose- and time course-responses induced by exposure to multi-walled carbon nanotubes. *Toxicology* **269**, 136-147, doi:10.1016/j.tox.2009.10.017 (2010).
147 Stuart, B. O. Deposition and clearance of inhaled particles. *Environ Health Perspect* **55**, 369-390 (1984).
148 Kagan, V. E. *et al.* Carbon nanotubes degraded by neutrophil myeloperoxidase induce less pulmonary inflammation. *Nat Nanotechnol* **5**, 354-359, doi:10.1038/nnano.2010.44 (2010).
149 U K Saarialho-Kere, A. P. P., H Birkedal-Hansen, W C Parks, and H G Welgus. Distinct populations of keratinocytes express stromelysin-1 and -2 in chronic wounds. *J Clin Invest* **94**, :79-88 (1994).
150 Sweeney, S., Grandolfo, D., Ruenraroengsak, P. & Tetley, T. D. Functional consequences for primary human alveolar macrophages following treatment with long, but not short, multiwalled carbon nanotubes. *Int J Nanomedicine* **10**, 3115-3129, doi:10.2147/IJN.S77867 (2015).
151 Wynn, T. A., Chawla, A. & Pollard, J. W. Macrophage biology in development, homeostasis and disease. *Nature* **496**, 445-455, doi:10.1038/nature12034 (2013).
152 Murray, P. J. & Wynn, T. A. Protective and pathogenic functions of macrophage subsets. *Nat Rev Immunol* **11**, 723-737, doi:10.1038/nri3073 (2011).
153 Lari, R. *et al.* Macrophage lineage phenotypes and osteoclastogenesis--complexity in the control by GM-CSF and TGF-beta. *Bone* **40**, 323-336, doi:10.1016/j.bone.2006.09.003 (2007).
154 Schlage, P., Kockmann, T., Sabino, F., Kizhakkedathu, J. N. & Auf dem Keller, U. Matrix metalloproteinase 10 degradomics in keratinocytes and epidermal tissue identifies bioactive substrates with pleiotropic functions. *Mol Cell Proteomics*, doi:10.1074/mcp.M115.053520 (2015).
155 Li, H., Xu, H. & Sun, B. Lipopolysaccharide regulates MMP-9 expression through TLR4/NF-kappaB signaling in human arterial smooth muscle cells. *Mol Med Rep* **6**, 774-778, doi:10.3892/mmr.2012.1010 (2012).
156 Jackson, L., Cady, C. T. & Cambier, J. C. TLR4-mediated signaling induces MMP9-dependent cleavage of B cell surface CD23. *J Immunol* **183**, 2585-2592, doi:10.4049/jimmunol.0803660 (2009).

157 Cho, J. S. *et al.* Lipopolysaccharide induces pro-inflammatory cytokines and MMP production via TLR4 in nasal polyp-derived fibroblast and organ culture. *PLoS One* **9**, e90683, doi:10.1371/journal.pone.0090683 (2014).
158 Rao, K. M. MAP kinase activation in macrophages. *J Leukoc Biol* **69**, 3-10 (2001).
159 Wu, L. *et al.* Regulation of MMP10 expression by the transcription factor CHF1/Hey2 is mediated by multiple E boxes. *Biochem Biophys Res Commun* **415**, 662-668, doi:10.1016/j.bbrc.2011.10.132 (2011).
160 Rothgiesser, K. M., Fey, M. & Hottiger, M. O. Acetylation of p65 at lysine 314 is important for late NF-kappaB-dependent gene expression. *BMC Genomics* **11**, 22, doi:10.1186/1471-2164-11-22 (2010).
161 Garcia-Irigoyen, O. *et al.* Matrix metalloproteinase 10 contributes to hepatocarcinogenesis in a novel crosstalk with the stromal derived factor 1/C-X-C chemokine receptor 4 axis. *Hepatology* **62**, 166-178, doi:10.1002/hep.27798 (2015).
162 Toft-Hansen, H. *et al.* Metalloproteinases control brain inflammation induced by pertussis toxin in mice overexpressing the chemokine CCL2 in the central nervous system. *J Immunol* **177**, 7242-7249 (2006).
163 Gharaee-Kermani, M., Denholm, E. M. & Phan, S. H. Costimulation of fibroblast collagen and transforming growth factor beta1 gene expression by monocyte chemoattractant protein-1 via specific receptors. *J Biol Chem* **271**, 17779-17784 (1996).
164 Elmore, S. Apoptosis: a review of programmed cell death. *Toxicol Pathol* **35**, 495-516, doi:10.1080/01926230701320337 (2007).
165 Burke, J. R. *et al.* BMS-345541 is a highly selective inhibitor of I kappa B kinase that binds at an allosteric site of the enzyme and blocks NF-kappa B-dependent transcription in mice. *J Biol Chem* **278**, 1450-1456, doi:10.1074/jbc.M209677200 (2003).
166 Frank, E. A., Birch, M. E. & Yadav, J. S. MyD88 mediates in vivo effector functions of alveolar macrophages in acute lung inflammatory responses to carbon nanotube exposure. *Toxicol Appl Pharmacol* **288**, 322-329, doi:10.1016/j.taap.2015.08.004 (2015).
167 Braber, S., Verheijden, K. A., Henricks, P. A., Kraneveld, A. D. & Folkerts, G. A comparison of fixation methods on lung morphology in a murine model of emphysema. *Am J Physiol Lung Cell Mol Physiol* **299**, L843-851, doi:10.1152/ajplung.00192.2010 (2010).
168 Manicone, A. M. *et al.* Epilysin (MMP-28) restrains early macrophage recruitment in Pseudomonas aeruginosa pneumonia. *J Immunol* **182**, 3866-3876, doi:10.4049/jimmunol.0713949 (2009).
169 Rohani, M. G. *et al.* uPARAP function in cutaneous wound repair. *PLoS One* **9**, e92660, doi:10.1371/journal.pone.0092660 (2014).

Curriculum Vitae

Tyler C. Vandivort

EDUCATION

University of Washington, Dept. of Envir. and Occup. Health Sci. Seattle, WA	Ph.D. Student Envir. Toxicology	09/10 to 12/15
Rhode Island College Providence, RI	Biology Chemistry minor *magna cum laude*	B. A., 2009

Honors thesis: *Mechanism of transcript diversity of shark aryl hydrocarbon receptor 2 (AHR2)*
Advisor: Dr. Rebeka Rand Merson

RESEARCH EXPERIENCE

April 2014 to present Cedars-Sinai Med. Ctr. Dept. of Medicine, Women's Guild Lung Institute Los Angeles, CA
Visiting Graduate Student
Continuing research with William C. Parks at a new institution

May 2011-April 2014 U. of Washington, Dept. of Medicine, Division of Pulmonary and Crit. Care Medicine, Seattle, WA
Graduate Researcher
Carrying out graduate research focusing on matrix metalloproteinase 10 (MMP10) in the context of the innate immune response to pulmonary injury, and the development of fibrosis. *S*tudies involve *in vivo* administration of a range of toxins and toxicants (e.g. bleomycin sulfate, *Pseudomonas aeruginosa* strain K, and multi-walled carbon nanotubes) via orotracheal intubation and oropharyngeal aspiration, as well as complementary *in vitro* work utilizing a myriad of immortalized and primary cell lines. Analyses include endpoints from gross damage and fibrogenesis, to specific signaling mechanisms (NFκB, MAPK, etc), and involve a range of activity assays, histology preparations, cell counts, immunobloting, flow cytometry, ELISAs, and more for their completion. PI: Dr. William C. Parks.

July 2009- July 2010 U. of New Mexico, Dept. of Pharmaceutical Sciences, Albuquerque, NM
Research Technician II
Research foci include the endogenous role of aryl hydrocarbon receptors (AhR) in blood pressure maintenance, and its mechanism of xenobiotic induced toxicity in response to halogenated aromatic hydrocarbons (HAH), such as the persistent environmental

contaminate 2,3,7,8-tetrachlorodibenzo-p-Dioxin (TCDD). Maintained generation breeding, tracked, and genotyped a total of 8 transgenic mouse colonies. Trained in the safe exposure and collection of tissues containing TCDD. Performed surgical implantations of various devices including subcutaneous osmotic minipumps, and blood pressure catheters in the carotid artery. PI: Dr. Mary K. Walker.

Jan. 2007-May 2009 Rhode Island College, Dept. of Biology, Providence, RI
Student Specialist
Designed and carried out studies regarding the function and diversity of the aryl hydrocarbon receptor (AhR) in early vertebrates. Utilized various experimental methods involved in understanding the molecular and organismal basis of receptor-mediated xenobiotic metabolism.
Extracted and sequenced AhR isoforms utilizing bioinformatic software, performed various blot and cellular analyses to discern AhR and Cyp1a1 expression. Carried out research both as an individual, and as part of an investigating team.

HONORS AND MEMBERSHIPS

August 2015	Outstanding Poster Award. Gordon Research Conference (GRC) on Pulmonary Injury and Repair. Andover, NH. August 16-21, 2015
October 2012	NIH Institutional Research Training Grant Recipient: Environmental Pathology and Toxicology Training Grant *(T32 ES007032-35)*
March 2011	Pacific Northwest Association of Toxicologists (PANWAT)
May 2009	Sigma Xi: The Scientific Research Society: Rhode Island College Chapter
March 14-16 2009	Society of Toxicology- Undergraduate Student and Advisor Travel Award
March 2009	Society of Toxicology Student Member

PRESENTATIONS

Platform

Zalobowski, T. W. & R.R. Merson. Unprecedented Diversity of Aryl Hydrocarbon Receptor 2 (AHR2) Transcripts from *Squalus acanthias*: Evidence for multiple AHR2 genes in sharks. Sigma Xi: The Scientific Research Society: Rhode Island College Chapter Conference. May 4, 2009. Rhode Island College. Providence, RI.

Zalobowski, T. W. & R.R. Merson. Unprecedented Diversity of Aryl Hydrocarbon Receptor 2 (AHR2) Transcripts from *Squalus acanthias*: Evidence for multiple AHR2 genes in sharks. 3rd Annual Biology New England South Meeting (BioNES). December 2, 2008 Roger Williams University, Bristol, RI.

Zalobowski, T. W. & R.R. Merson. Extensive variability of the shark Aryl Hydrocarbon Receptor 2 (AHR2) in a domain containing multiple tandem octapeptide repeats.

RIC-WHOI Joint Meeting, August 7, 2008 Wood's Hole Oceanographic Institution, Woods Hole, MA.

Posters

Vandivort, T.C., Birkland, T. P., Domiciano, T., Kavanagh, T. J., Parks, W.C. Matrix metalloproteinase 10 (MMP10) modulates pulmonary clearance, inflammation and cell death following long multi-walled carbon nanotube (L-MWCNT) exposure. Gordon Research Conference: Lung Development, Injury & Repair. Proctor Academy, August 16-21, 2015, Andover, NH.

Vandivort, T., Birkland, T, Dowon, A., Parks., W.C. (2013) The role of Matrix Metalloproteinase 10 (MMP-10) in Modulating Bleomycin-induced lung Injury. Gordon Research Conference: Lung Development, Injury & Repair. Proctor Academy, August 18-23, 2013, Andover, NH.

Vandivort, T. C., Birkland, T., An, D., Parks, W. C. The Role of Matrix Metalloproteinase 10 (Mmp10) in Modulating Bleomycin-induced Lung Injury. Environmental Pathology and Toxicology Training Grant Meeting. University of Washington, May 30, 2013. Seattle, WA

Zalobowski, T. W., Birkland, T., Parks, W. C. The Role of MMP-10 in Modulating the Polarization State of Bone Marrow Derived Macrophages. Environmental Pathology and Toxicology Training Grant Meeting. University of Washington, May 1, 2012. Seattle, WA

Zalobowski, T. W. & R.R. Merson. Transcript diversity of aryl hydrocarbon receptor 2 (AHR2) in sharks Annual Society of Toxicology Meeting. Baltimore Convention Center, May 4-16, 2009 Baltimore, MD, ACCEPTED

Zalobowski, T. W. & R.R. Merson. Extensive variability of the shark Aryl Hydrocarbon Receptor 2 (AHR2) in a domain containing multiple tandem octapeptide repeats. New England Membrane Enzyme Group (NUTMEG) Conference. Woods Hole Oceanographic Institution, October 5-7, 2008 Woods Hole, MA.

Zalobowski, T. W. & R.R. Merson. Extensive variability of the shark Aryl Hydrocarbon Receptor 2 (AHR2) in a domain containing multiple tandem octapeptide repeats. 2008 Summer Undergraduate Research Fellows Conference. University of Rhode Island August 4, 2008 Kingston, RI.

Zalobowski, T. W., M. Schmidt & R.R. Merson. How do we get from there to here? Bench training and aberrant methylation of DNA following exposure to environmental chemicals. Rhode Island Research Alliance Symposium, RI Convention Center June 3, 2008 Providence, RI,

PUBLICATIONS (In 2012 I legally changed my name from Tyler Zalobowski to Tyler Vandivort)

Vandivort, T.C., Birkland, T. P., Domiciano, T., Kavanagh, T. J., Parks, W.C. Stromelysin-2 (MMP-10) Facilitates Clearance and Moderates Inflammation and Cell Death Following Lung Exposure to Long Multi-walled Carbon Nanotubes (L-MWCNT). **In Prep.**

Vandivort, T. C., Parks, W. C. Induction of Stromeolysin-2 (MMP-10) in Macrophages Is Meditated via Diverse Mitogen Activated Protein (MAP) Kinase Pathways That Converge on NFkB. **In Prep.**

Vandivort, T. C., Birkland, Dowon, A., T. B., Parks, W. C. Pulmonary Stromelysin-2 (MMP-10) Protects against Acute Lung Injury and Fibrogenesis in Mice. **In Prep.**

Vandivort, T.C., Parks, W.C. (2014) An Improved Method for Rapid Intubation of Bleomycin in Mi. JoVE. **In Press.**

Vandivort, T.C., Eaton, D.L. (2014) Principles of Toxicology. Reference Module in Biomedical Sciences. Elsevier. doi:10.1016/B978-0-12-801238-3.00203-8

Zhang, N., Agbor, L. N., Scott, J. A., ***Zalobowski, T**., Elased, K. M., Trujillo, A., Walker, M. K. (2010). An activated renin-angiotensin system maintains normal blood pressure in aryl hydrocarbon receptor heterozygous mice but not in null mice. *Biochemical Pharmacology*, *80*(2), 197–204. doi:10.1016/j.bcp.2010.03.023